

# Realistic Reaction Evaluations for Fission Products Off Stability

G.P.A. Nobre<sup>1</sup>, Kyle Wendt<sup>2</sup>, Alexander Voinov<sup>3</sup>, Dave Brown<sup>1</sup>,  
Emanuel Chimanski<sup>1</sup>, Shusen Liu<sup>2</sup>, Aman Sharma<sup>2</sup>

<sup>1</sup>National Nuclear Data Center, Brookhaven National Laboratory

<sup>2</sup>Lawrence Livermore National Laboratory

<sup>3</sup>Ohio University



@BrookhavenLab

Technical Meeting on Neutron-induced Reactions on

Short-lived Nuclides

25-29 August 2025

# Outline

- Project Goals and Objectives
- Team Introduction
- Nuclear Data & Evaluations
- Methodology
  - Fast region
  - Resonance region
  - Experimental component
- Status and perspectives

**DEPARTMENT OF ENERGY (DOE)  
OFFICE OF SCIENCE (SC), NUCLEAR PHYSICS (NP)  
NATIONAL NUCLEAR SECURITY ADMINISTRATION (NNSA), DEFENSE  
NUCLEAR NONPROLIFERATION RESEARCH AND DEVELOPMENT**



**NUCLEAR DATA INTERAGENCY WORKING GROUP  
(NDIAWG) RESEARCH PROGRAM**

**FUNDING OPPORTUNITY ANNOUNCEMENT (FOA) NUMBER:  
DE-FOA-0003238**

**FOA TYPE: Initial  
CFDA NUMBER: 81.049**

# Project Goals and Objectives

## Goals:

- To develop a reproducible method to produce realistic evaluations for nuclei off-stability
- Apply the method to produce new evaluations of fission products off stability

## Key Objectives:

- To provide evaluated files for the main off-stability fission products of  $^{235}\text{U}$  and submit them to the ENDF/B nuclear data library
- Develop a robust and reproducible method for such evaluations
- Stretch goal: develop evaluated files for all off-stability fission products from  $^{235}\text{U}$ ,  $^{239}\text{Pu}$ ,  $^{252}\text{Cf}$



# Project Goals and Objectives

The **core-goal nuclei** (mostly produced by  $^{235}\text{U}$  fission):

- 1<sup>st</sup> Fission yield bump:  $^{87-89}\text{Br}$ ,  $^{88-92}\text{Kr}$ ,  $^{91-94}\text{Rb}$ ,  $^{92-97}\text{Sr}$ ,  $^{95-99}\text{Y}$ ,  $^{97-102}\text{Zr}$ ,  $^{101-103}\text{Nb}$
- 2<sup>nd</sup> Fission yield bump:  $^{131-133}\text{Sb}$ ,  $^{132-136}\text{Te}$ ,  $^{135-138}\text{I}$ ,  $^{136-141}\text{Xe}$ ,  $^{139-143}\text{Cs}$ ,  $^{141-146}\text{Ba}$ ,  $^{144-145}\text{La}$ ,  $^{147-148}\text{Ce}$

**Secondary goal** (main fission products from  $^{239}\text{Pu}$  and  $^{252}\text{Cf}$ ):

- 1<sup>st</sup> Fission yield bump:  $^{94,100}\text{Y}$ ,  $^{96,103}\text{Zr}$ ,  $^{99,100,104,105}\text{Nb}$ ,  $^{102-108}\text{Mo}$ ,  $^{105-110}\text{Tc}$ ,  $^{107-112}\text{Ru}$ ,  $^{110-114}\text{Rh}$ ,  $^{112-116}\text{Pd}$ ,  $^{114}\text{Ag}$
- 1<sup>st</sup> Fission yield bump:  $^{131}\text{Te}$ ,  $^{134}\text{I}$ ,  $^{135}\text{Xe}$ ,  $^{137,138,144}\text{Cs}$ ,  $^{140}\text{Ba}$ ,  $^{143,146-148}\text{La}$ ,  $^{145,146,149,150}\text{Ce}$ ,  $^{149-152}\text{Pr}$ ,  $^{151-153}\text{Nd}$

**Stretch goal** (whole isotopic chain of fission products from  $^{235}\text{U}$ ,  $^{239}\text{Pu}$ , and  $^{252}\text{Cf}$ ):

- $^{66}\text{V}$ ,  $^{66-67}\text{Cr}$ ,  $^{66-71}\text{Mn}$ ,  $^{66-75}\text{Fe}$ ,  $^{66-77}\text{Co}$ ,  $^{66-80}\text{Ni}$ ,  $^{66-82}\text{Cu}$ ,  $^{66-85}\text{Zn}$ ,  $^{68-87}\text{Ga}$ ,  $^{70-90}\text{Ge}$ ,  $^{72-92}\text{As}$ ,  $^{75-95}\text{Se}$ ,  $^{77-98}\text{Br}$ ,  $^{79-101}\text{Kr}$ ,  $^{81,83-103}\text{Rb}$ ,  $^{83-106}\text{Sr}$ ,  $^{87-109}\text{Y}$ ,  $^{88-112}\text{Zr}$ ,  $^{91-114}\text{Nb}$ ,  $^{93-117}\text{Mo}$ ,  $^{97-119}\text{Tc}$ ,  $^{98-121,124}\text{Ru}$ ,  $^{101-125}\text{Rh}$ ,  $^{103-126,128}\text{Pd}$ ,  $^{106-132}\text{Ag}$ ,  $^{108-134}\text{Cd}$ ,  $^{111-137}\text{In}$ ,  $^{113-139}\text{Sn}$ ,  $^{118-140}\text{Sb}$ ,  $^{120-143}\text{Te}$ ,  $^{123,125,126,128-145}\text{I}$ ,  $^{125,128,130-148}\text{Xe}$ ,  $^{131-151}\text{Cs}$ ,  $^{132-153}\text{Ba}$ ,  $^{135,137-155}\text{La}$ ,  $^{137-157}\text{Ce}$ ,  $^{139-159}\text{Pr}$ ,  $^{142-161}\text{Nd}$ ,  $^{144-163}\text{Pm}$ ,  $^{147-165}\text{Sm}$ ,  $^{149,151-168}\text{Eu}$ ,  $^{152-170}\text{Gd}$ ,  $^{155-172}\text{Tb}$ ,  $^{157-172}\text{Dy}$ ,  $^{161-172}\text{Ho}$ ,  $^{162-172}\text{Er}$ ,  $^{165-172}\text{Tm}$ ,  $^{168-172}\text{Yb}$ ,  $^{171-172}\text{Lu}$








Project will be successful if **core-goal** is achieved. However, when the methods are well-established, generalization to secondary and stretch goals should be possible with relative low effort.



# Project impact on the program

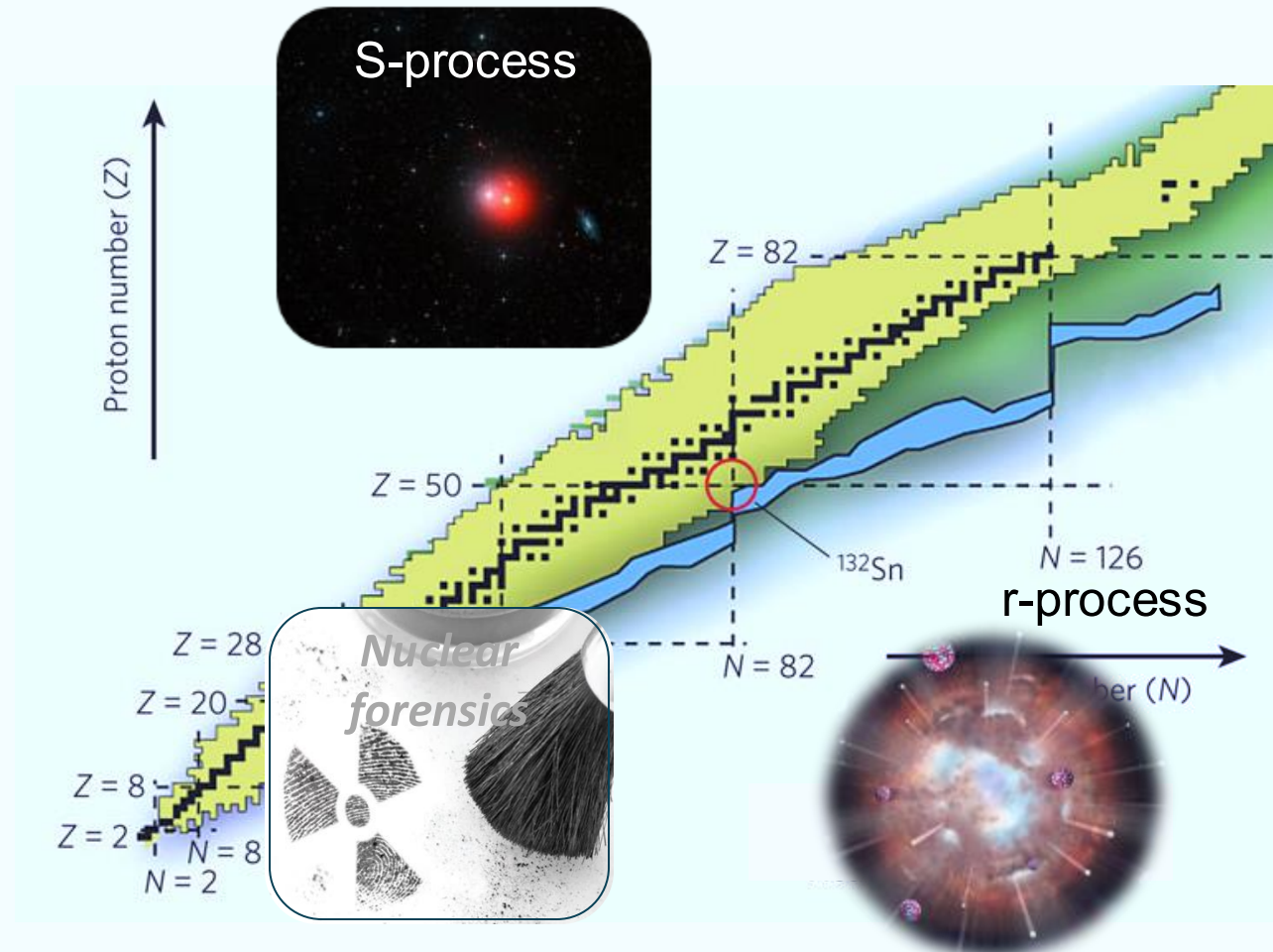
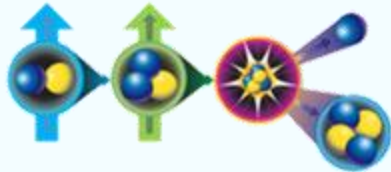
- Applications such **nonproliferation, post-detonation forensics, spent-fuel assay, reactor burnup and design**, as well as **astrophysics**, rely on the accurate description of the neutron interaction with unstable fission products.
- Current cross-section descriptions of these nuclei are either **non-existent** or based on **simplified assumptions**, leading to unquantified impacts on predicted cross-sections.
- By project completion, more **predictive/realistic** new nuclear data will be produced, improving the **reliability** of applications involving **fission products off stability!**

# Team Introduction

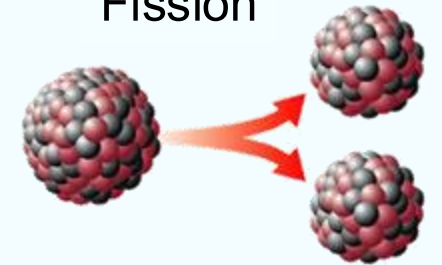
Team Member		Past/Current Leveraging Activities	Project Role
	Gustavo Nobre (BNL, PI)	<ul style="list-style-type: none"><li>• Led many previous evaluations, on and off stability</li><li>• Reaction model developer with many published works related to deformed nuclei, predictive models, and machine learning.</li><li>• ENDF/B library manager and EMPIRE co-developer</li></ul>	<ul style="list-style-type: none"><li>• Project Coordination</li><li>• Lead fast region calculations, mentoring postdoc</li><li>• Complete evaluated file assembly and submit to ENDF/B library</li></ul>
	David Brown (BNL)	<ul style="list-style-type: none"><li>• Extensive work and experience on resolved and unresolved resonances and analytical methods related cross-section probabilities and synthetic resonance generation.</li><li>• ENDF evaluator and NNDC and CSEWG chair</li></ul>	<ul style="list-style-type: none"><li>• Lead resonance treatment</li><li>• Implement transitions between different energy regions</li></ul>
	Kyle Wendt (LLNL)	<ul style="list-style-type: none"><li>• Theoretical nuclear physicist with extensive experience in modeling low energy phenomena.</li><li>• Lead develop on nuclear data UQ suite at LLNL</li><li>• Theory/AI team co-lead on SI-LDRD on ML for nuclear data</li></ul>	<ul style="list-style-type: none"><li>• Lead ML effort to provide cross-section priors off-stability for threshold reactions</li></ul>
	Alexander Voinov (OU)	<ul style="list-style-type: none"><li>• Experimentalist with extensive experience in nuclear level density measurements</li></ul>	<ul style="list-style-type: none"><li>• Perform experiments and data analysis for stable nuclei in the mass region of fission products</li></ul>
	Aman Sharma (LLNL, postdoc)	<ul style="list-style-type: none"><li>• Postdoc working on LLNL SI-LDRD on ML for nuclear data</li><li>• Experience on both experimental and theoretic physics, with an emphasis on UQ in both context.</li><li>• Has conducted experiments and evaluations as PhD student.</li></ul>	<ul style="list-style-type: none"><li>• Will work with Gustavo Nobre to learn about EMPIRE and to perform most of fast-region calculations.</li></ul>
	Shusen Liu (LLNL)	<ul style="list-style-type: none"><li>• Machine intelligence scientist with extensive experience on signal modeling and interpretable machine learning.</li><li>• Theory/AI team co-lead on SI-LDRD on ML for nuclear data.</li></ul>	<ul style="list-style-type: none"><li>• Will adapt the LLNL ML to specific needs of this project.</li></ul>
	Emanuel Chimanski (BNL)	<ul style="list-style-type: none"><li>• Evaluator and model developer, with published works on microscopic models and preequilibrium</li><li>• EMPIRE co-developer</li></ul>	<ul style="list-style-type: none"><li>• Fast-region preequilibrium modeling</li></ul>

# Nuclear Data is the interface between nuclear physics and science and technical application that depend nuclear physics

Thermonuclear  
Fusion



Fission



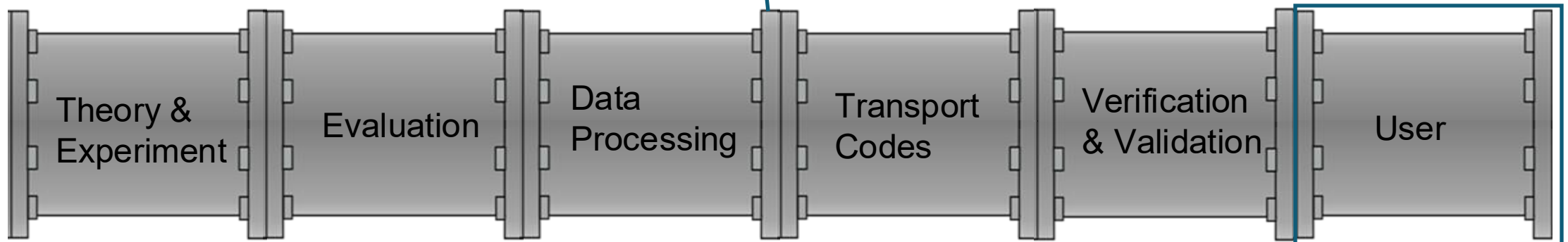
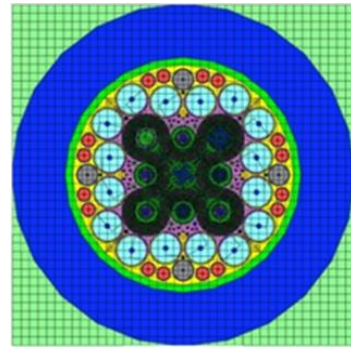
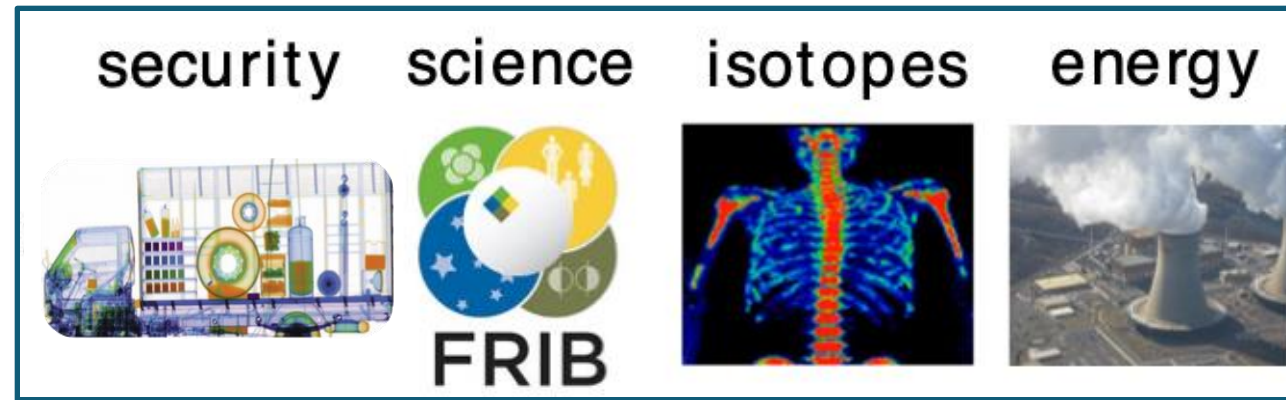
Neutron stars





# The Nuclear Data Pipeline

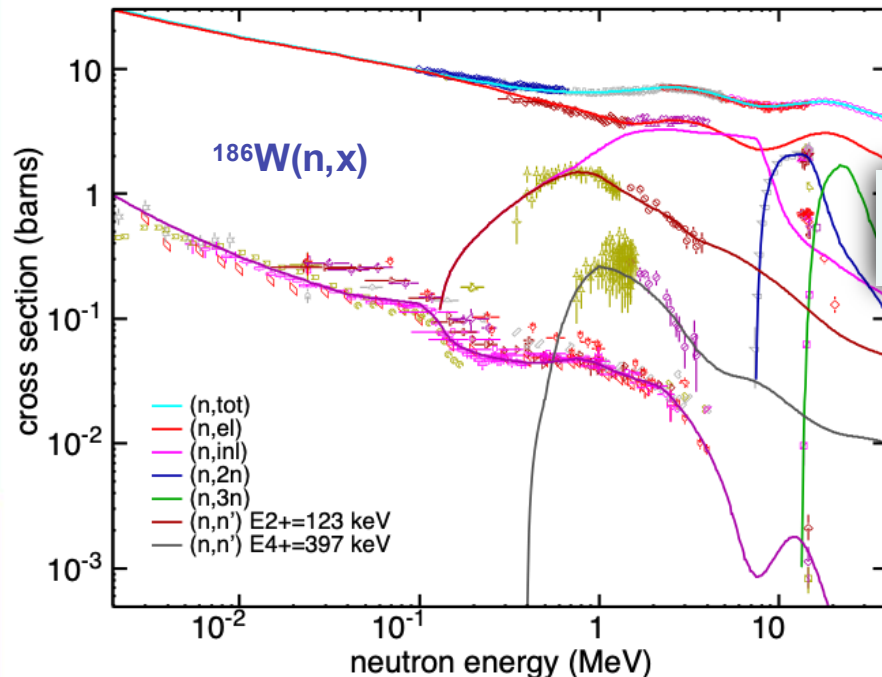
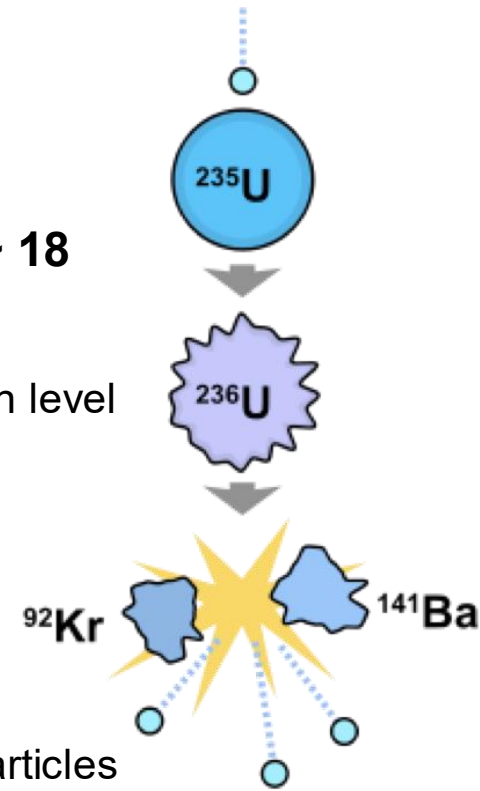
Our goal is to get the highest quality data to users



# Evaluated Nuclear Data File: Nuclear reactions

A **reaction evaluation** is the description of **everything** that can happen from the nuclear reaction between a **projectile** and a **target**

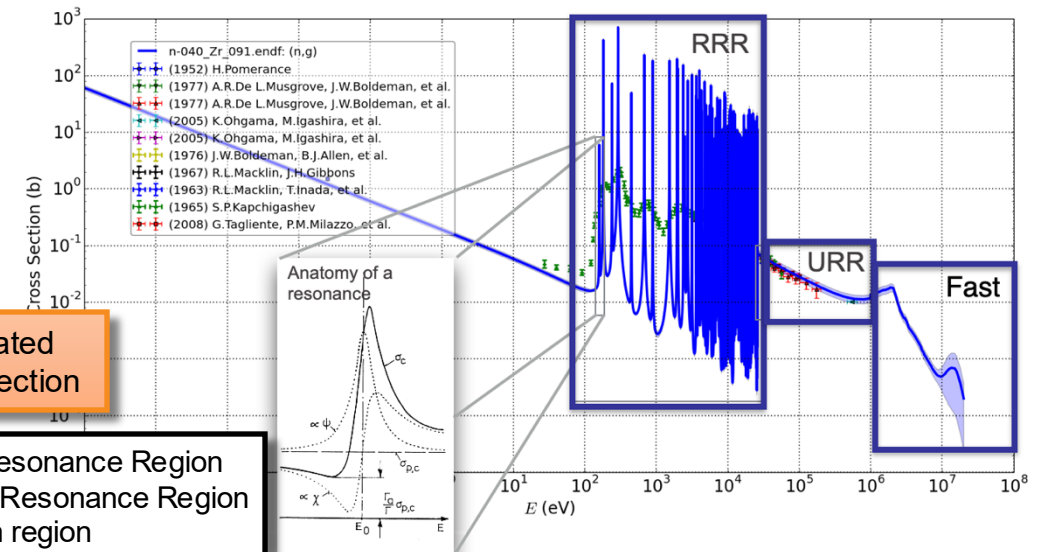
- **Typical neutron incident on non-actinide has ~ 18 relevant reactions**
  - ~ 5 threshold reactions: (n,2n), (n,3n), (n,p), etc.
  - ~ 10 discrete level excitation reactions: (n,n') for each level in residual nucleus
  - 3 non-threshold reactions: (n,tot), (n,el), (n, $\gamma$ )
- **Actinides add fission, (n,f)**
- **For transport studies, need:**
  - Cross sections
  - Multiplicities of all emitted particles
  - Outgoing energy-angle distributions for all emitted particles



Experimental data  
never enough: need  
theory to fill in gaps

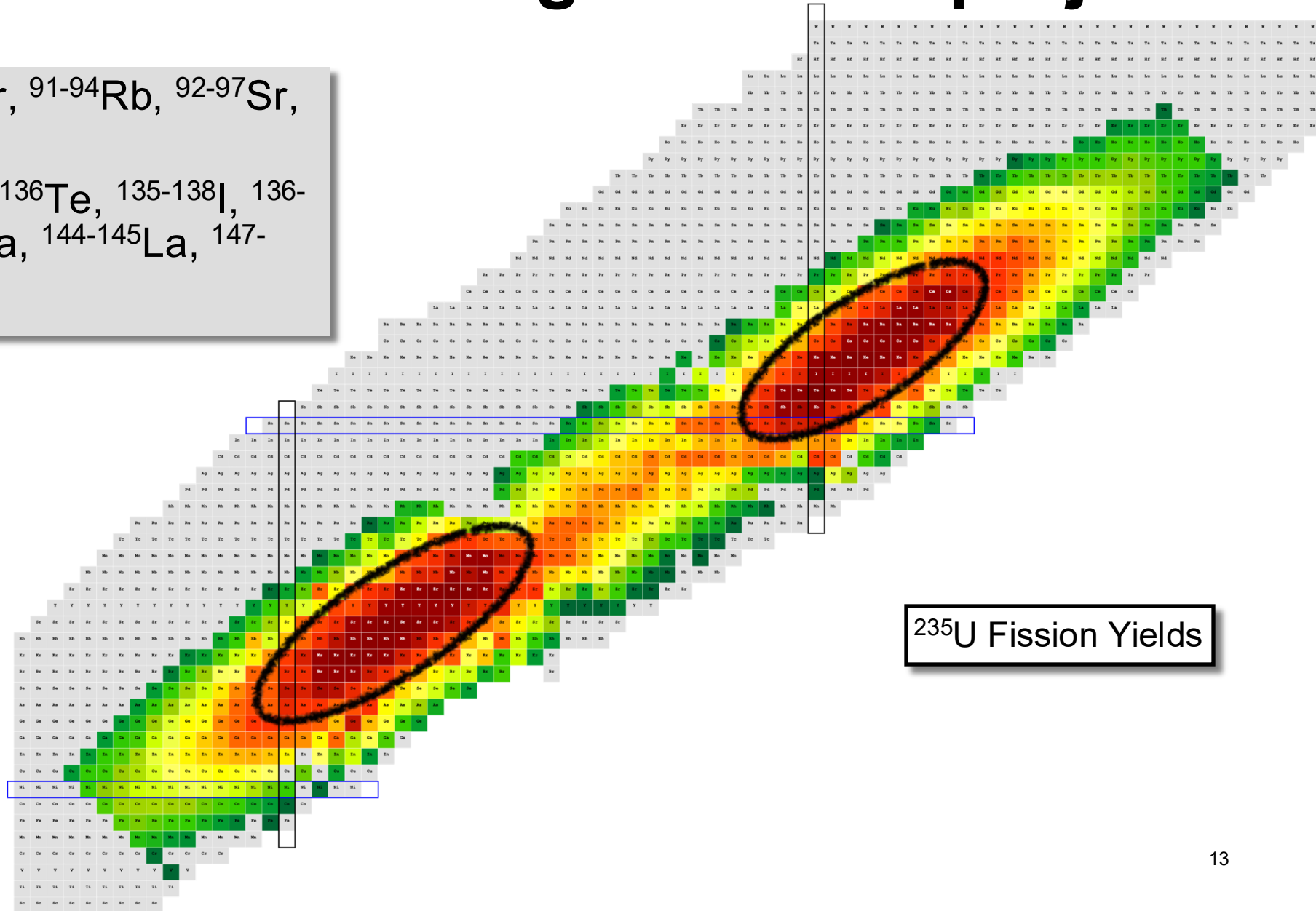
Typical evaluated  
capture cross section

RRR: Resolved Resonance Region  
URR: Unresolved Resonance Region  
Fast: Fast-neutron region



# Which nuclei are we focusing on in this project?

- 1<sup>st</sup> Bump:  $^{87-89}\text{Br}$ ,  $^{88-92}\text{Kr}$ ,  $^{91-94}\text{Rb}$ ,  $^{92-97}\text{Sr}$ ,  $^{95-99}\text{Y}$ ,  $^{97-102}\text{Zr}$ ,  $^{101-103}\text{Nb}$
- 2<sup>nd</sup> Bump:  $^{131-133}\text{Sb}$ ,  $^{132-136}\text{Te}$ ,  $^{135-138}\text{I}$ ,  $^{136-141}\text{Xe}$ ,  $^{139-143}\text{Cs}$ ,  $^{141-146}\text{Ba}$ ,  $^{144-145}\text{La}$ ,  $^{147-148}\text{Ce}$





# Which nuclei are we focusing on in this project?

- 1<sup>st</sup> Bump:  $^{87-89}\text{Br}$ ,  $^{88-92}\text{Kr}$ ,  $^{91-94}\text{Rb}$ ,  $^{92-97}\text{Sr}$ ,  $^{95-99}\text{Y}$ ,  $^{97-102}\text{Zr}$ ,  $^{101-103}\text{Nb}$
- 2<sup>nd</sup> Bump:  $^{131-133}\text{Sb}$ ,  $^{132-136}\text{Te}$ ,  $^{135-138}\text{I}$ ,  $^{136-141}\text{Xe}$ ,  $^{139-143}\text{Cs}$ ,  $^{141-146}\text{Ba}$ ,  $^{144-145}\text{La}$ ,  $^{147-148}\text{Ce}$

Off-stability = few data constraints

Half-lives

# Which nuclei are we focusing on in this project?

- 1<sup>st</sup> Bump:  $^{87-89}\text{Br}$ ,  $^{88-92}\text{Kr}$ ,  $^{91-94}\text{Rb}$ ,  $^{92-97}\text{Sr}$ ,  $^{95-99}\text{Y}$ ,  $^{97-102}\text{Zr}$ ,  $^{101-103}\text{Nb}$
- 2<sup>nd</sup> Bump:  $^{131-133}\text{Sb}$ ,  $^{132-136}\text{Te}$ ,  $^{135-138}\text{I}$ ,  $^{136-141}\text{Xe}$ ,  $^{139-143}\text{Cs}$ ,  $^{141-146}\text{Ba}$ ,  $^{144-145}\text{La}$ ,  $^{147-148}\text{Ce}$

Off-stability = few data constraints

Many are (highly-)deformed!

$E_{4+} / E_{2+}$   
(Indication of deformation)

# Approach in fast region



# Employing a more predictive approach for deformed nuclei: Adiabatic model

Adiabatic approach:

A very non-rigorous description

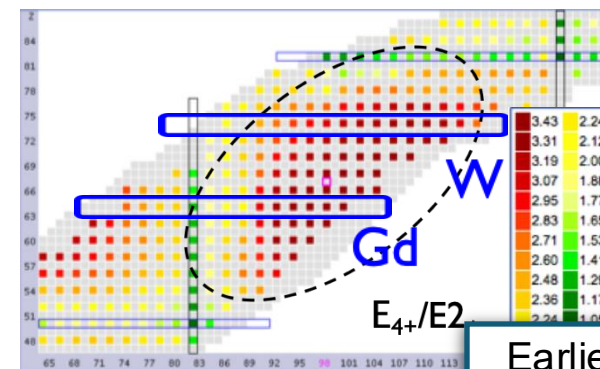
$$H_{\text{deformed}} = H_{\text{spherical}} + H_{\text{rotational}}$$

Spher. OMP      CC rot. band

Fitted parameters

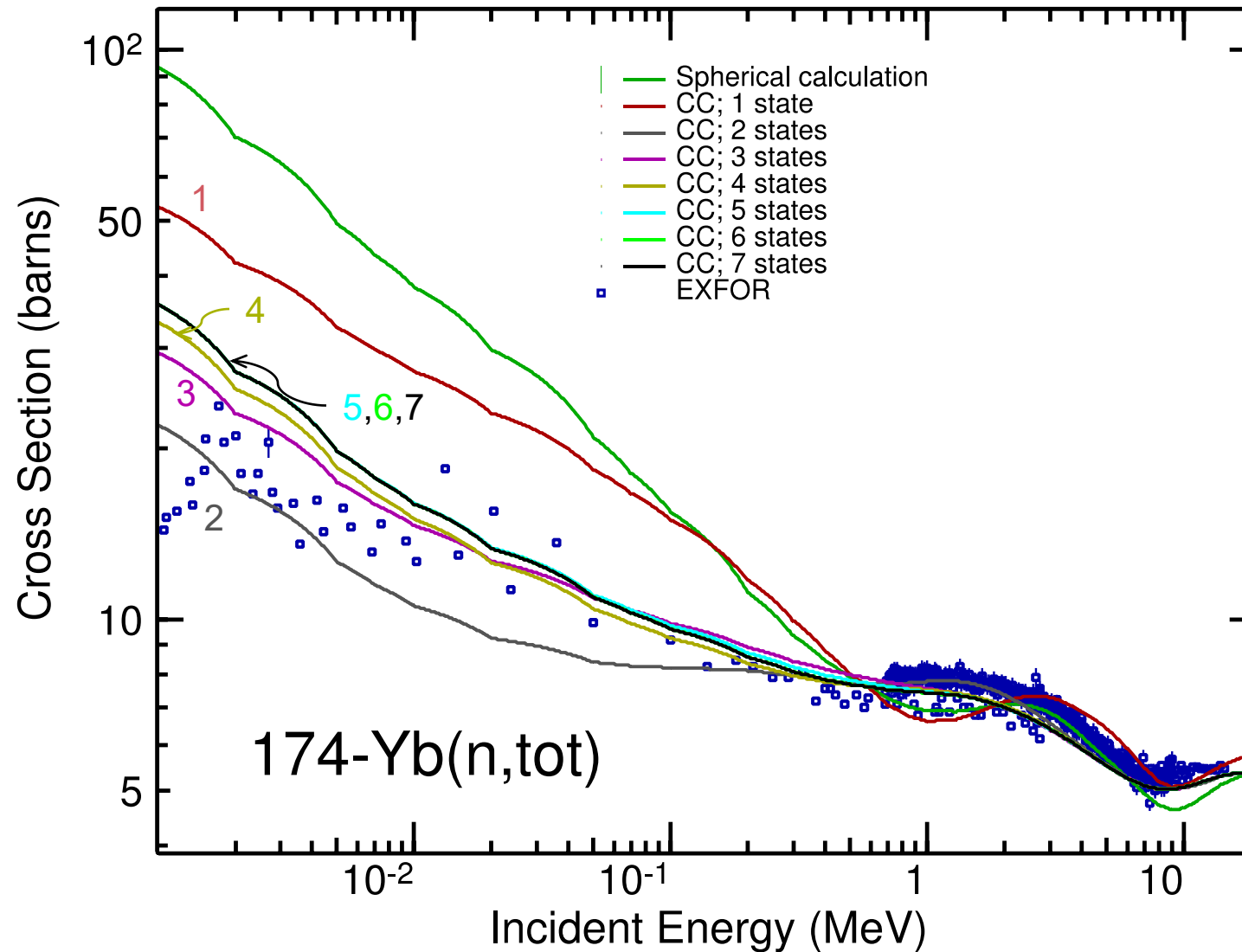
## Motivation:

- Predictive theory helps reaction research, evaluations and applications
  - Extrapolation to regions where data is scarce
  - Mitigate compensation of errors
- Lack of existing regional optical potentials for statically deformed nuclei
- Many fission products are deformed nuclei



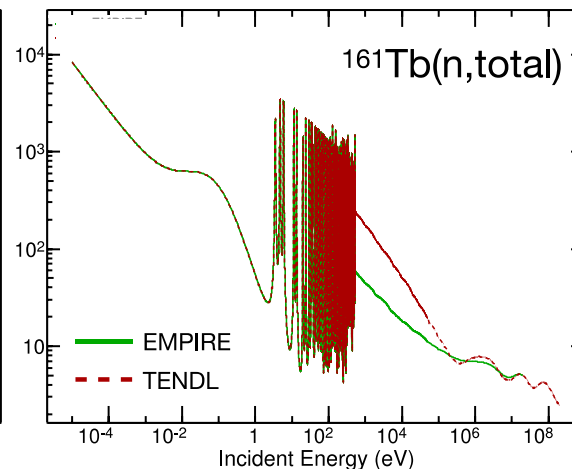
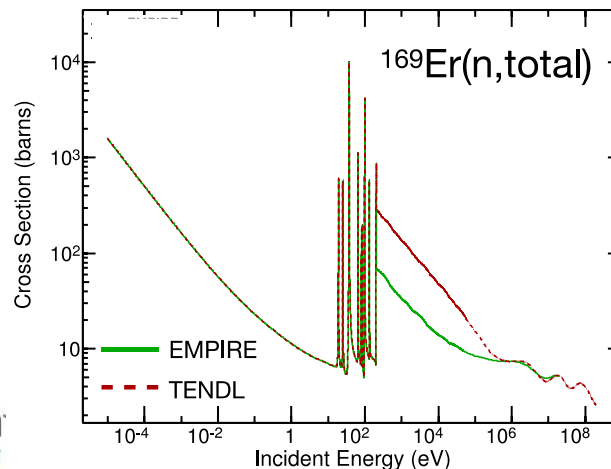
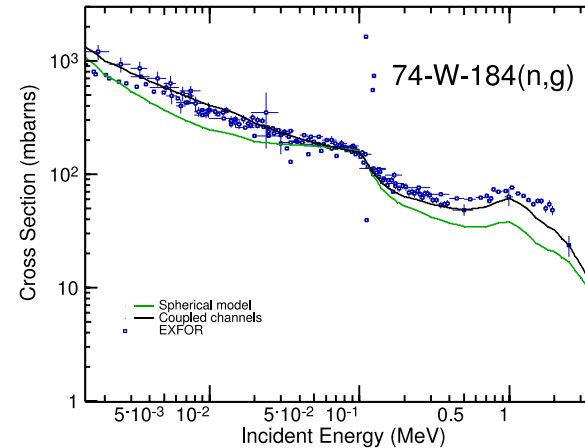
Earlier works had shown that scattering from highly deformed nuclei is near adiabatic limit, thus deforming a spherical global potential may be suitable with only minor modifications.

# Convergence on number of channels



# Fast region: We will leverage previous experience with deformed nuclei

- Predictive: takes as input
  - An spherical OMP
  - Deformation paramters
- Deformation treatment changes total/elastic cross sections by orders of magnitude
- Indirectly impacts capture



PHYSICAL REVIEW C **91**, 024618 (2015)  
**Derivation of an optical potential for statically deformed rare-earth nuclei from a global spherical potential**

G. P. A. Nobre,\* A. Palumbo, M. Herman, D. Brown, and S. Hoblit  
 National Nuclear Data Center, Brookhaven National Laboratory, Upton, New York 11973-5000, USA

F. S. Dietrich  
 P.O. Box 30423, Walnut Creek, California 94598, USA  
 (Received 23 December 2014; published 25 February 2015)

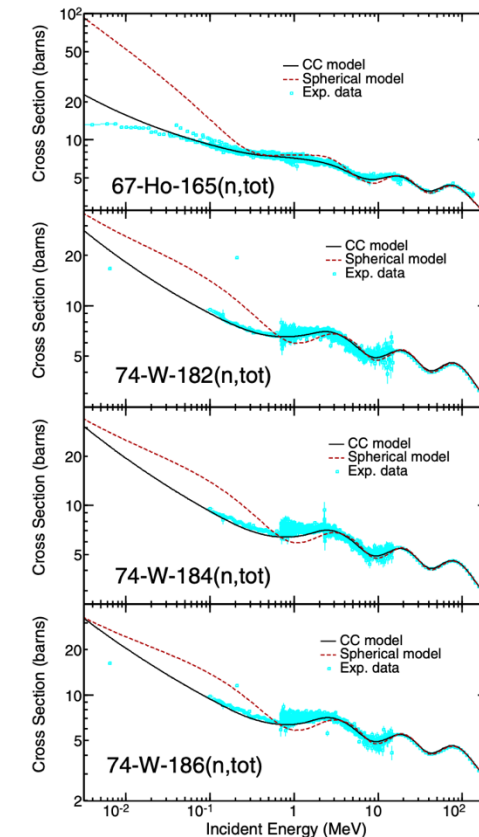
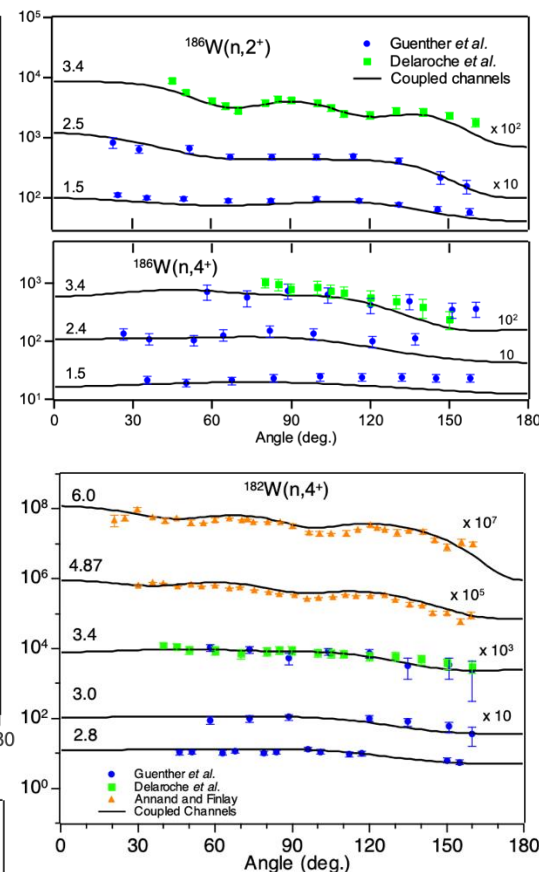
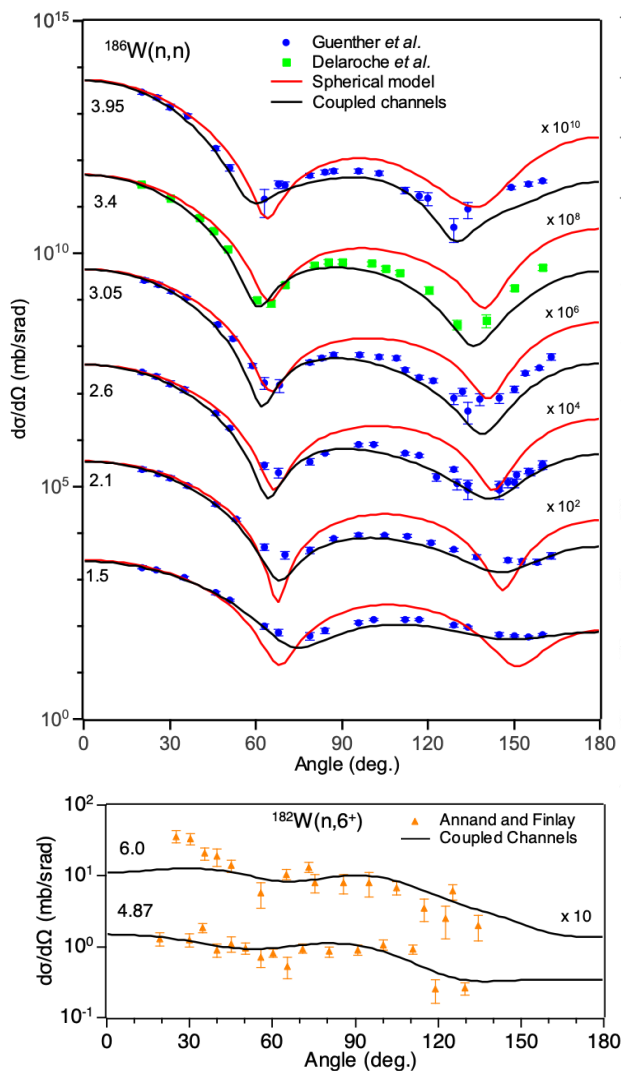
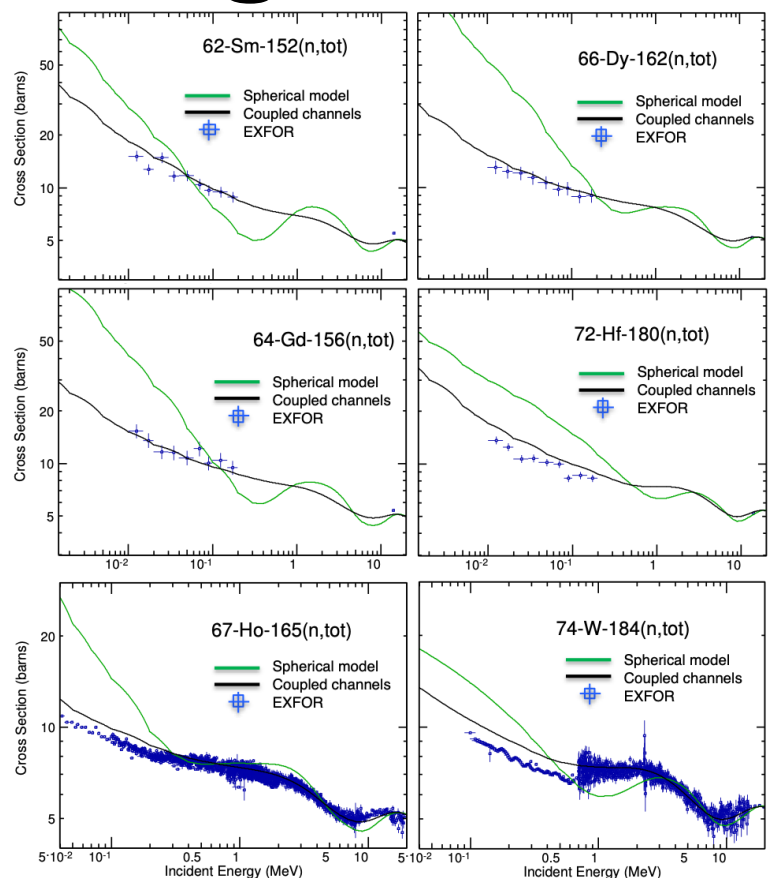


FIG. 1. (Color online) Total cross sections for neutrons scattered by a  $^{165}\text{Ho}$  and  $^{182,184,186}\text{W}$  targets for incident energies ranging from as low as  $\approx 3$  keV to as high as 200 MeV, which is the upper limit of validity for the KD optical potential [2]. The solid black curves correspond to the predictions of our CC model, while the dashed red curves are the results of calculations within the spherical model. The experimental data were taken from the EXFOR nuclear data library [39].



# Good agreement with data!



The fact that deforming KD allows to consistently describe observed total cross section and elastic and inelastic angular distributions remarkably well is very supportive of the model and of the adiabatic approximation.

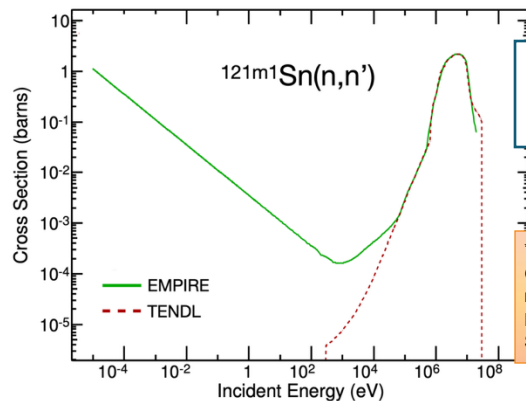
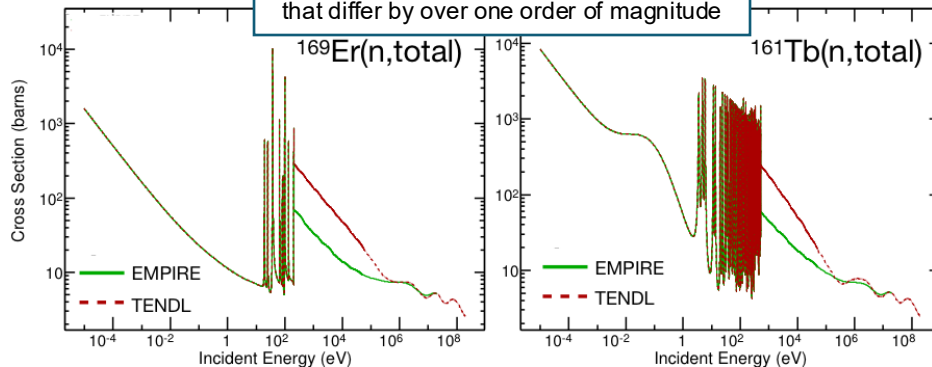
## More on this:

- G.P.A. Nobre *et al.*, Physical Review C 91, 024618 (2015),
- G.P.A. Nobre *et al.*, AIP Conf. Proc. 1625, 45 (2014),
- M.W. Herman *et al.*, EPJ Web of Conf. 69, 00007 (2014),
- G.P.A. Nobre *et al.*, Nuclear Data Sheets 118 (2014) 266-269

# Extending to unstable nuclei

- This approach was applied to evaluations of unstable nuclei: 74+ evaluations accepted into ENDF/B-VIII.0\*
- Activation studies require reliable cross section knowledge for unstable nuclei and long-lived isomers, as well as all the nuclides in the decay chain towards stability
- Machine Learning techniques can be used to train the system to choose the best set of models and parametrization in each case

Different models can predict cross sections that differ by over one order of magnitude



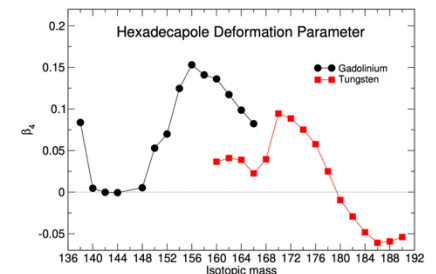
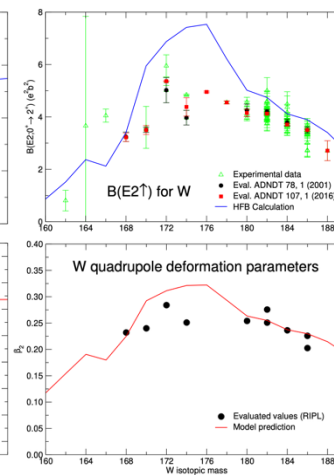
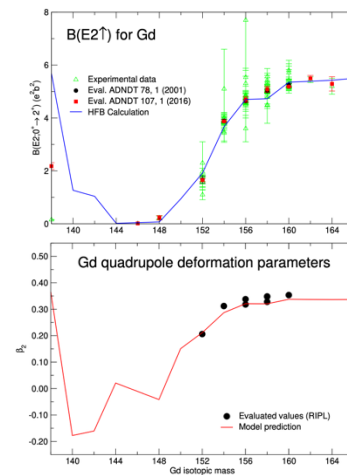
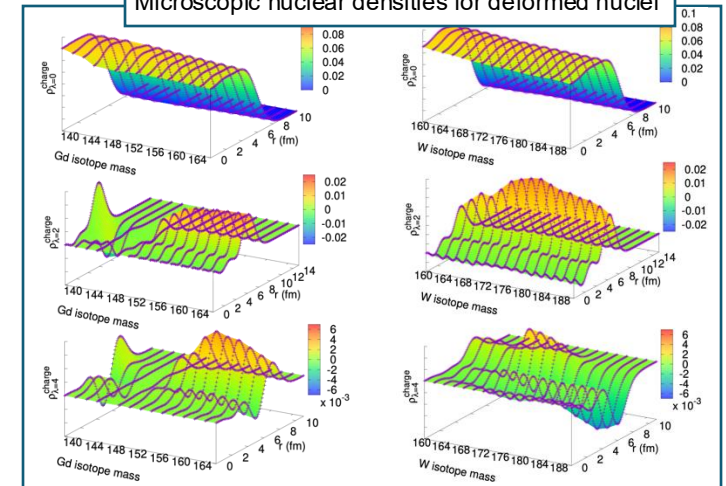
Proper treatment of reactions with isomeric projectiles

References:  
G. P. A. Nobre *et al.*, BNL technical report BNL-114256-2017-IR.  
D. A. Brown *et al.*, Nuclear Data Sheets 148, (2018) 1



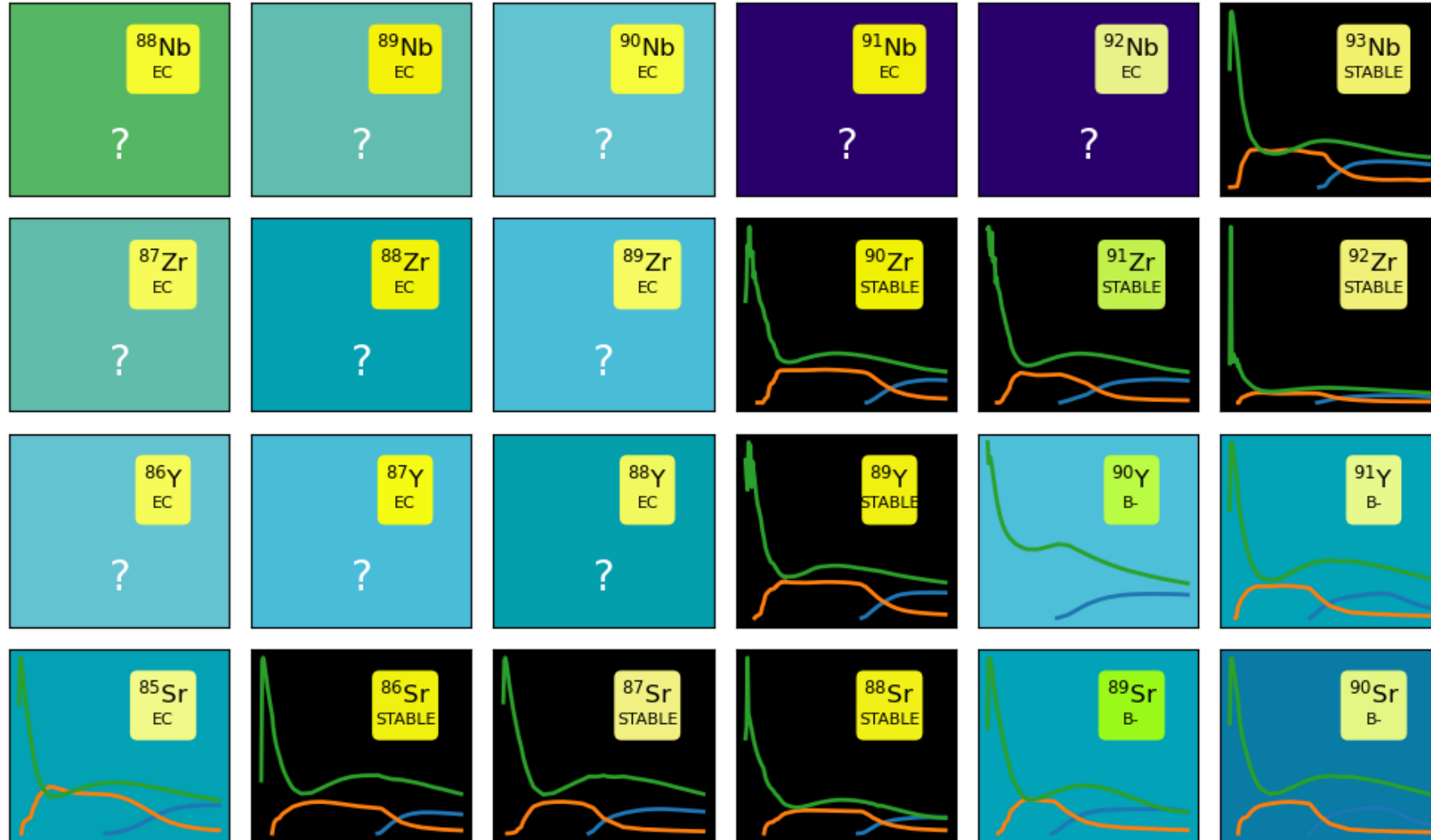
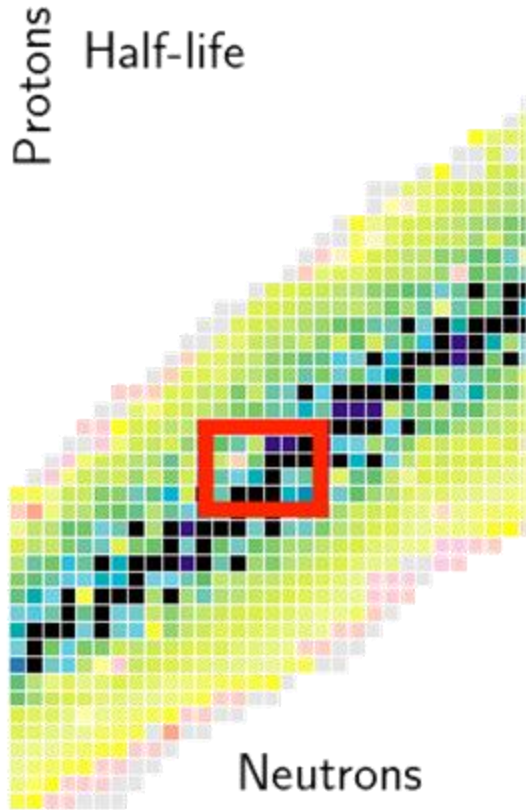
Previous exploration into extending approach to rare-earths off stability

Microscopic nuclear densities for deformed nuclei



Using microscopic HFB densities to make predictions of deformation parameters off stability.

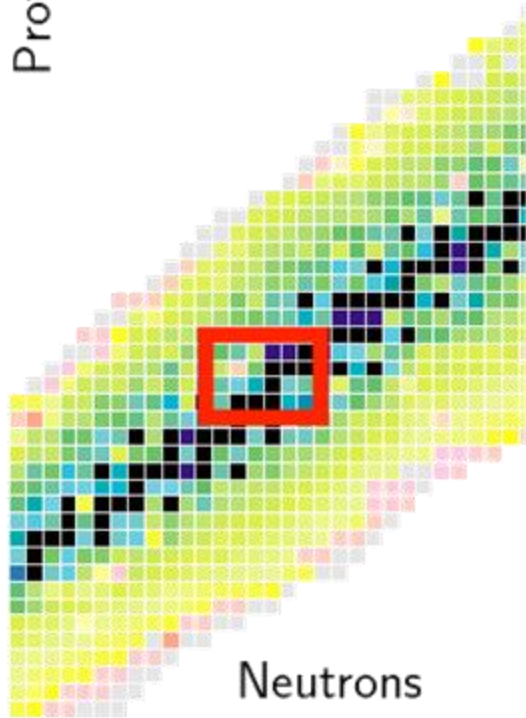
# Under LDRD at LLNL, we are using existing calculations and measurements to learn how cross sections transform across the nuclear chart



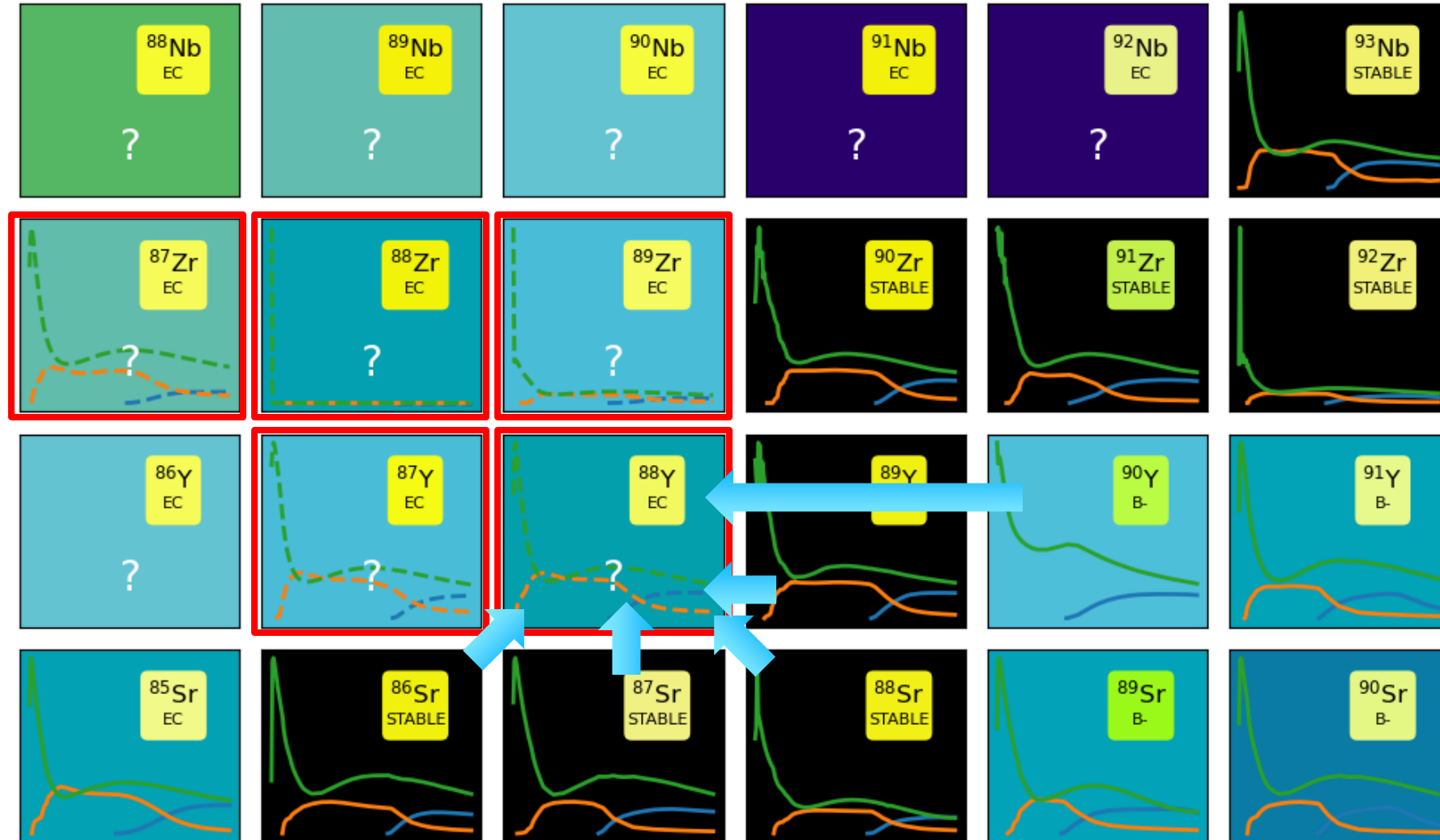
# Under LDRD at LLNL, we are using existing calculations and measurements to learn how cross sections transform across the nuclear chart

Protons

Half-life

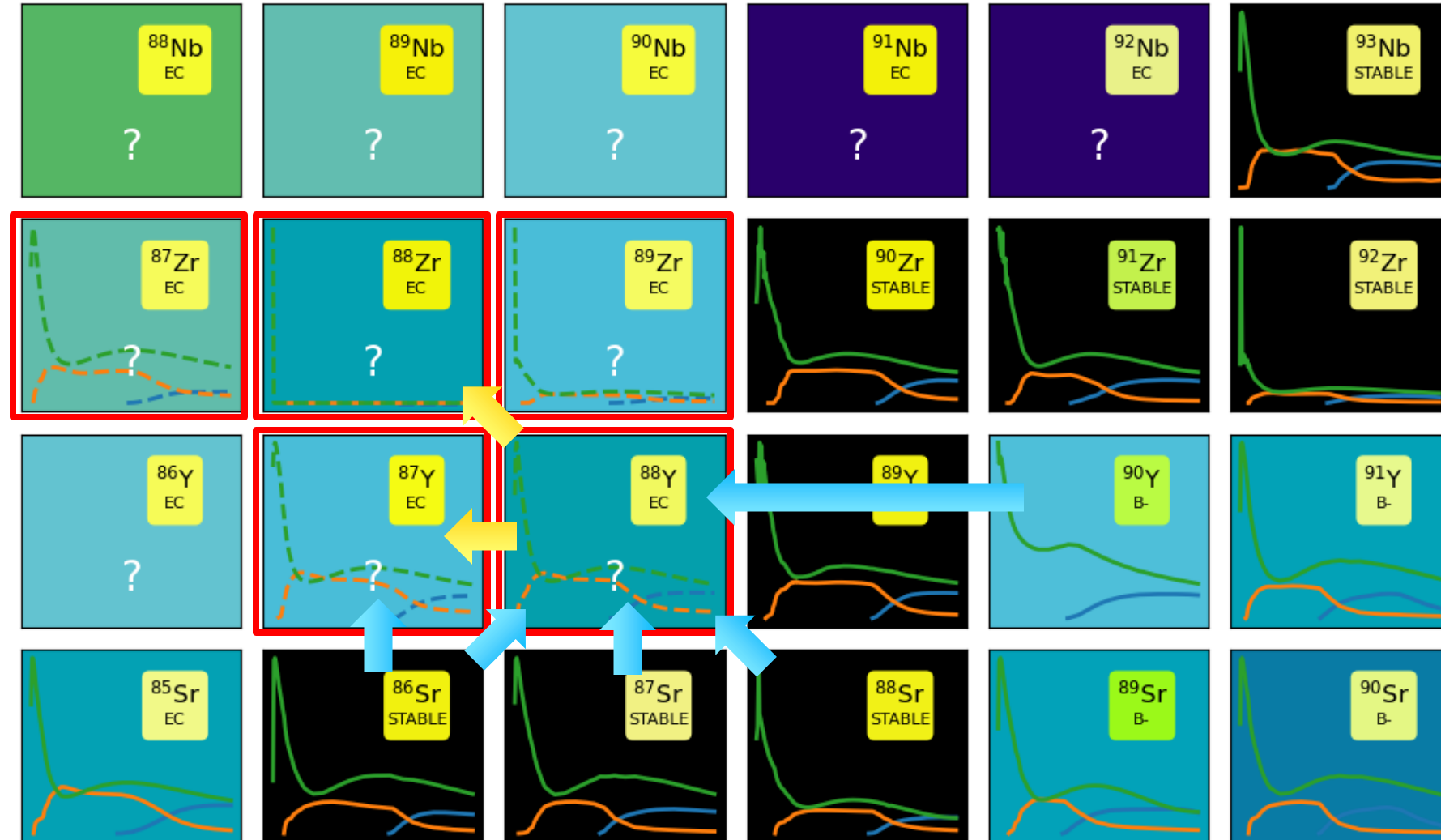
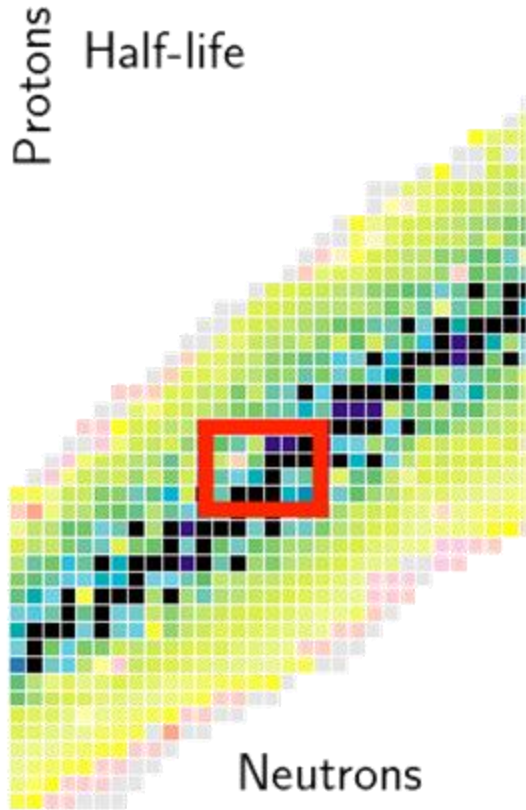


Neutrons



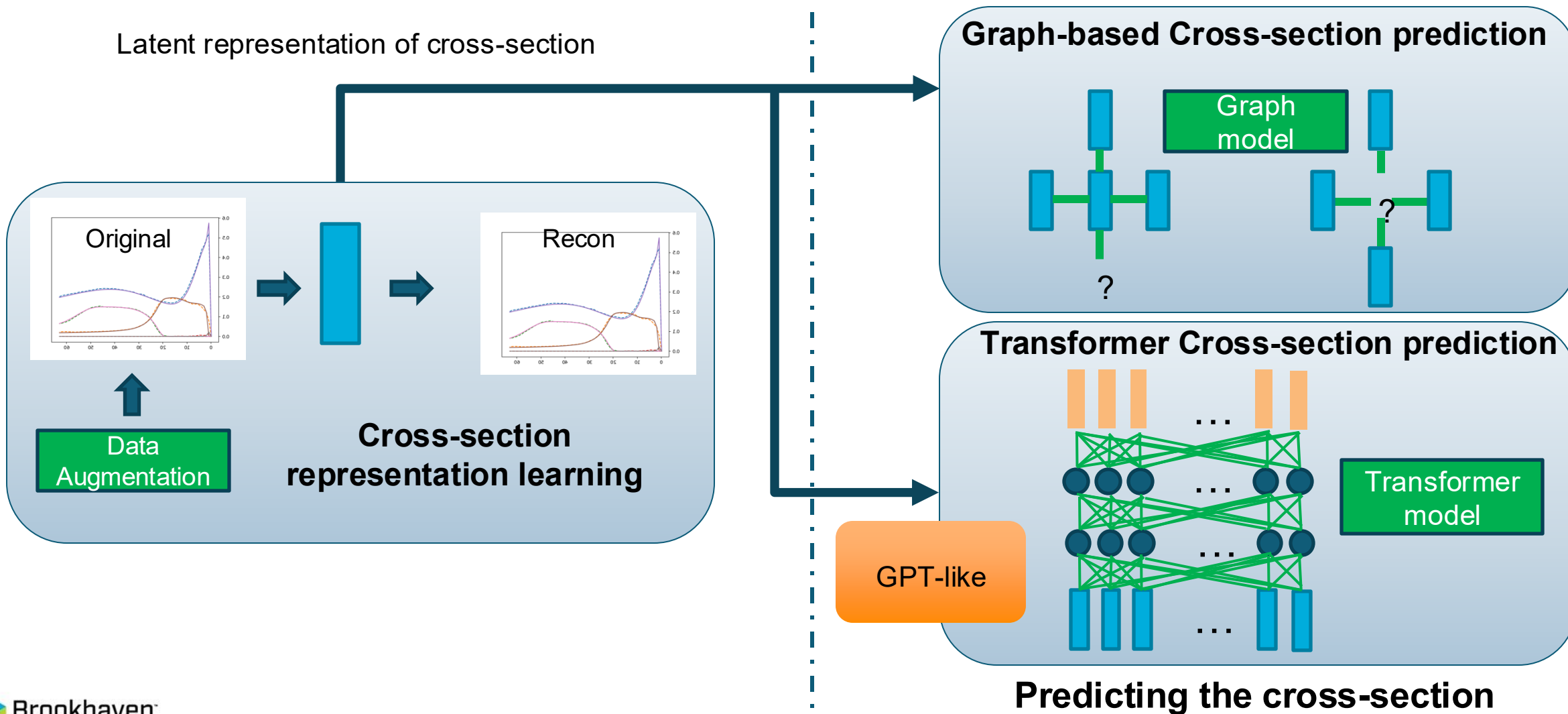


We will leverage the tools from this LDRD to provide “systematic” priors for evaluations on unstable nuclei.

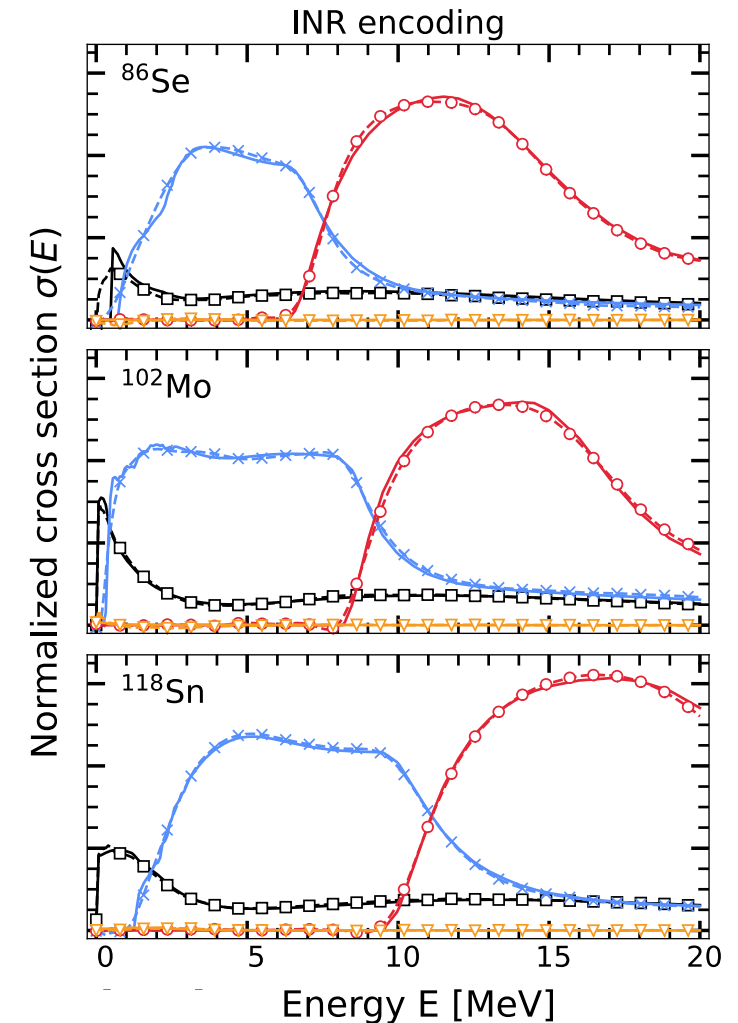
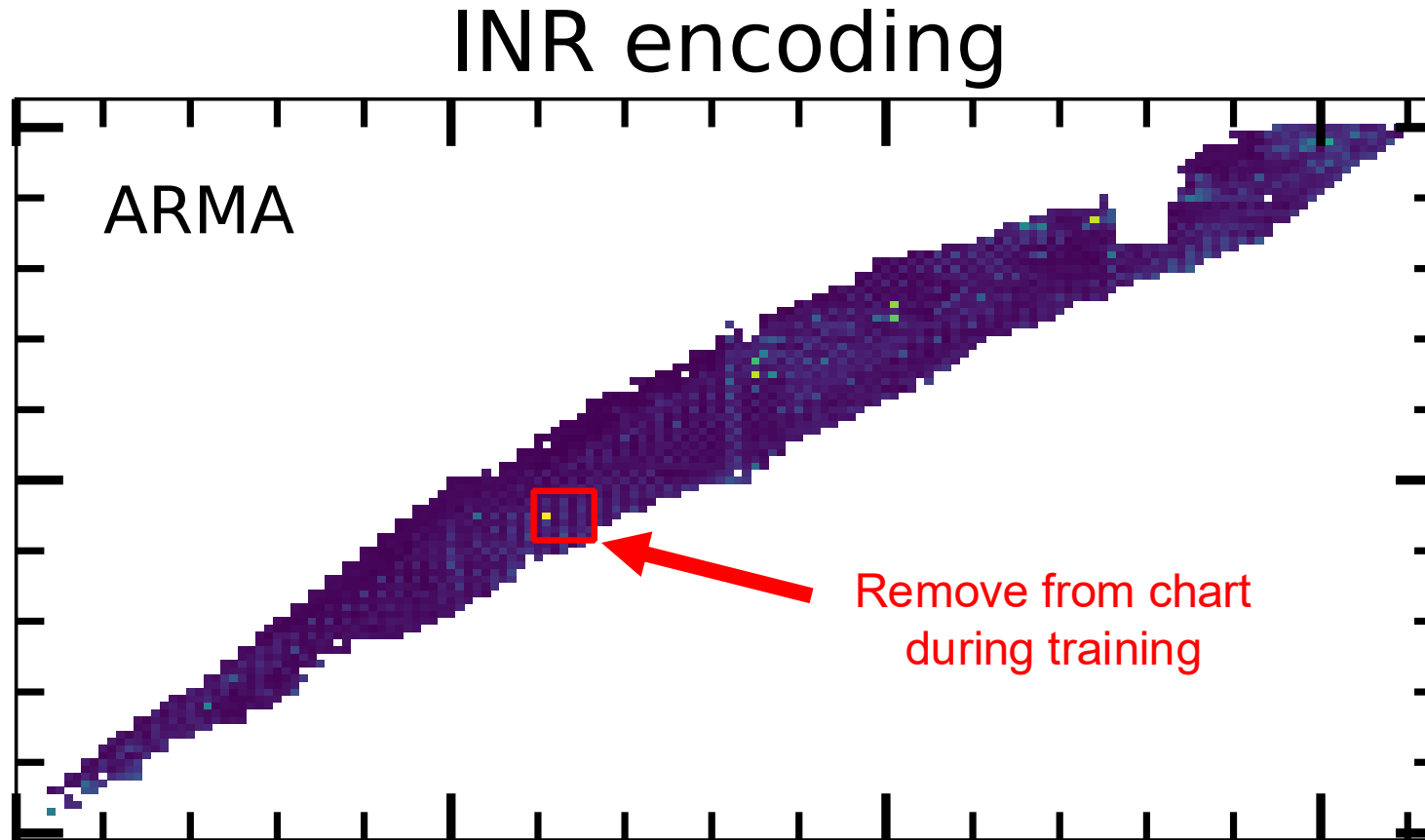


# We have developed a framework for learning and predicting cross sections across the chart.

Representation learning



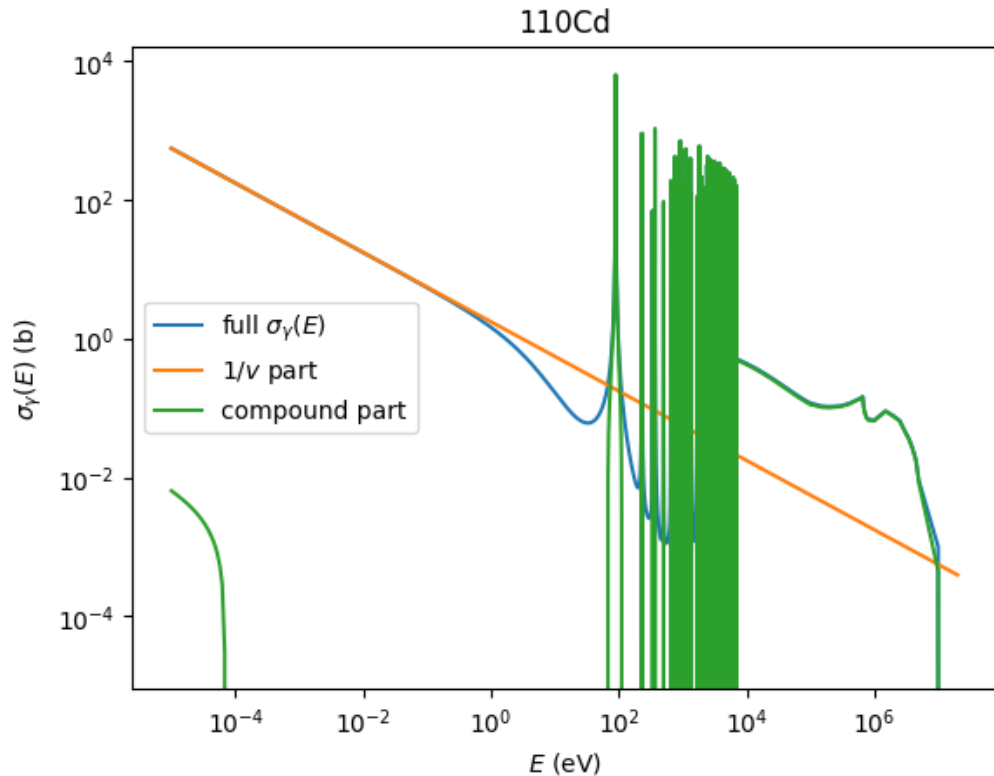
# Graph framework can precisely infer missing data



# Approach in resonance region



# Capture cross-sections at low energies



Capture cross-sections have

- A 1/v part – the shape is analytic, the magnitude must be measured
- A compound nuclear part consisting of many resonances
- A smooth high-energy part that peaks around 14 MeV with  $\sigma \sim 100$  mb

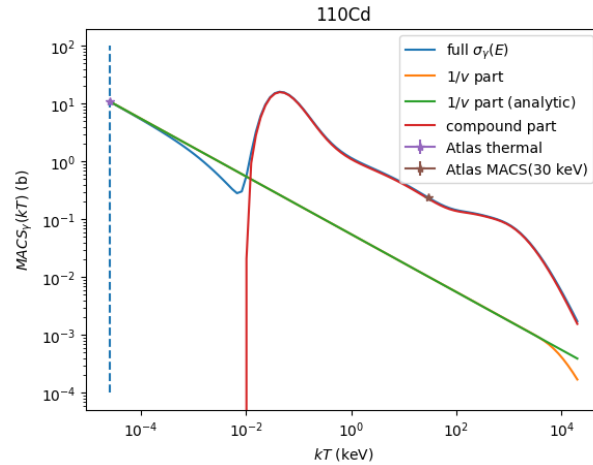
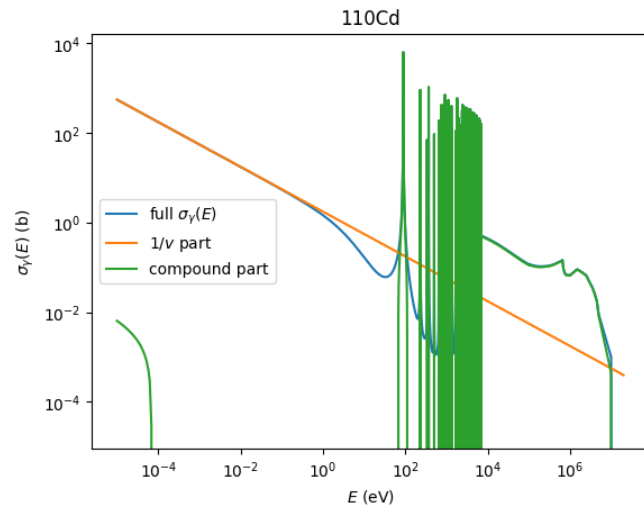
Practical division:

$$\sigma_\gamma(E) = \underbrace{\sigma_{th} \sqrt{\frac{E_{th}}{E}}}_{\text{Thermal component}} + \underbrace{\sigma_{CN}(E)}_{\text{Compound nucleus component}}$$

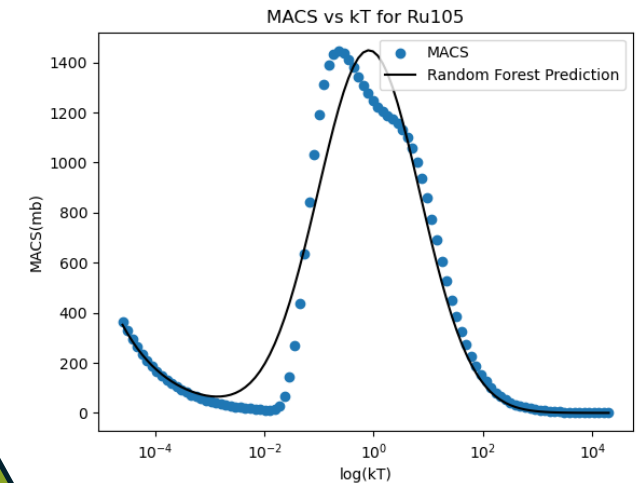
- There are **too many** resonances.
- It is **not possible** to predict their position or width
- We focus on an “average” cross section and some probability distribution that captures the size of fluctuations

# Capture cross-section average values

Build reduced order model of MACS



Learn parametric (Z,A) dependence of reduced order model



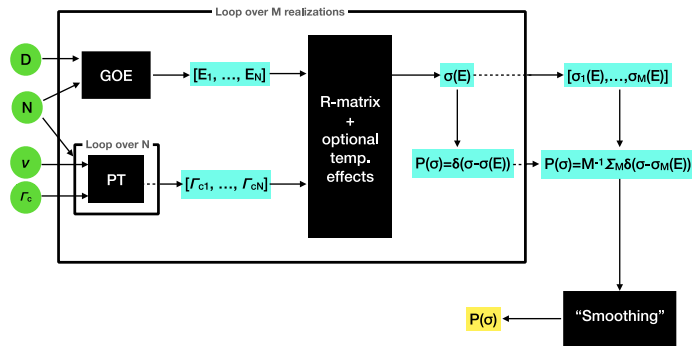
Leveraging preliminary work under NA-22 Intentional Forensics Venture

Test against original cross-sections or MACS

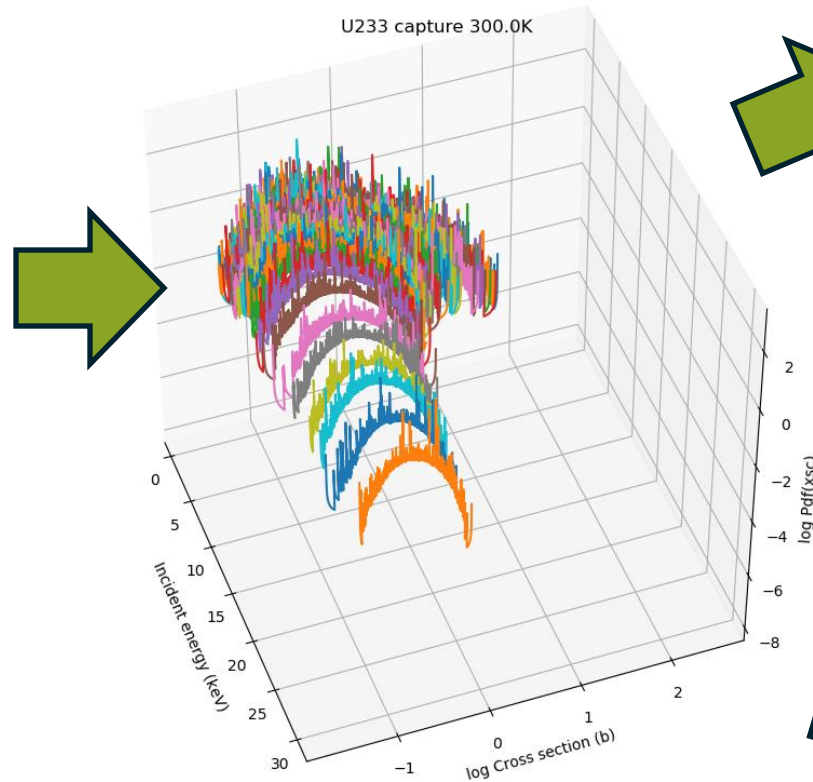
*“magic” function*  
 $\sigma_\gamma(Z,A,E)$

Transform model back to cross-section space

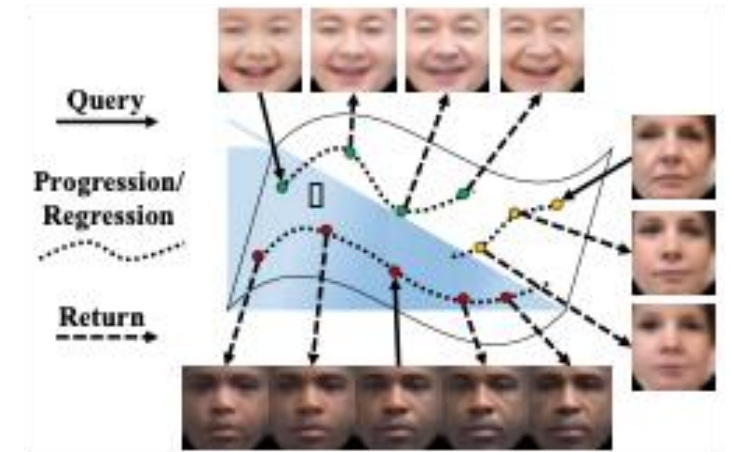
# Capture cross-section fluctuations



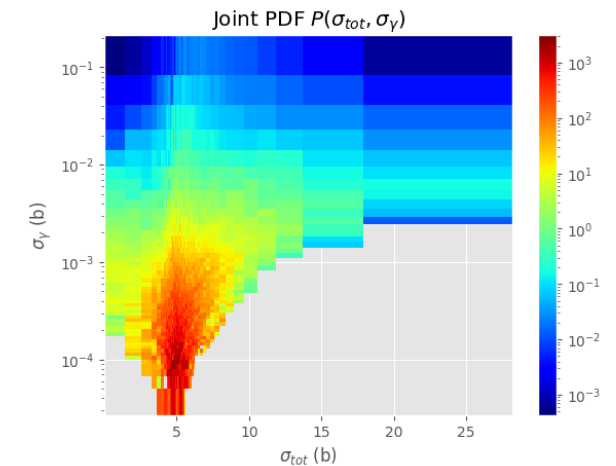
Use FUDGE as a generative model to simulate cross-section probability distribution function (PDF)



$^{238}\text{U}(n,g)$  cross-section PDF



Use age-progression software to learn the temperature (and energy?) dependence of the cross-section PDF



Alternatively, we can use the PDFs directly with estimates of RRR spacings & widths

Leveraging preliminary work under NCSP AM-6

# Experimental constraints: Nuclear Level Densities



# Experimental level density constraints at Edwards lab, Ohio University

**Goal:** to improve systematics of the level density model parameters in the mass region of fission products thereby enhancing the **predictive power** of level density models for nuclear data evaluations when **extrapolating to nuclei off stability**.

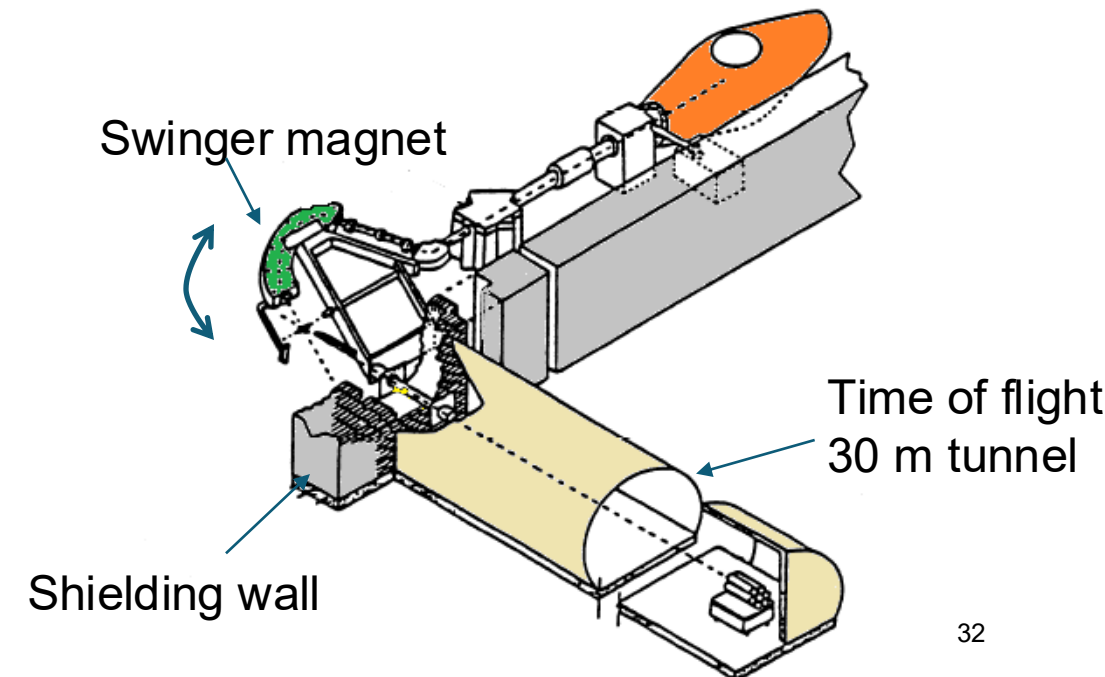
## Method:

- to review and validate available literature data on level densities measured with the different techniques over the mass range of the fission products (about 20 data sets are available).
- to address gaps in level density systematics by conducting targeted experiments at the Edwards Lab and benchmark models against experimental data

Swinger magnet

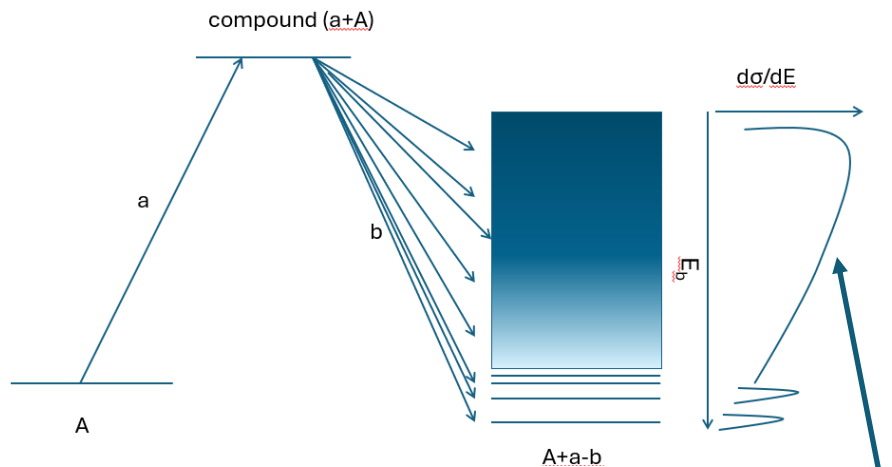


Accelerator



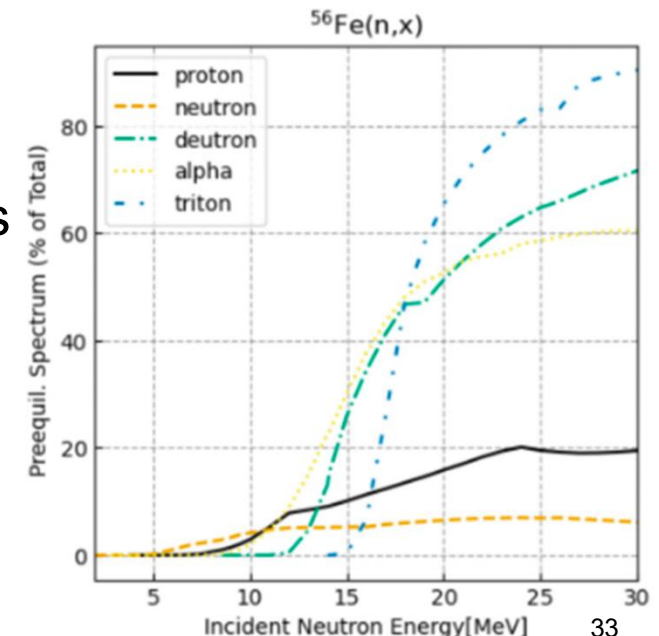
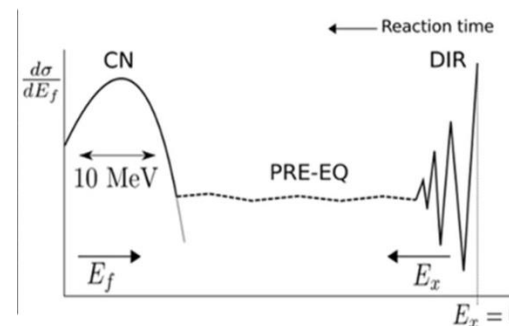
# Particle evaporation technique to study level densities at the Edwards Lab

1. Create a reaction which proceeds through the compound reaction mechanism. This implies selecting appropriate beam species and energies.
2. Differential spectra of particles emitted from compound reactions depends on level density of nuclei populated.



We will use (p,n) reactions to measure neutron  $d\sigma/dE$  spectra

- **Preequilibrium** emissions become dominant at high energies
- We will use experimental information to constrain microscopic PE models
- Increase confidence in the description at stable isotopes before applying to unstable ones



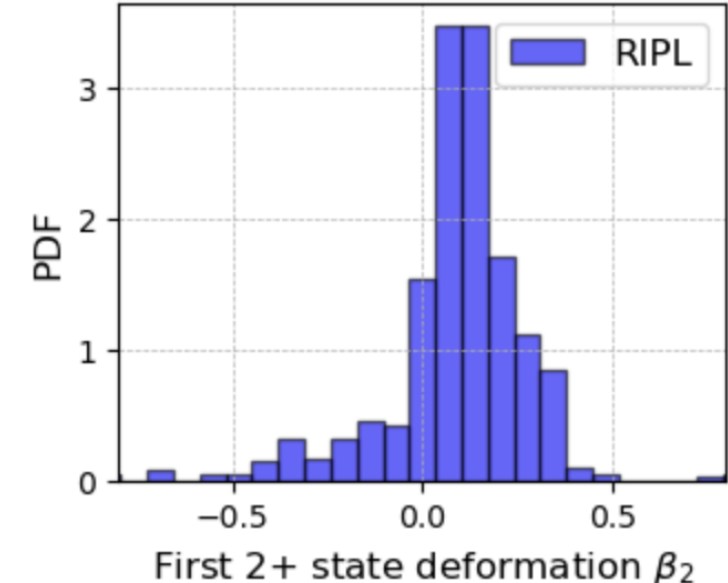
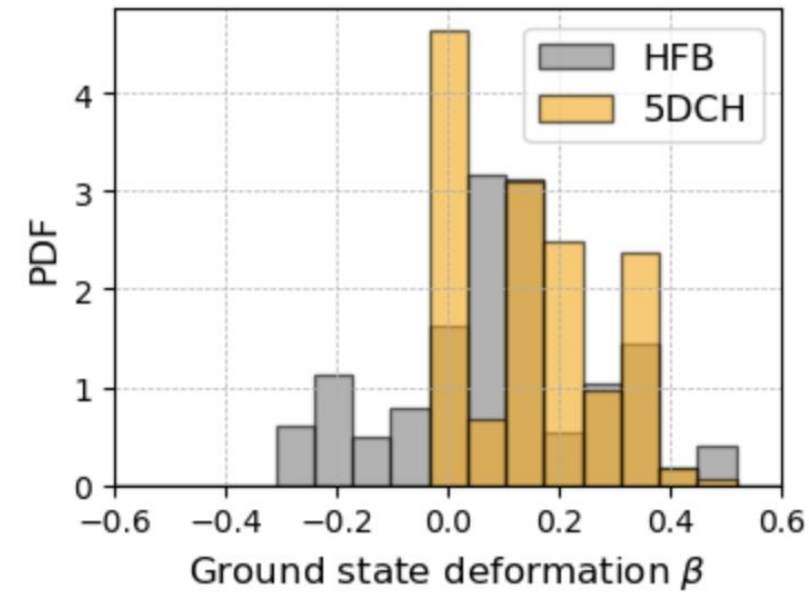
# Status and perspectives

# Current status

- In the 1<sup>st</sup> year (out of 3), most effort was dedicated to coordination and laying out groundwork
- Most of technical effort has focused on
  - Building the infrastructure
    - Creating (multiple) database(s) of nuclear deformations
    - Script to create EMPIRE inputs for all relevant nuclei and run them on the NNDC cluster
  - First experimental campaign
    - Measurement of  $^{96}\text{Zr}(p,n)$  evaporation neutron spectra
    - Data analysis

# Nuclear deformation database

- Collected and organized information on nuclear deformations for different approaches:
  - CEA [1]
    - Nuclear structure deformation parameters Hartree-Fock-Bogoliubov (HFB) and Gogny Force (DS1). This self-consistent mean-field approach incorporates pairing correlations and is commonly used in microscopic nuclear structure modeling.
    - Nuclear structure deformation parameters computed using the Five-Dimensional Collective Hamiltonian (5DCH) including triaxial deformations.
  - RIPL-3 [2]
    - Recommended deformation parameters for nuclear levels from optical model section
    - Ground state properties calculated within the Finite Range Droplet Model (FRDM 1995), from the masses section



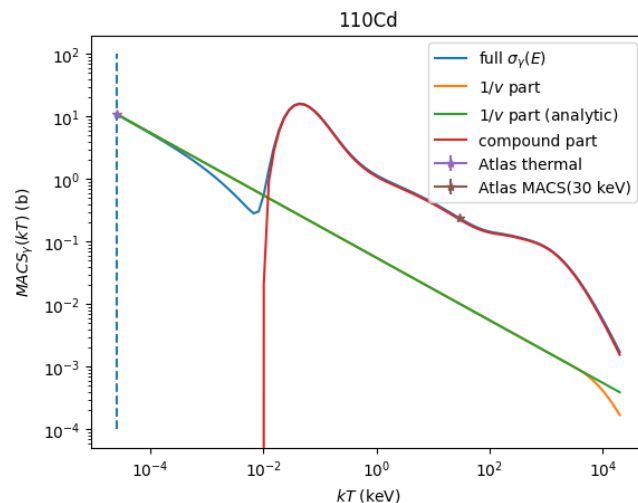
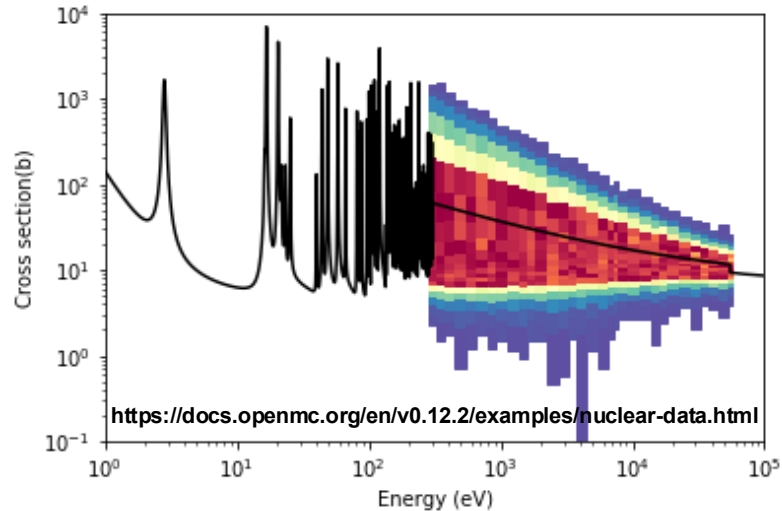


# Data infrastructure

- Collected information for all of the 900+ nuclides relevant to the project and organized them by goal priority, Z, A, half-life, prior existence in the ENDF/B library
- Assessed experimental data availability
  - for the nuclei in the primary goal list, we investigated the existence of any experimental data in the EXFOR compilation
  - We found, as expected, that there are none for the vast majority, with only a few exceptions consisting basically of derived Maxwellian Averaged Cross Sections (MACS)
  - In the future, we may expand this to all nuclei across the priority goals.
- Wrote a main script to cycle through the relevant nuclei
  - Generate EMPIRE inputs
  - Run and generate fast-region ENDF-6 files
  - Still needs to be fully integrated with deformation library and with ML priors

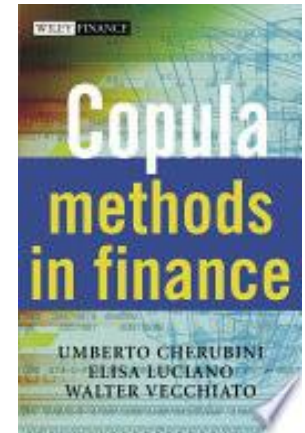
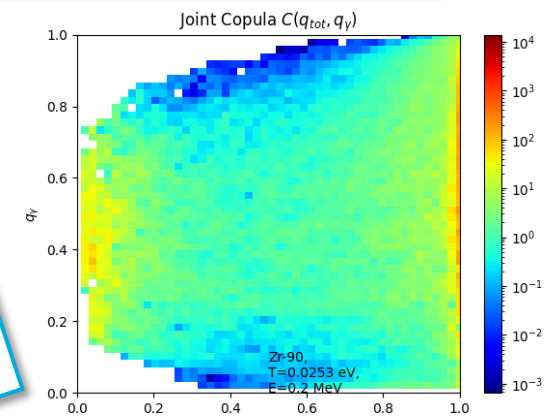
# Developments in resonance range

If we “don’t know anything” we must treat the problem probabilistically



- Developing model for MACS functional

- Exploring the alternative approaches from the usual probability tables
- Replaces PDF by cumulative functions: copula



Cherubini, Luciano, Vecchiato.  
*Copula Methods in Finance*.  
John Wiley & Sons, Ltd, 2004

See D. Brown's  
talks at ND 2025

Estimation of Maxwellian averaged cross-sections with machine learning methods

David Brown<sup>a</sup>, Christian Stanley<sup>b</sup>,  
Amber Lauer-Coles<sup>c</sup>, Daniel  
Quinter<sup>d</sup>, Emanuel Chimanski<sup>e</sup>

<sup>a</sup> NNDC, Brookhaven National Laboratory, USA  
<sup>b</sup> Indiana University, USA  
<sup>c</sup> Savannah River National Laboratory, USA  
<sup>d</sup> Stony Brook University, USA

Tests of the probability table method for unresolved resonances

David Brown<sup>a</sup>, Gustavo Nobre<sup>a</sup>,  
Matteo Vorabbi<sup>a,b</sup>, Marie-Anne Descalle<sup>c</sup>,  
Caleb Mattoon<sup>a</sup>, Bret Beck<sup>d</sup>, Godfree Gert<sup>e</sup>

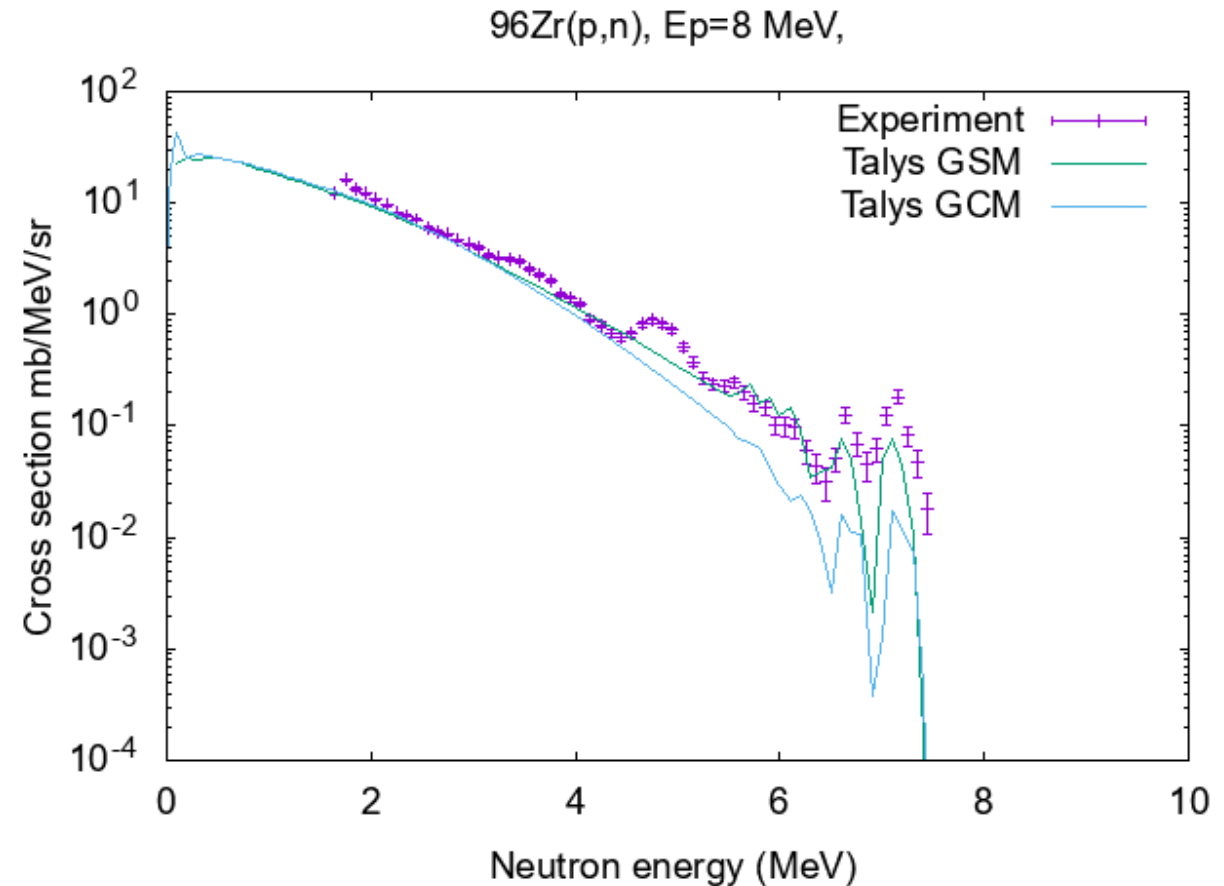
<sup>a</sup> NNDC, Brookhaven National Lab, USA  
<sup>b</sup> University of Surrey, UK  
<sup>c</sup> Lawrence Livermore National Lab, USA

2025

2025

# Level density measurement

- First experimental campaign at Ohio University
  - Measurement of  $^{96}\text{Zr}(p,n)$  evaporation neutron spectra
  - Data analysis revealed peaks coming from  $^{92}\text{Zr}$  present in the  $^{96}\text{Zr}$ -enriched sample
  - Additional measurement of  $^{92}\text{Zr}(p,n)$  to quantify the contamination in the  $^{96}\text{Zr}$  measurement.



# Perspectives

- Tasks underway or soon-to-be initiated:
  - Generate a pool of training data for resonance region
  - Library of ML-extrapolated cross-section priors
  - Generation of preliminary evaluated files
- Challenges in defining validation possibilities
  - Spent fuel
  - Depletion
  - Astrophysics
  - ?
- Feedback, especially regarding model approaches and validation are appreciated

# Acknowledgements

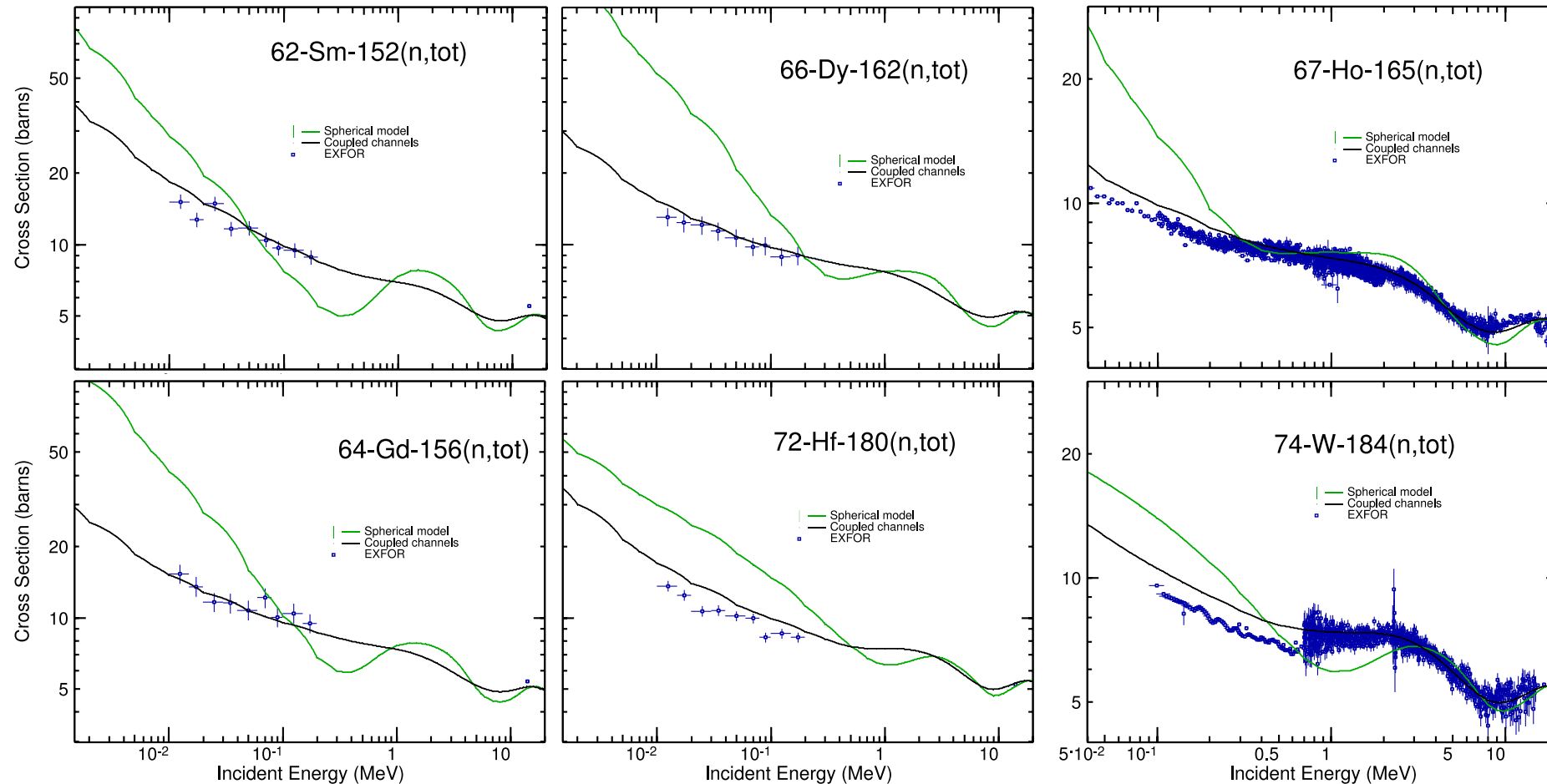
This work was supported by the Office of Defense Nuclear Nonproliferation Research and Development within the U.S. Department of Energy's National Nuclear Security Administration. This work was supported by the Nuclear Criticality Safety Program, funded and managed by the National Nuclear Security Administration for the U.S. Department of Energy. Additionally, work at Brookhaven National Laboratory was sponsored by the Office of Nuclear Physics, Office of Science of the U.S. Department of Energy under Contract No. DE-SC0012704 with Brookhaven Science Associates, LLC. This project was supported in part by the Brookhaven National Laboratory (BNL), National Nuclear Data Center under the BNL Supplemental Undergraduate Research Program (SURP) and by the U.S. Department of Energy, Office of Science, Office of Workforce Development for Teachers and Scientists (WDTS) under the Science Undergraduate Laboratory Internships Program (SULI).





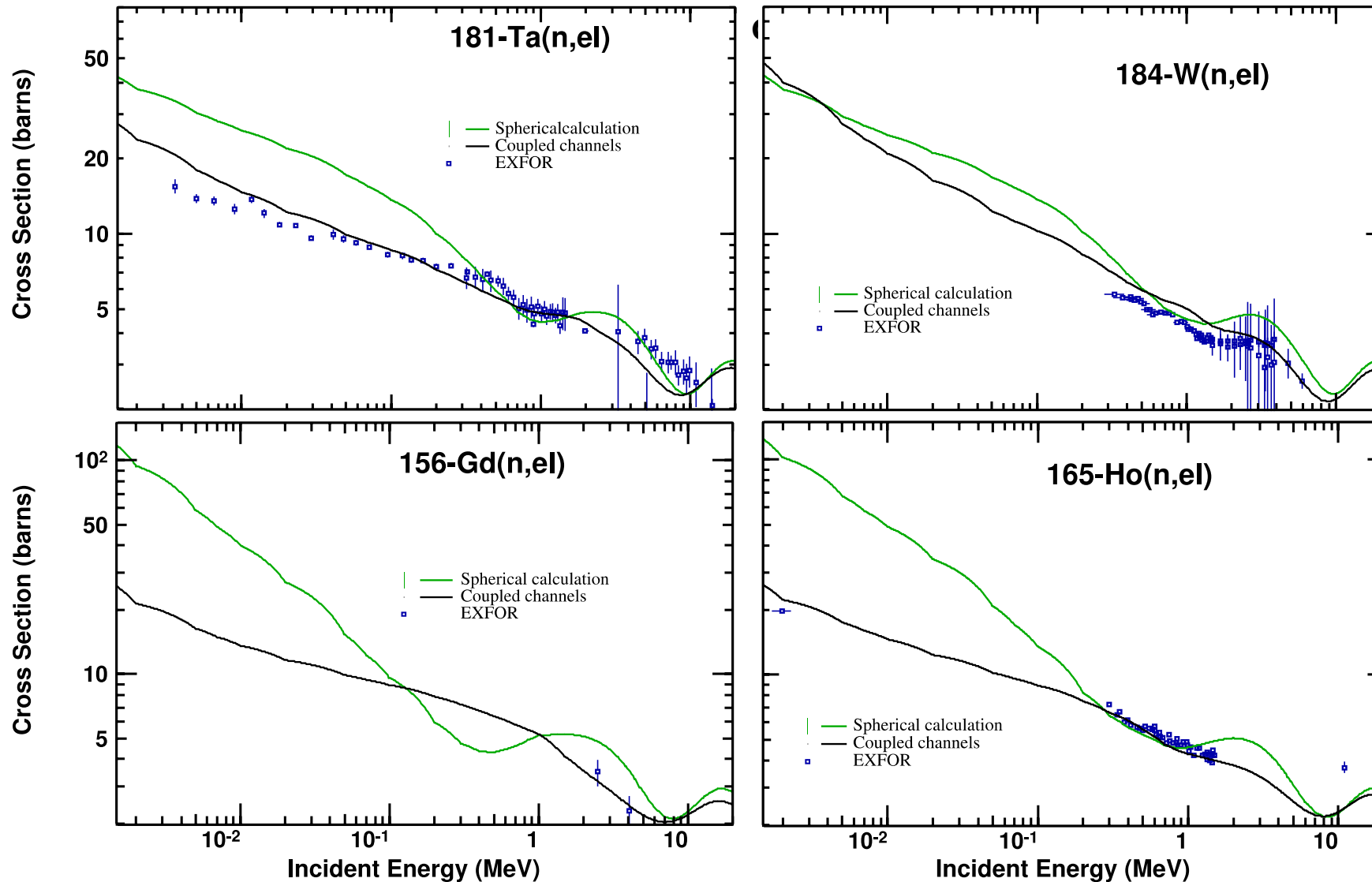
# Backup slides

# Comparison between spherical and CC



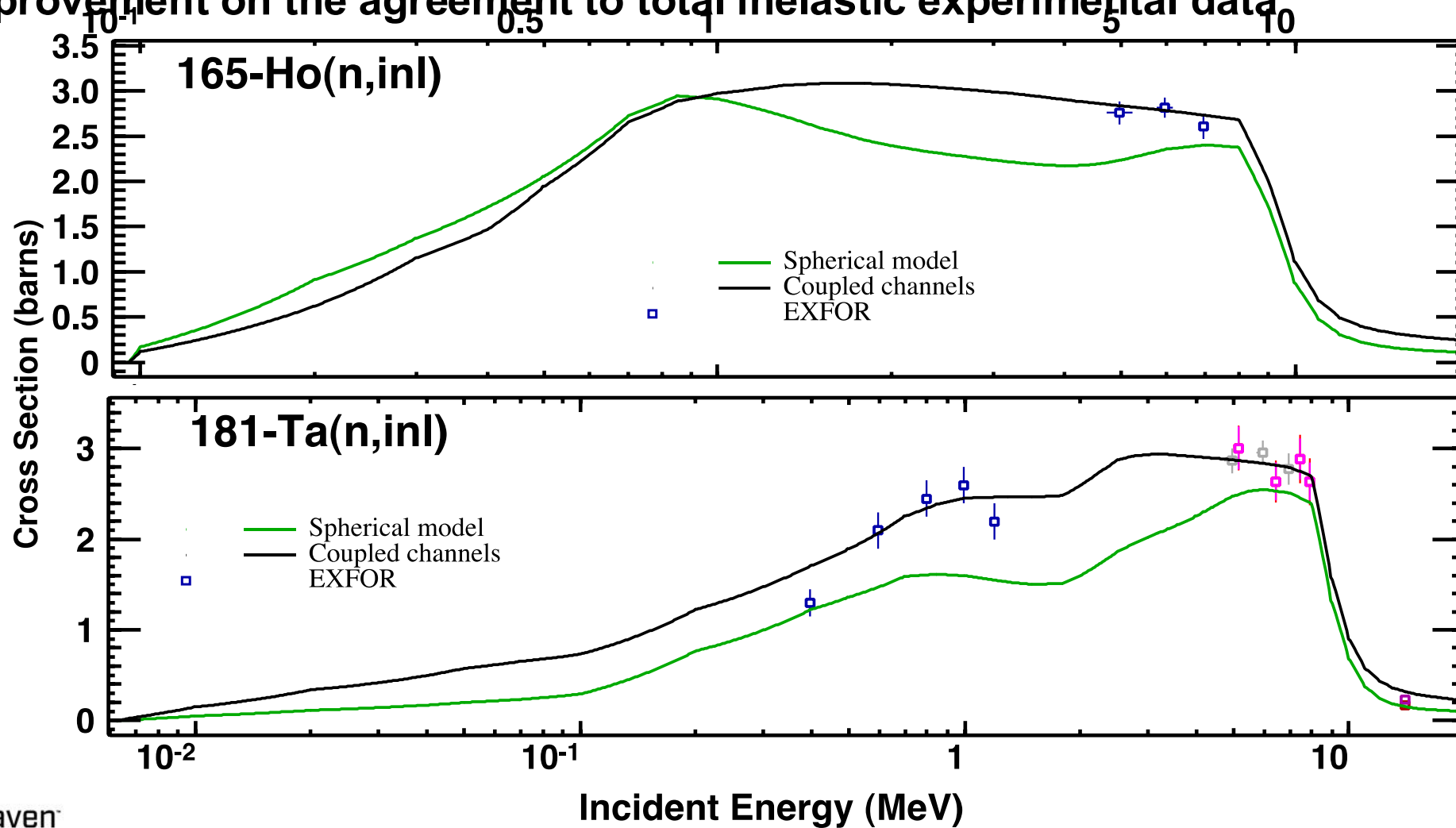
Spherical approach fails at low energy and its shape often is in disagreement with experimental data, while deforming KD potential provides a good description of the observed total cross sections

# Elastic cross section (shape + compound)

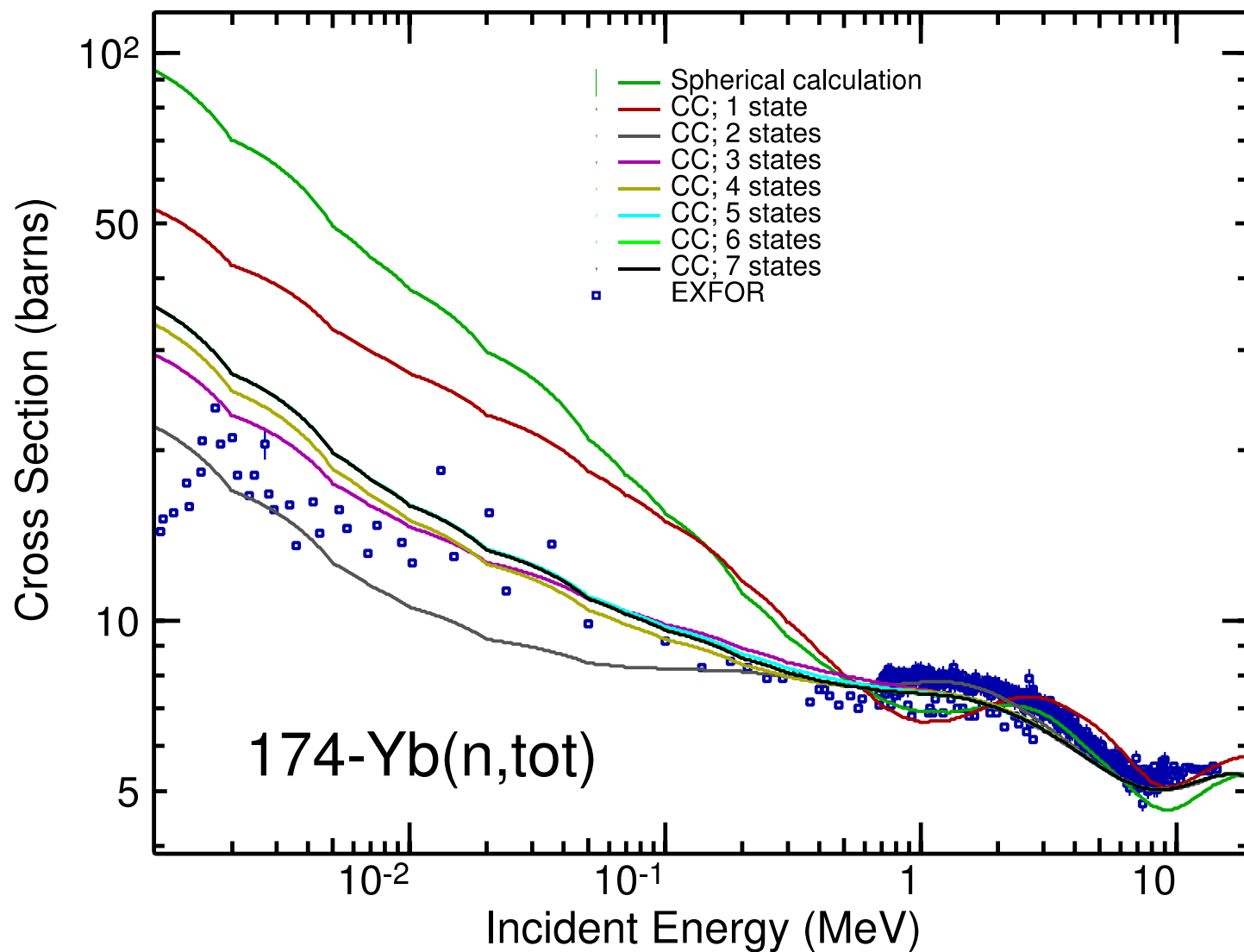


# Total inelastic

Clear improvement on the agreement to total inelastic experimental data

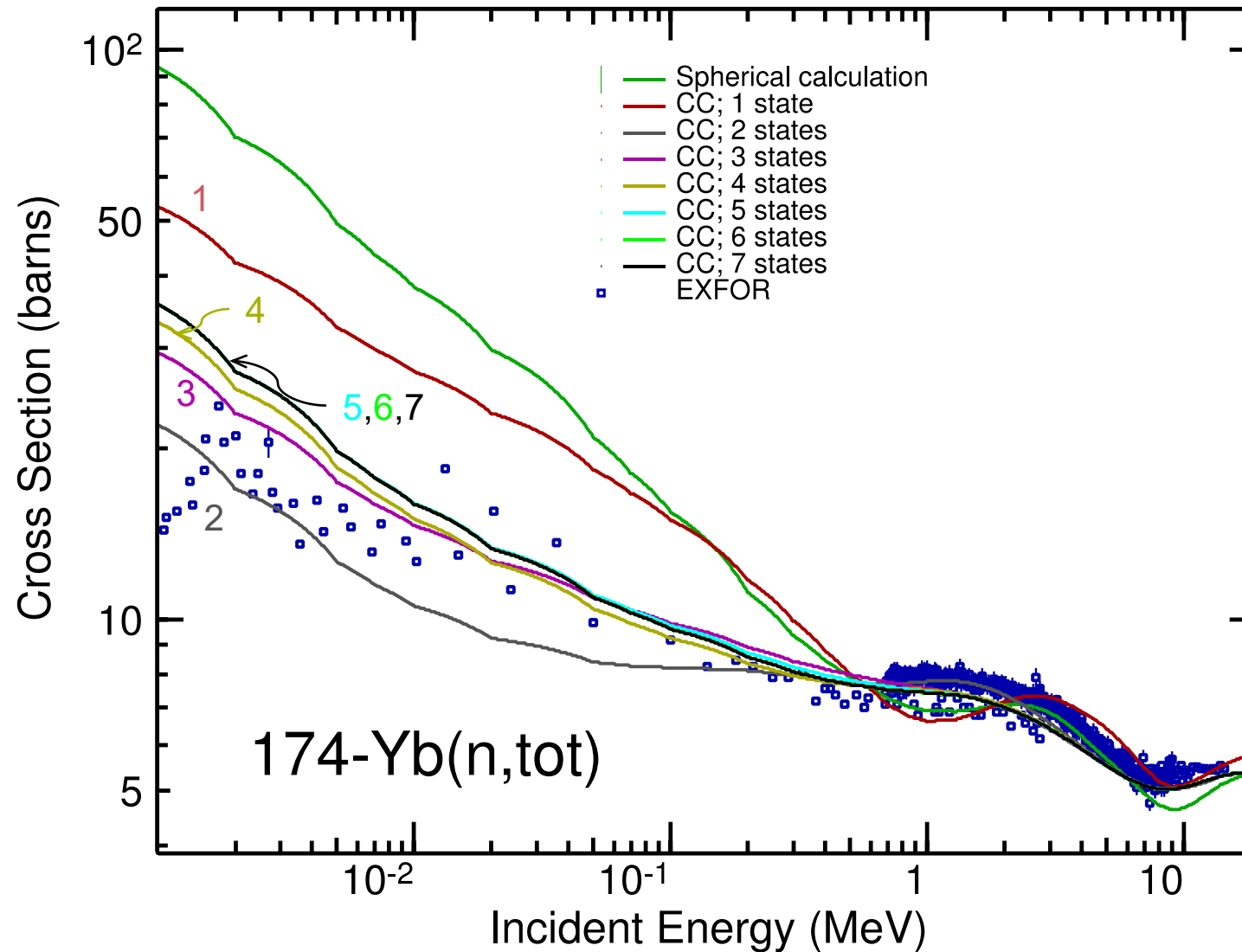


# Convergence on number of channels

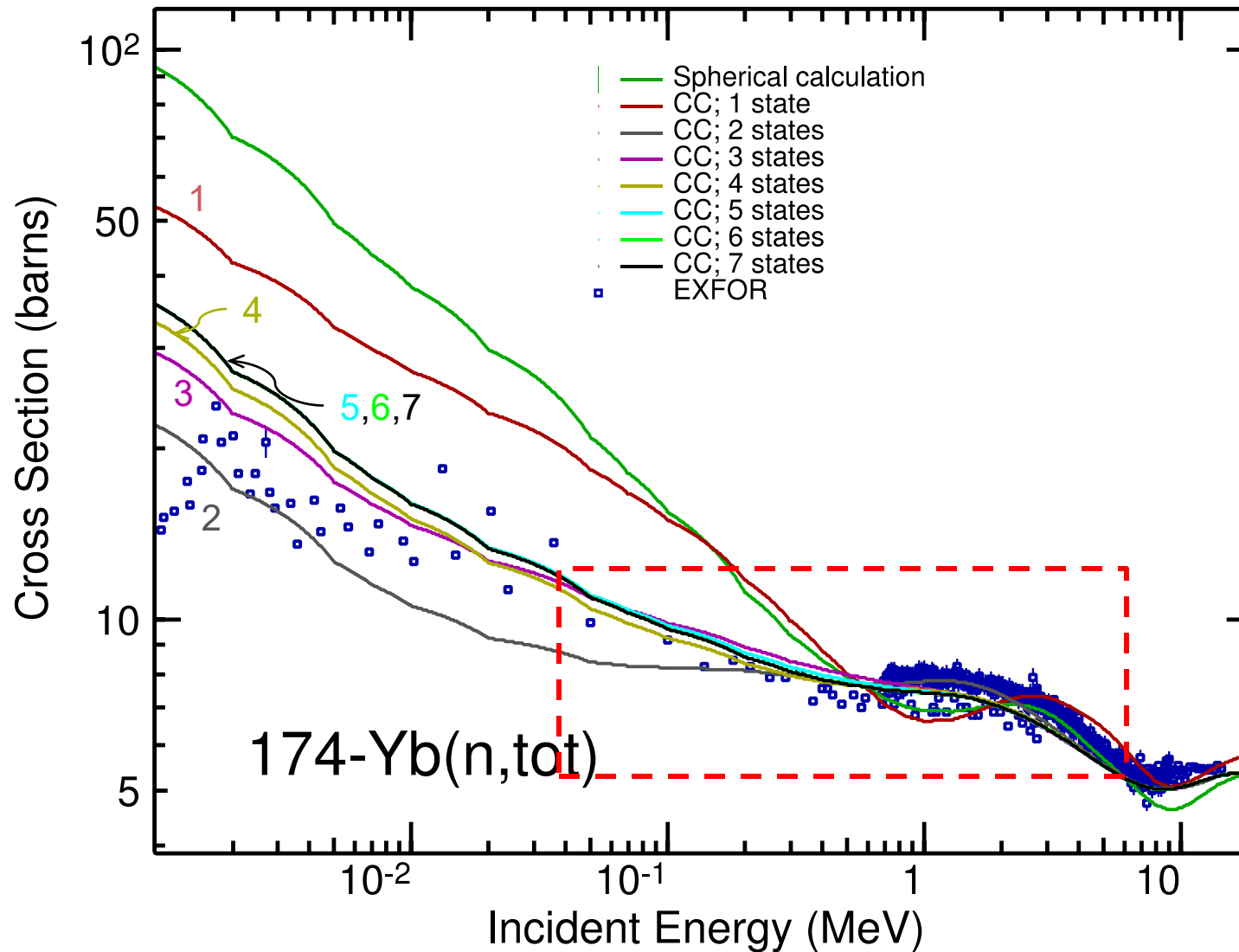




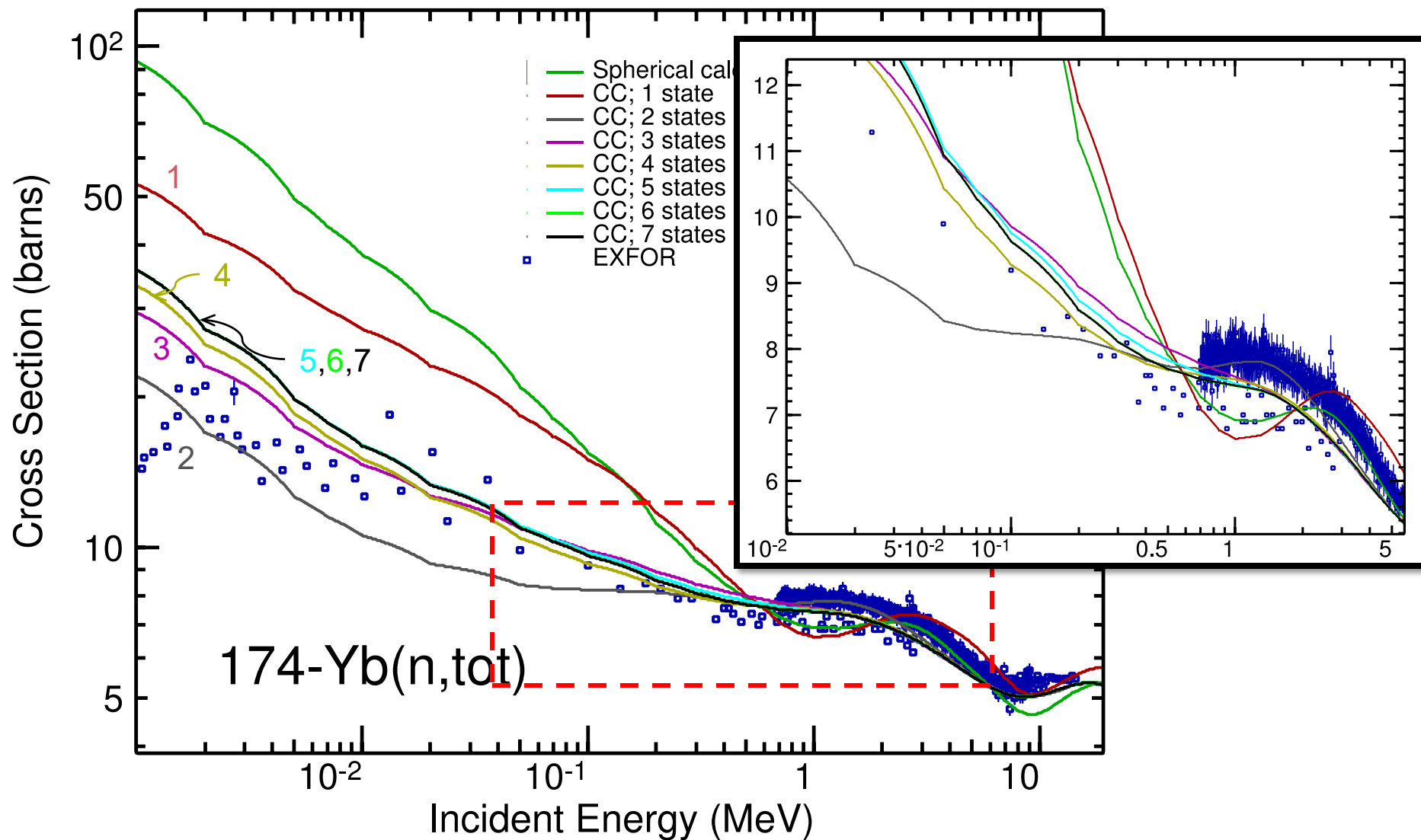
# Convergence on number of channels



# Convergence on number of channels

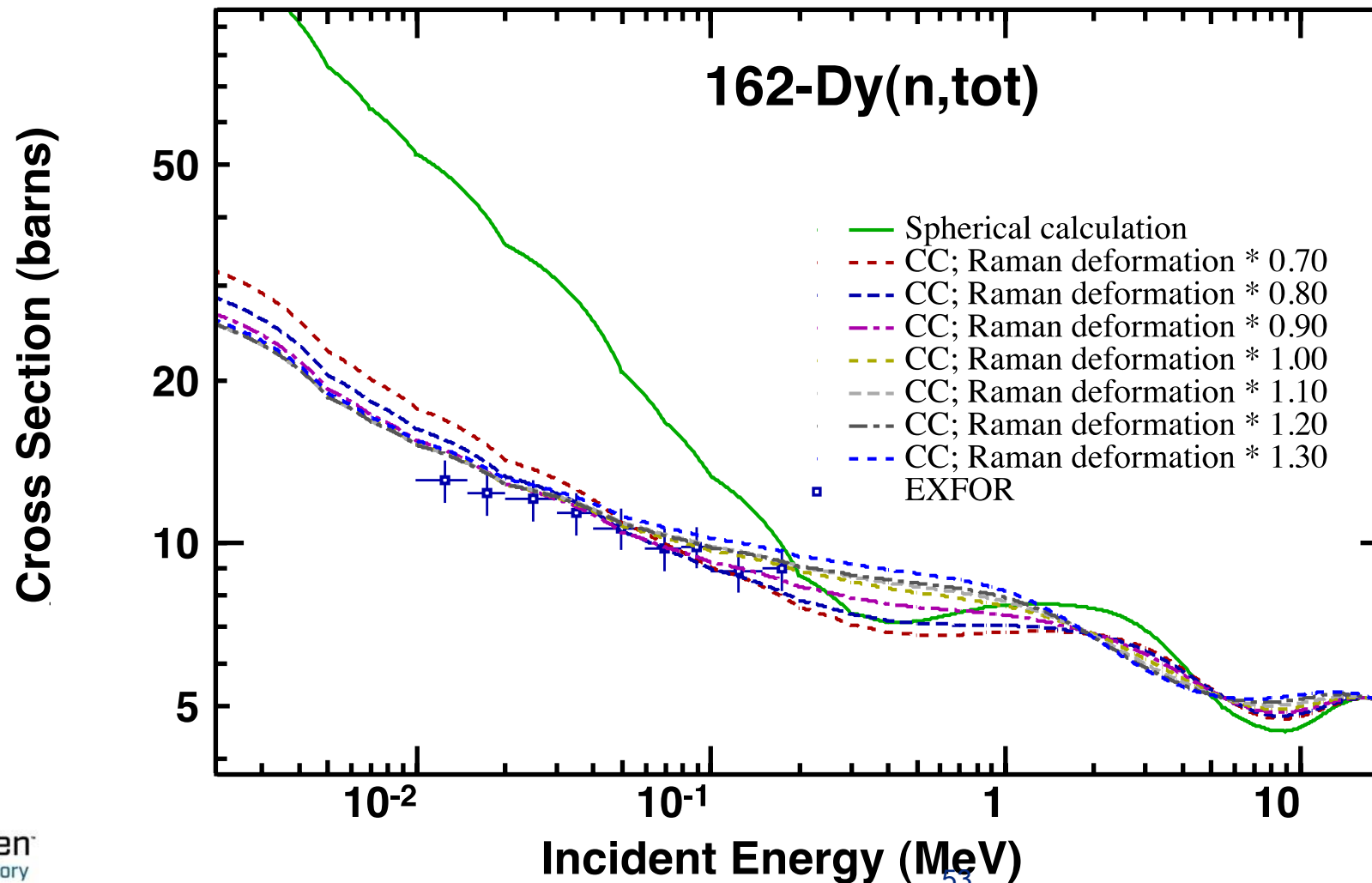


# Convergence on number of channels



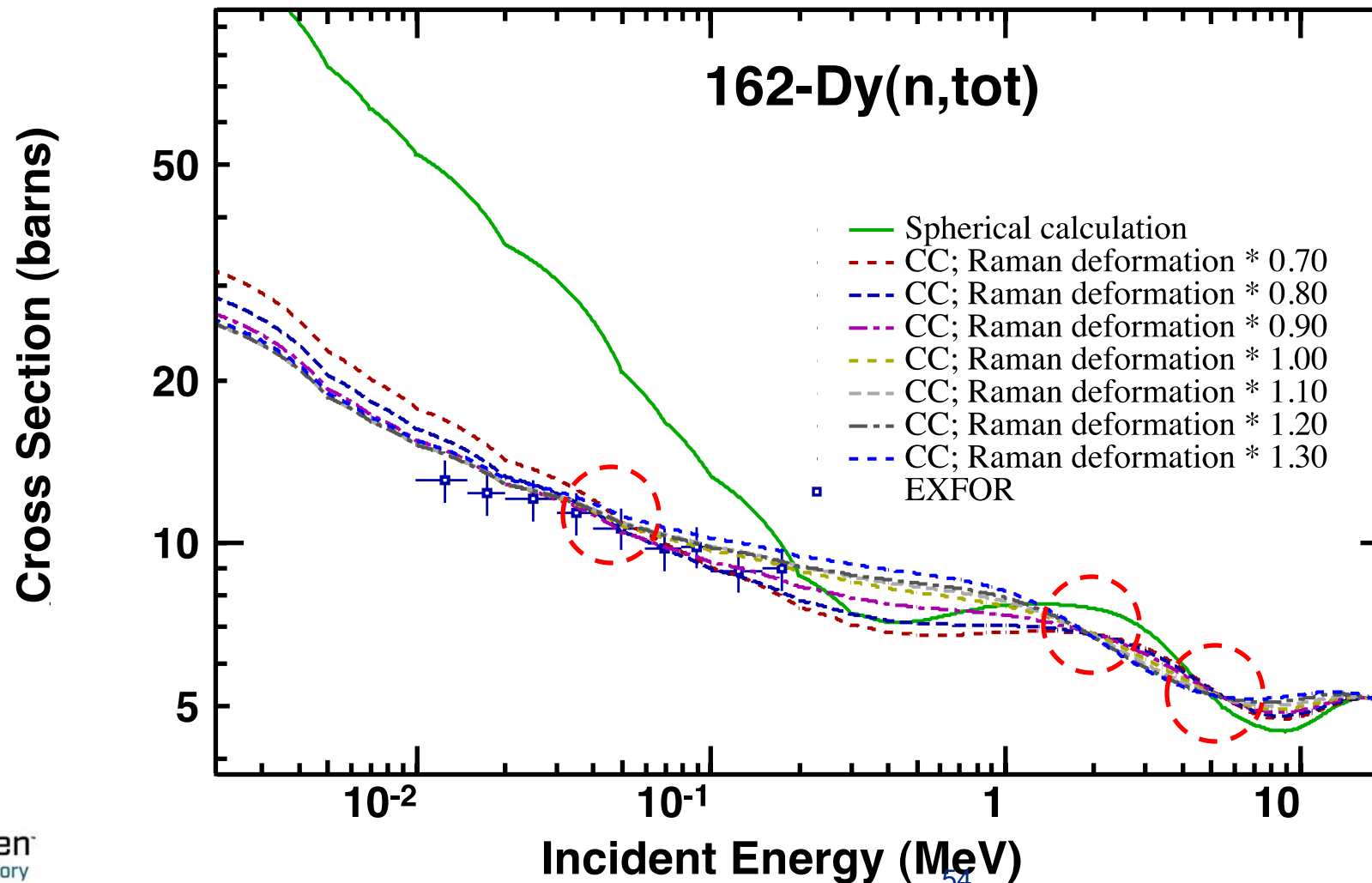
# Sensitivity to deformation

Deformation uncertainty relates to cross-section uncertainty



# Sensitivity to deformation

Deformation uncertainty relates to cross-section uncertainty

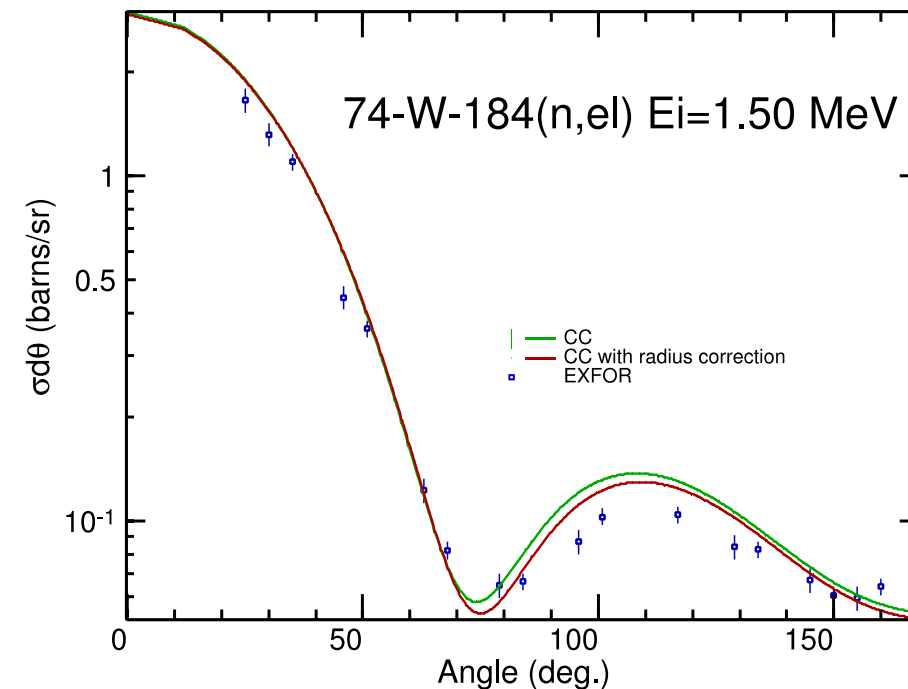
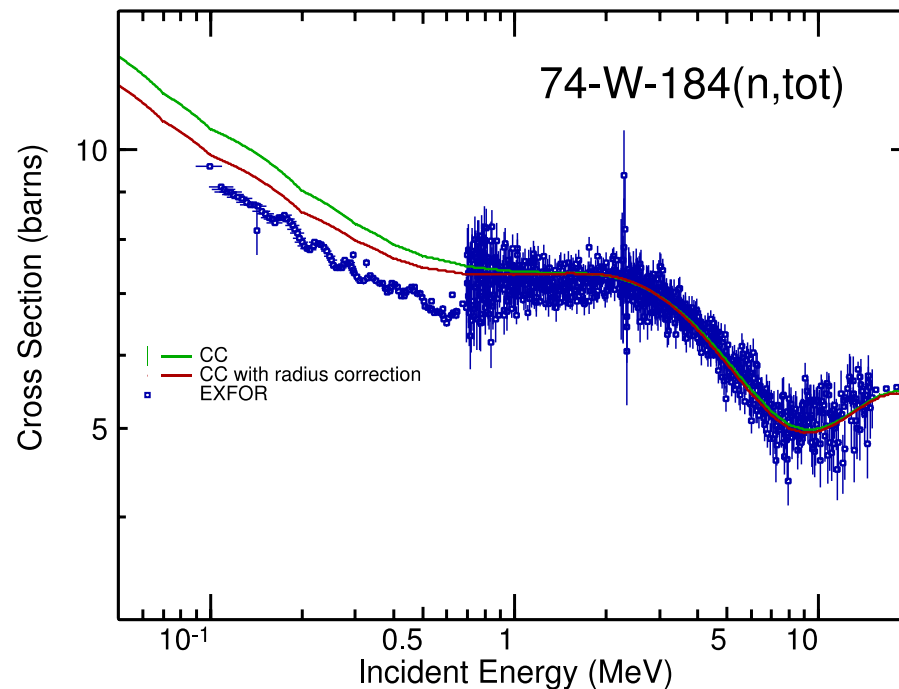


# When deforming the potential, the volume should be conserved

Bang & Vaagen  $R'_0 = R_0(1 - \Sigma \beta_\lambda^2 / 4\pi)$

For  $^{184}\text{W}$ :  $\beta_2 = 0.236$   $\square$   $\Delta < 0.5\%$

Most deformed:  $^{160}\text{Gd}$ :  $\beta_2 = 0.353$   $\square$   $\Delta < 1\%$





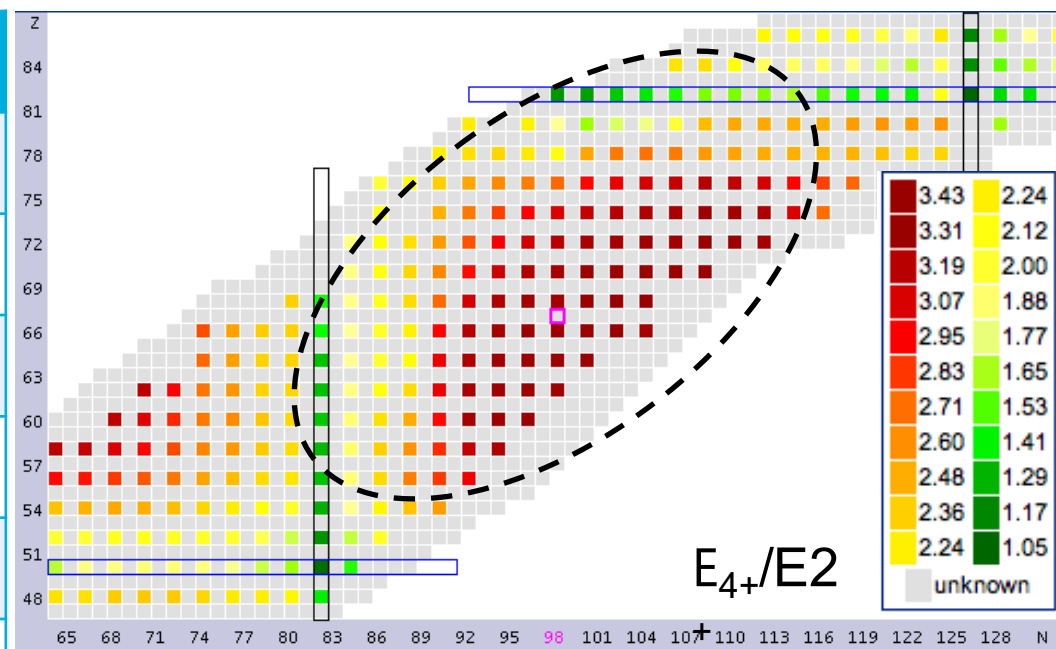
# Angular distributions: Gd, Ho, W

More detailed analysis on the experimental data sets

Some elastic ang. dist. data actually contained inelastics

Ensured convergence regarding number of rotational channels

nucleus	$\beta_2^*$	$\beta_4^{\S}$	$\Delta_R$	$\beta_2^{(sys)\P}$
$^{158}\text{Gd}$	0.348	0.056	0.990	0.362
$^{160}\text{Gd}$	0.353	0.056	0.990	0.372
$^{165}\text{Ho}$	0.293	-0.020	0.993	0.385
$^{182}\text{W}$	0.251	-0.080	0.995	0.268
$^{184}\text{W}$	0.236	-0.080	0.996	0.255
$^{186}\text{W}$	0.226	-0.080	0.996	0.226



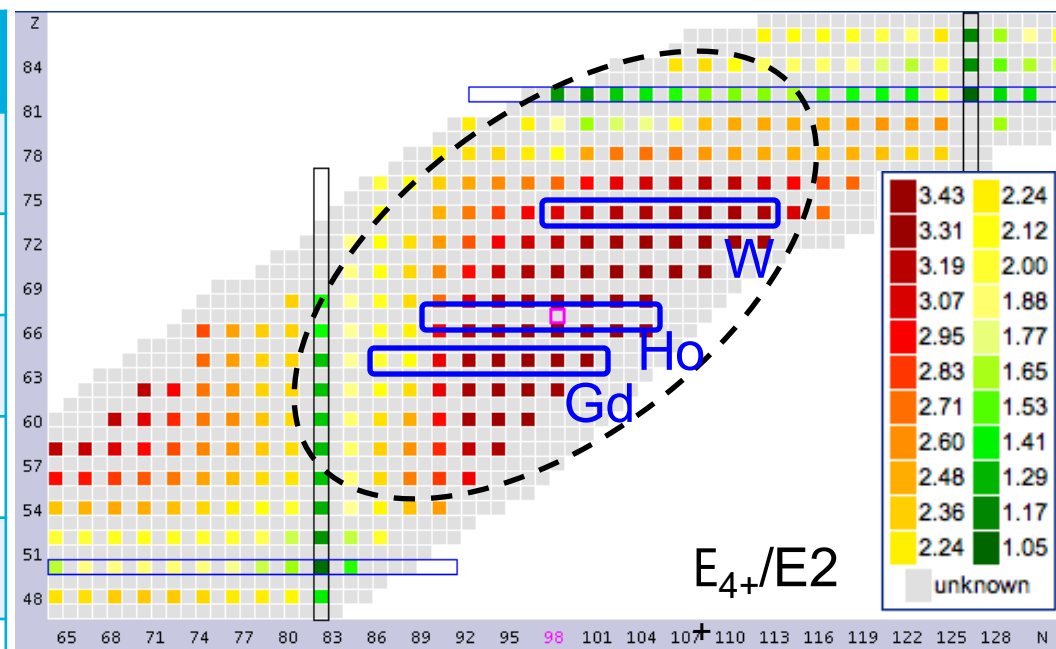
# Angular distributions: Gd, Ho, W

More detailed analysis on the experimental data sets

Some elastic ang. dist. data actually contained inelastics

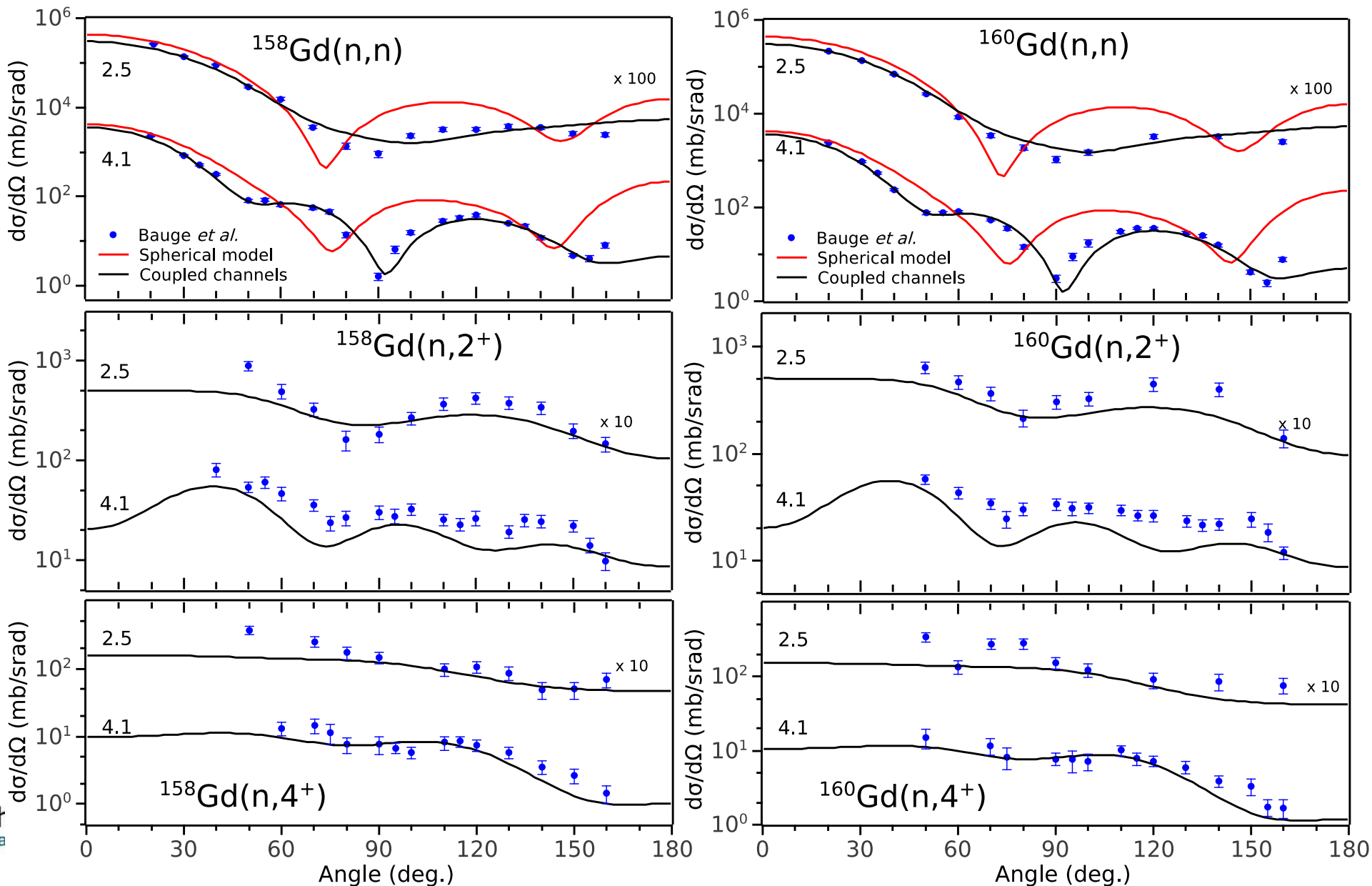
Ensured convergence regarding number of rotational channels

nucleus	$\beta_2^*$	$\beta_4^{\S}$	$\Delta_R$	$\beta_2^{(sys)\P}$
$^{158}\text{Gd}$	0.348	0.056	0.990	0.362
$^{160}\text{Gd}$	0.353	0.056	0.990	0.372
$^{165}\text{Ho}$	0.293	-0.020	0.993	0.385
$^{182}\text{W}$	0.251	-0.080	0.995	0.268
$^{184}\text{W}$	0.236	-0.080	0.996	0.255
$^{186}\text{W}$	0.226	-0.080	0.996	0.226

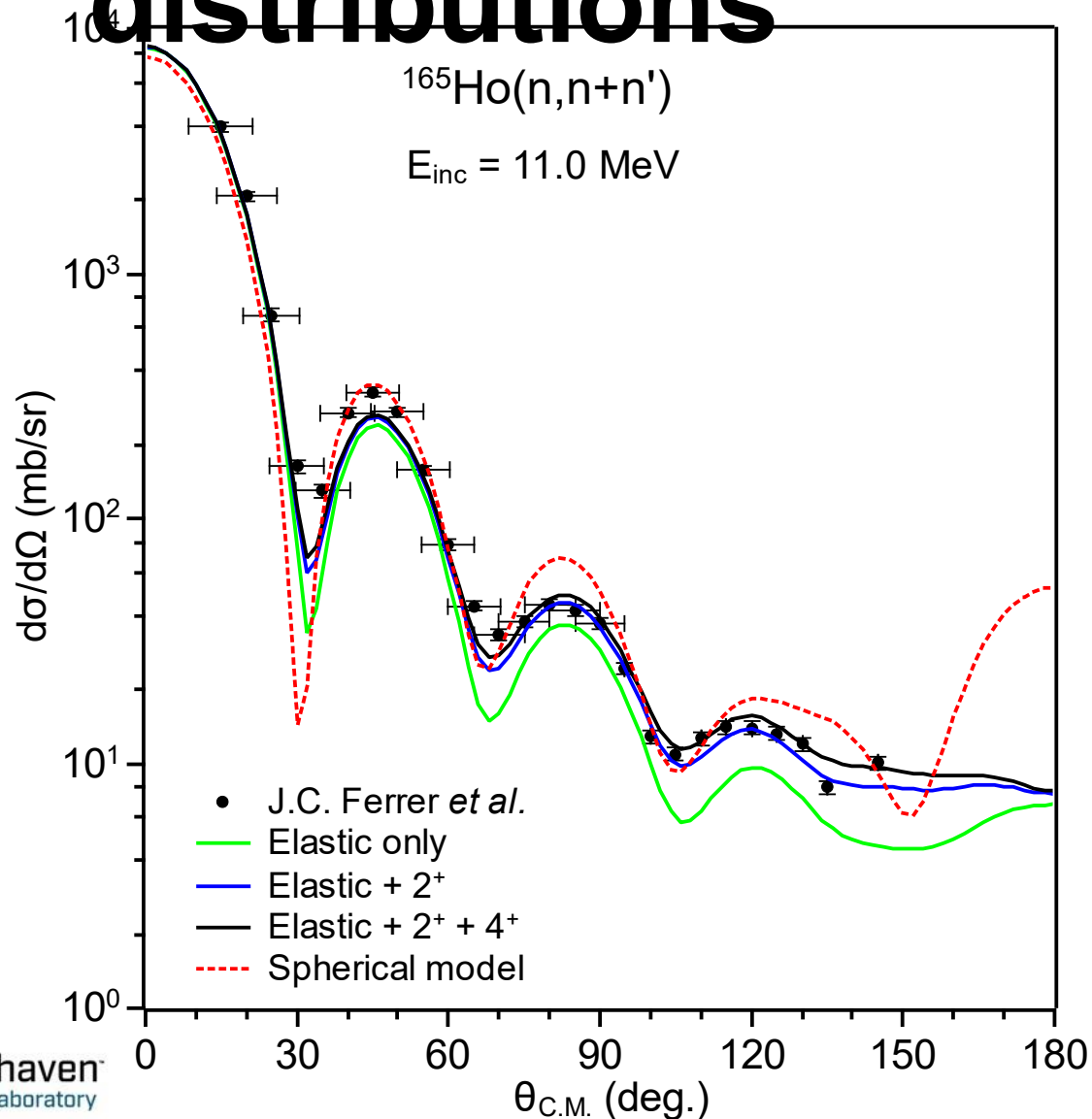


# 158, 160Gd Angular distributions

Good agreement with experimental data obtained by the model

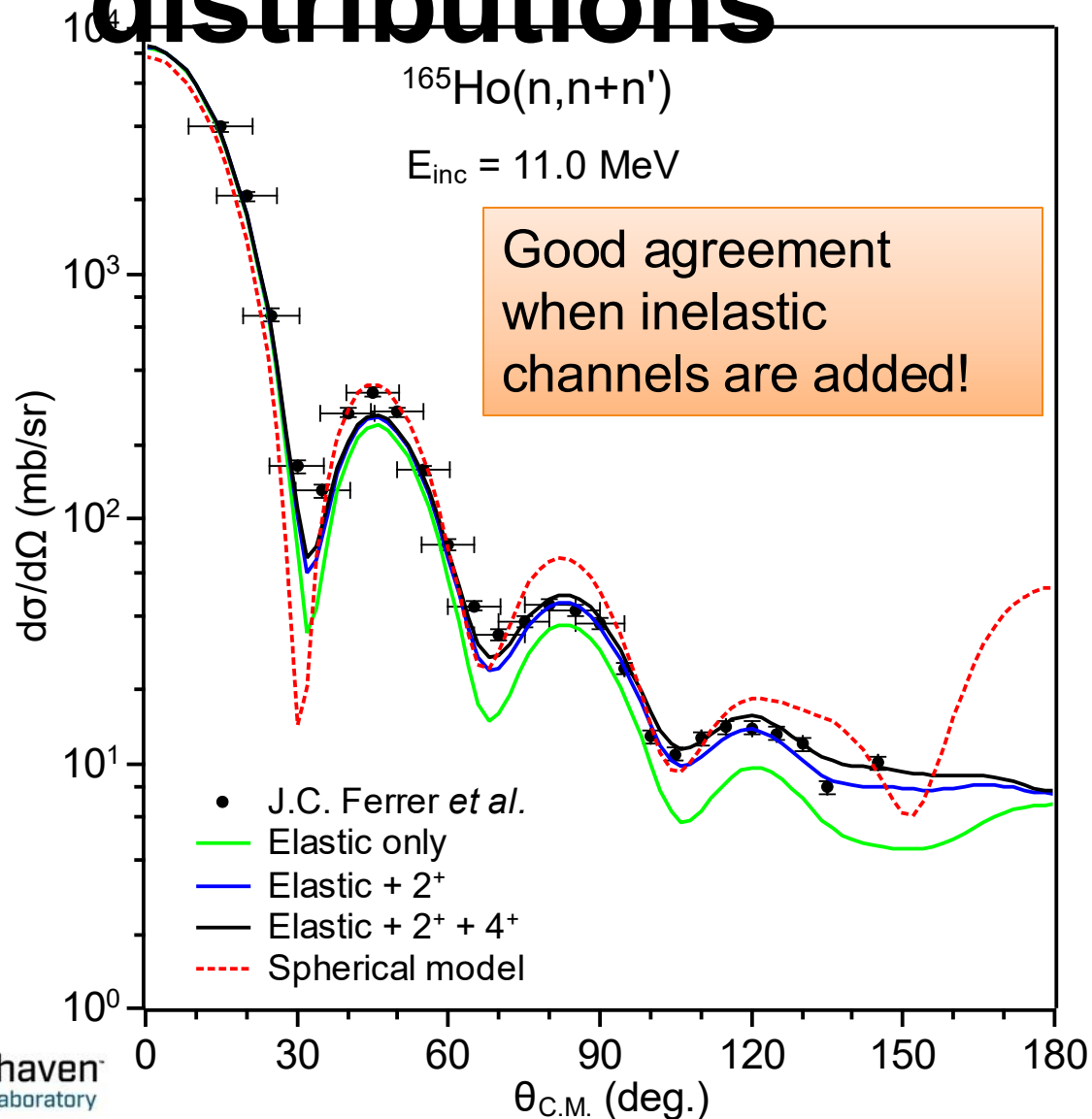


# $^{165}\text{Ho}$ “Quasi-elastic” angular distributions



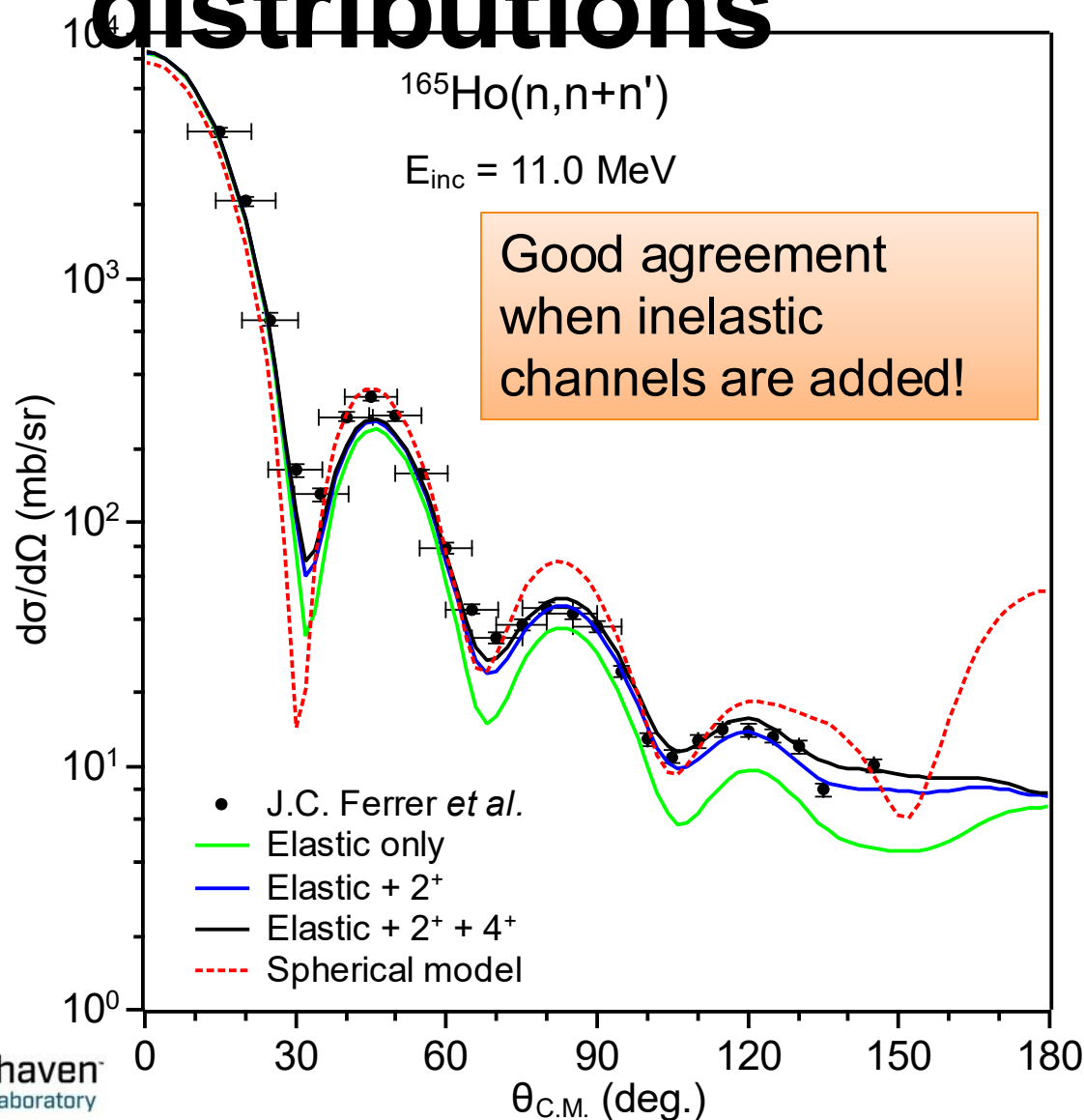
$^{165}\text{Ho}$  experimental angular distributions contain inelastic contributions (above  $\sim 1\text{MeV}$ )

# $^{165}\text{Ho}$ “Quasi-elastic” angular distributions



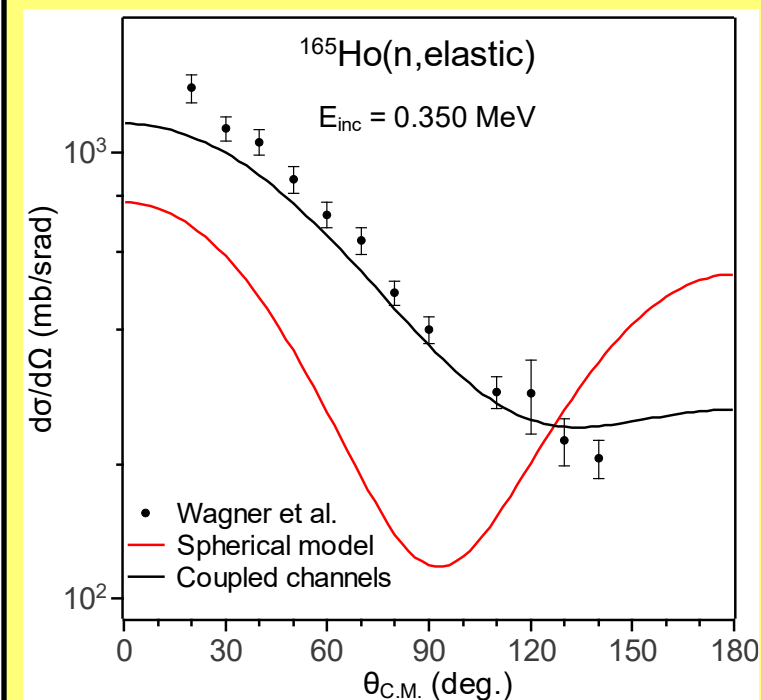
$^{165}\text{Ho}$  experimental angular distributions contain inelastic contributions (above  $\sim 1\text{MeV}$ )

# $^{165}\text{Ho}$ “Quasi-elastic” angular distributions



$^{165}\text{Ho}$  experimental angular distributions contain inelastic contributions (above  $\sim 1\text{MeV}$ )

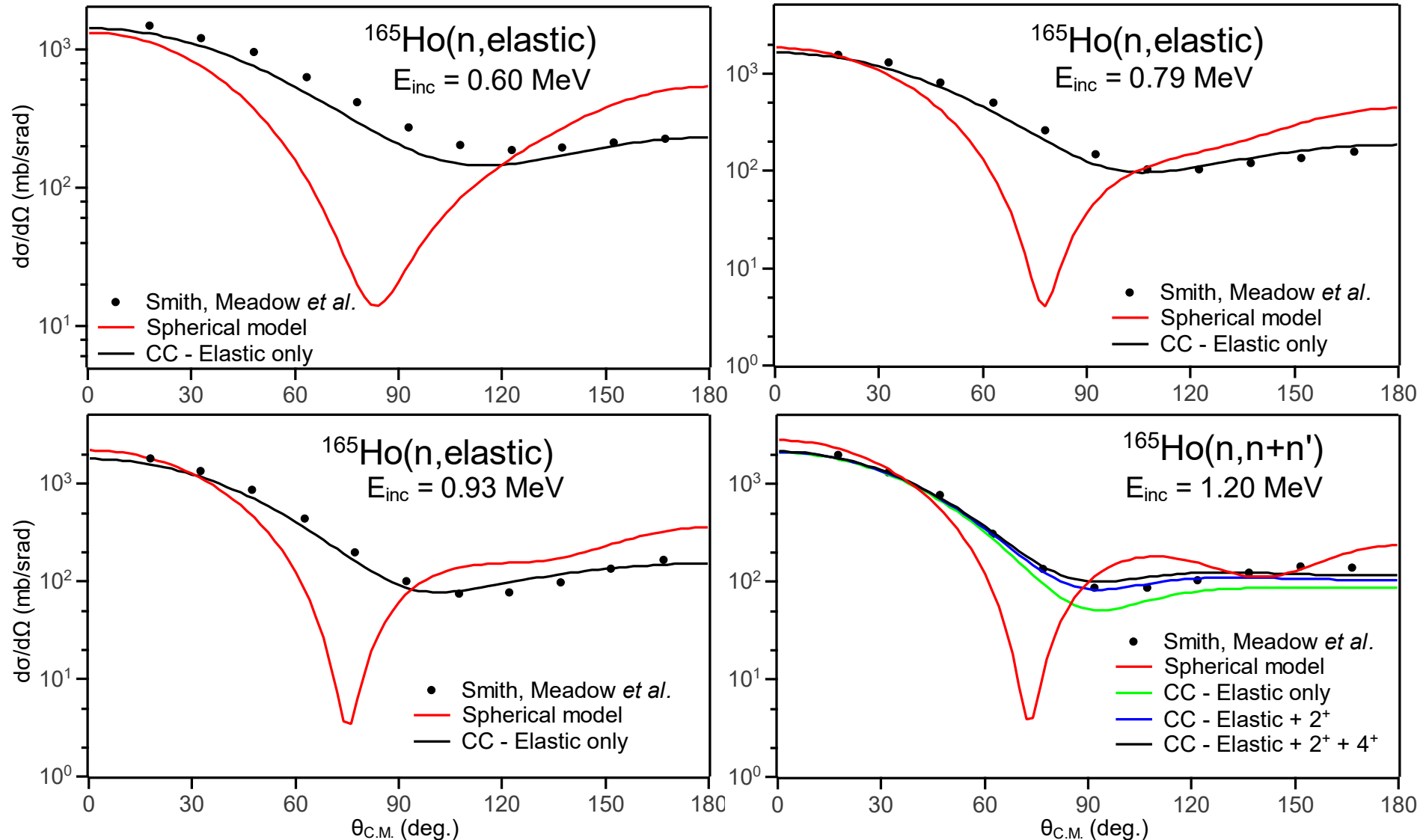
Below  $\sim 1 \text{ MeV}$ : Elastic only





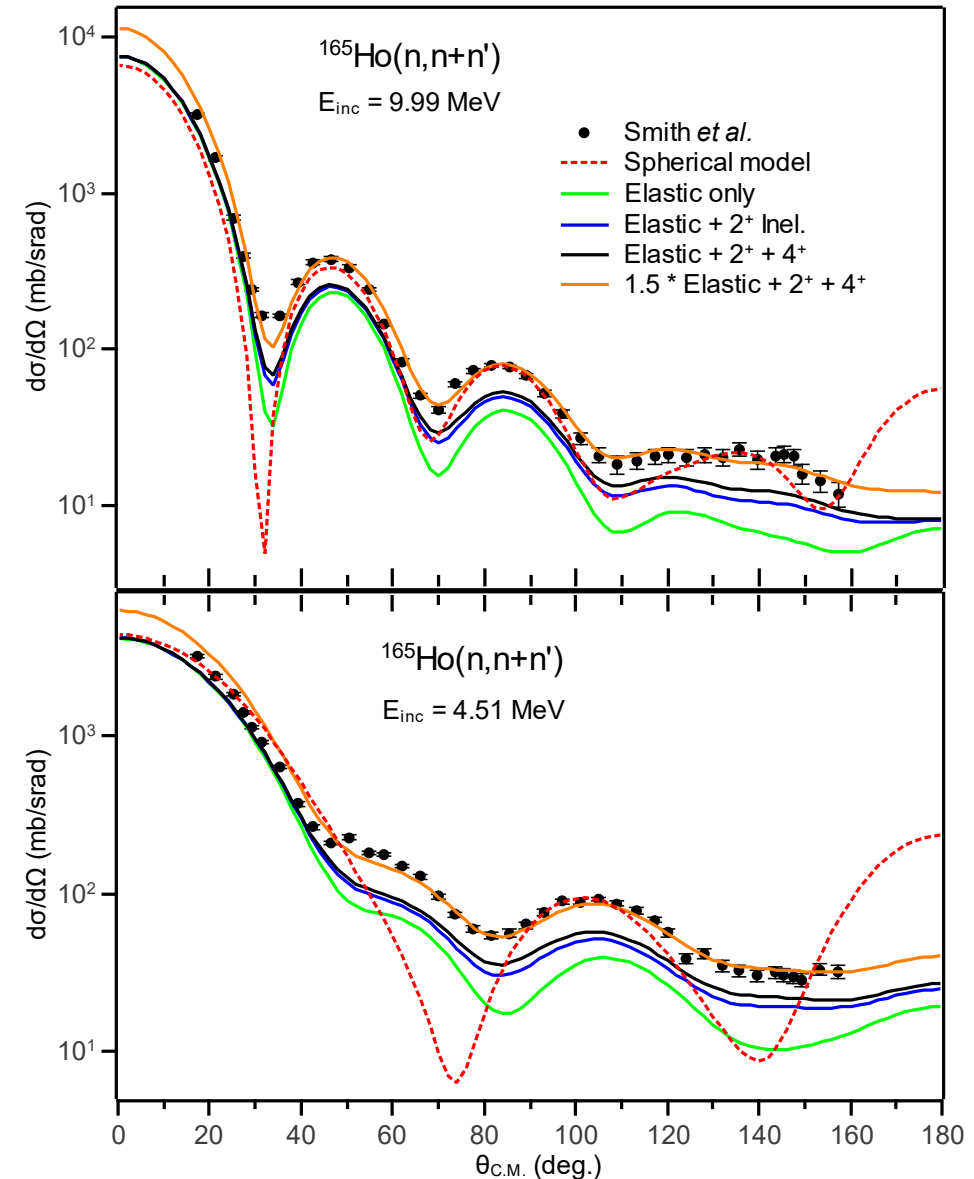
# $^{165}\text{Ho}$ (Quasi-)elastic angular distributions

Good agreement with experimental data obtained by the model



# $^{165}\text{Ho}$ “Quasi-elastic” angular distributions

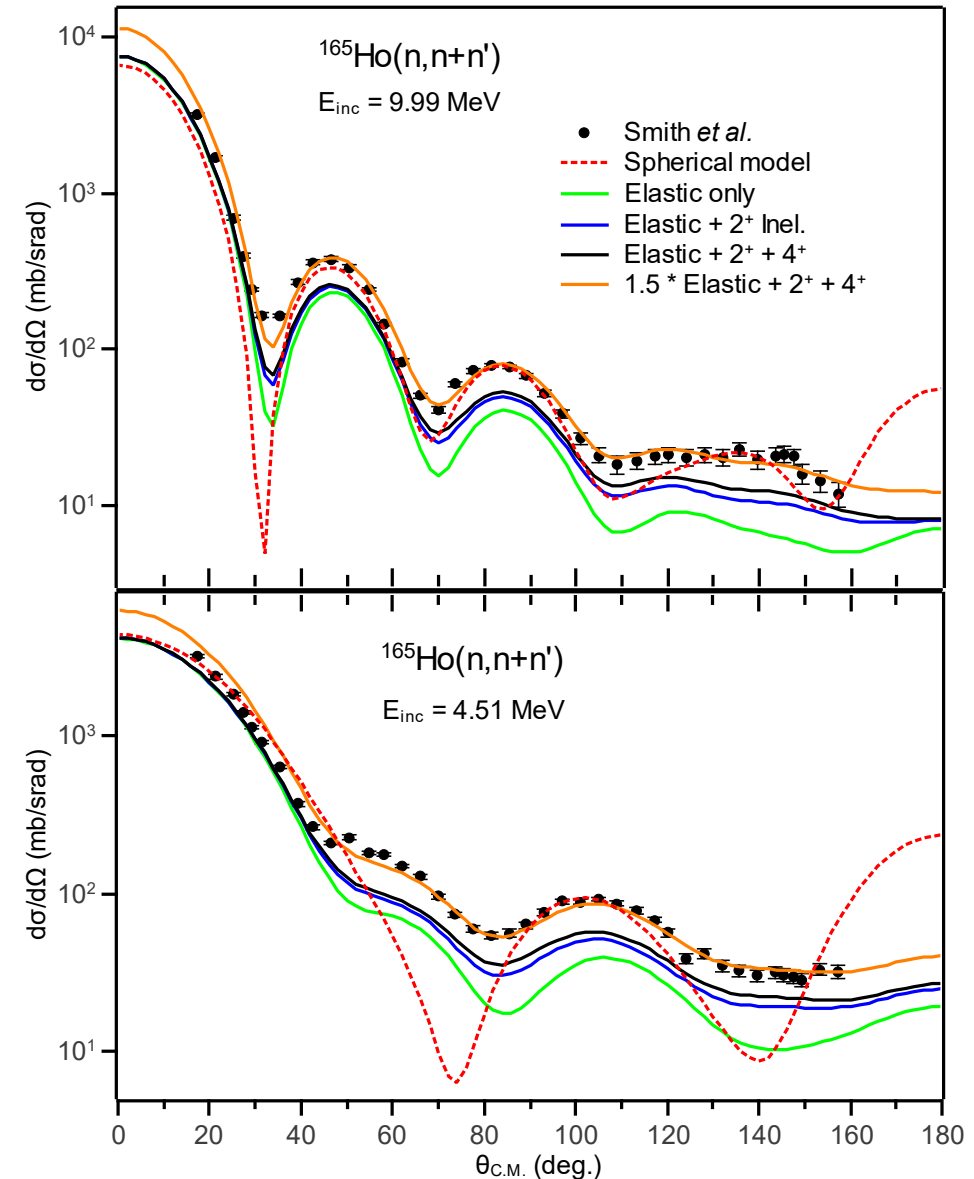
In 2001, A. B. Smith published measurements of quasi-elastic angular distributions for  $n + ^{165}\text{Ho}$ , at  $4.51 \text{ MeV} \leq E_{\text{inc}} \leq 9.99 \text{ MeV}$



# $^{165}\text{Ho}$ “Quasi-elastic” angular distributions

In 2001, A. B. Smith published measurements of quasi-elastic angular distributions for  $n + ^{165}\text{Ho}$ , at  $4.51 \text{ MeV} \leq E_{\text{inc}} \leq 9.99 \text{ MeV}$

Inconsistency with other experiments

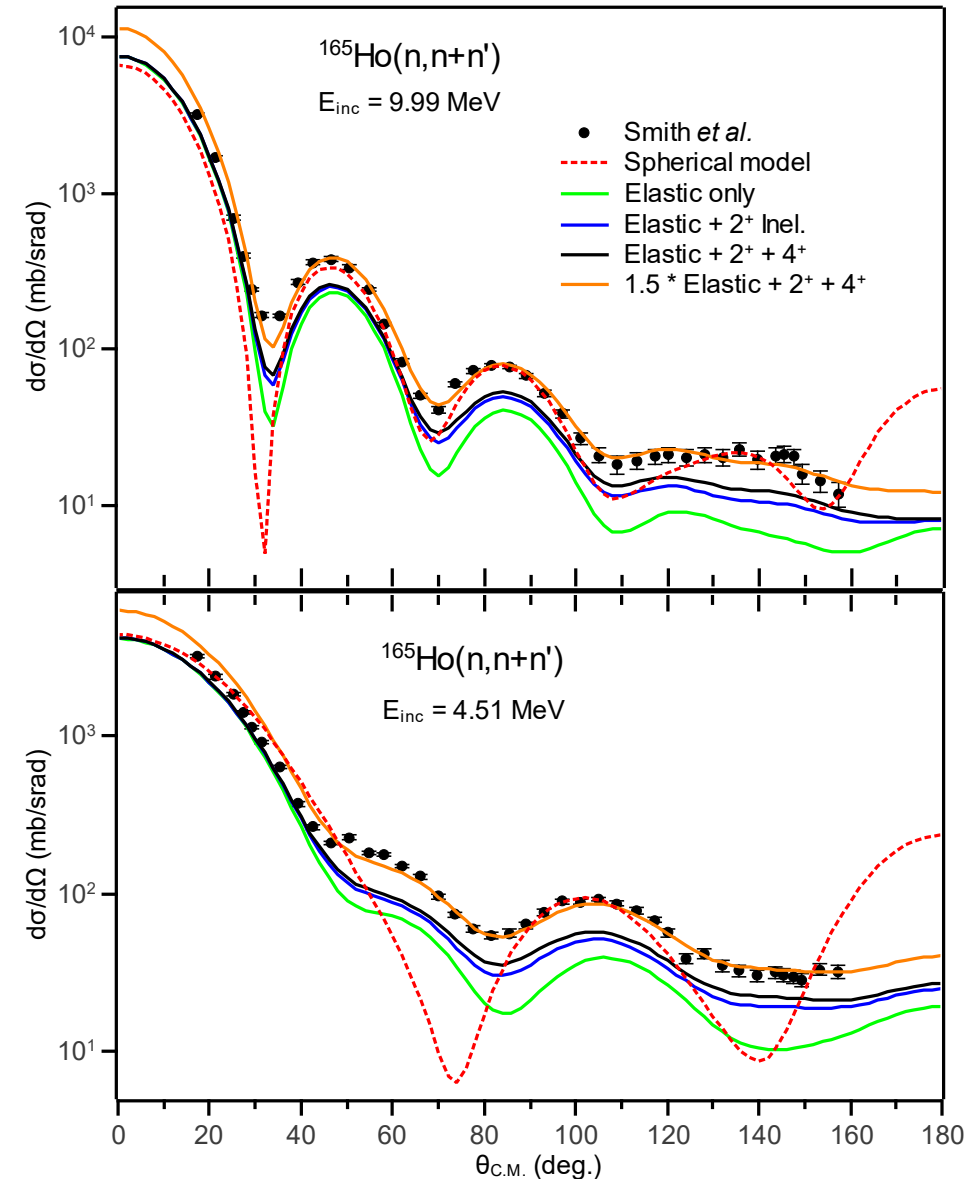


# $^{165}\text{Ho}$ “Quasi-elastic” angular distributions

In 2001, A. B. Smith published measurements of quasi-elastic angular distributions for  $n + ^{165}\text{Ho}$ , at  $4.51 \text{ MeV} \leq E_{\text{inc}} \leq 9.99 \text{ MeV}$

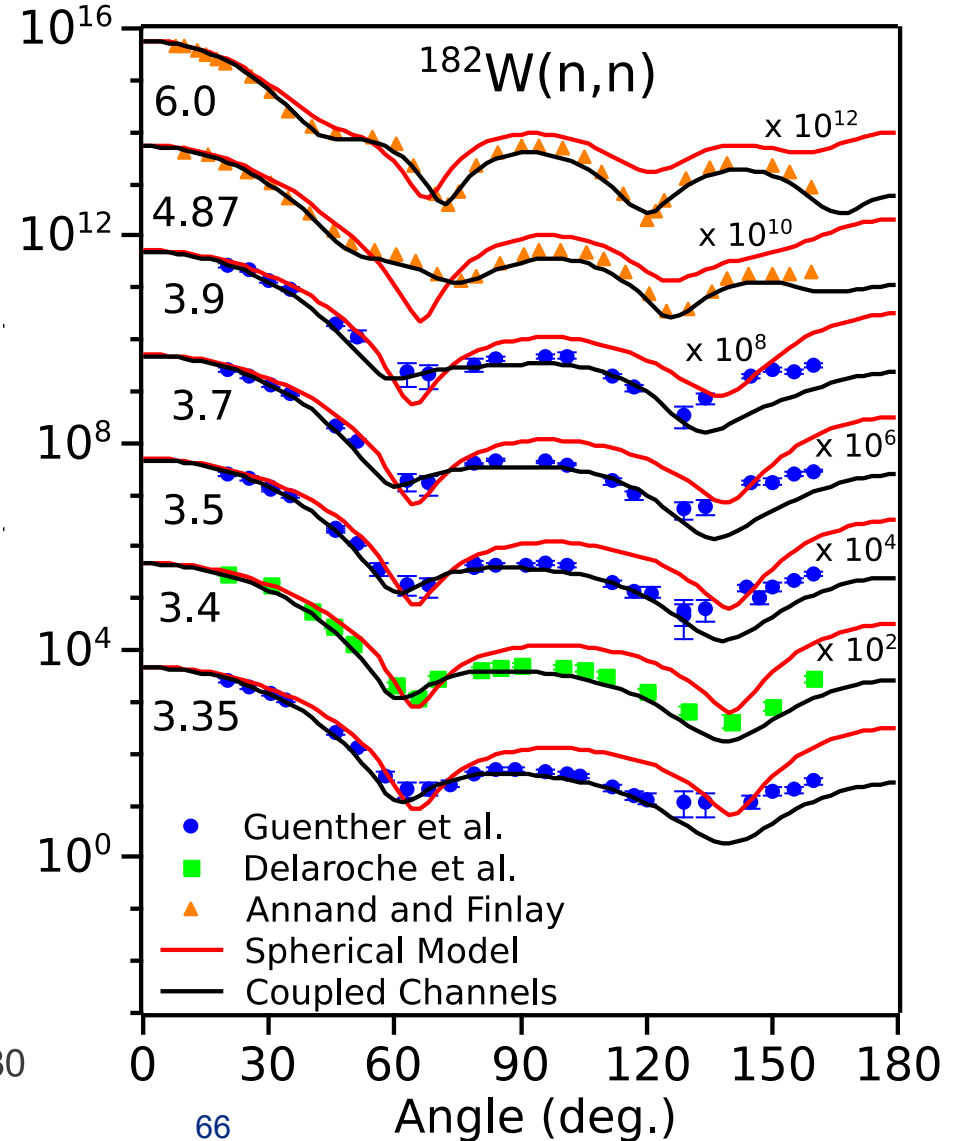
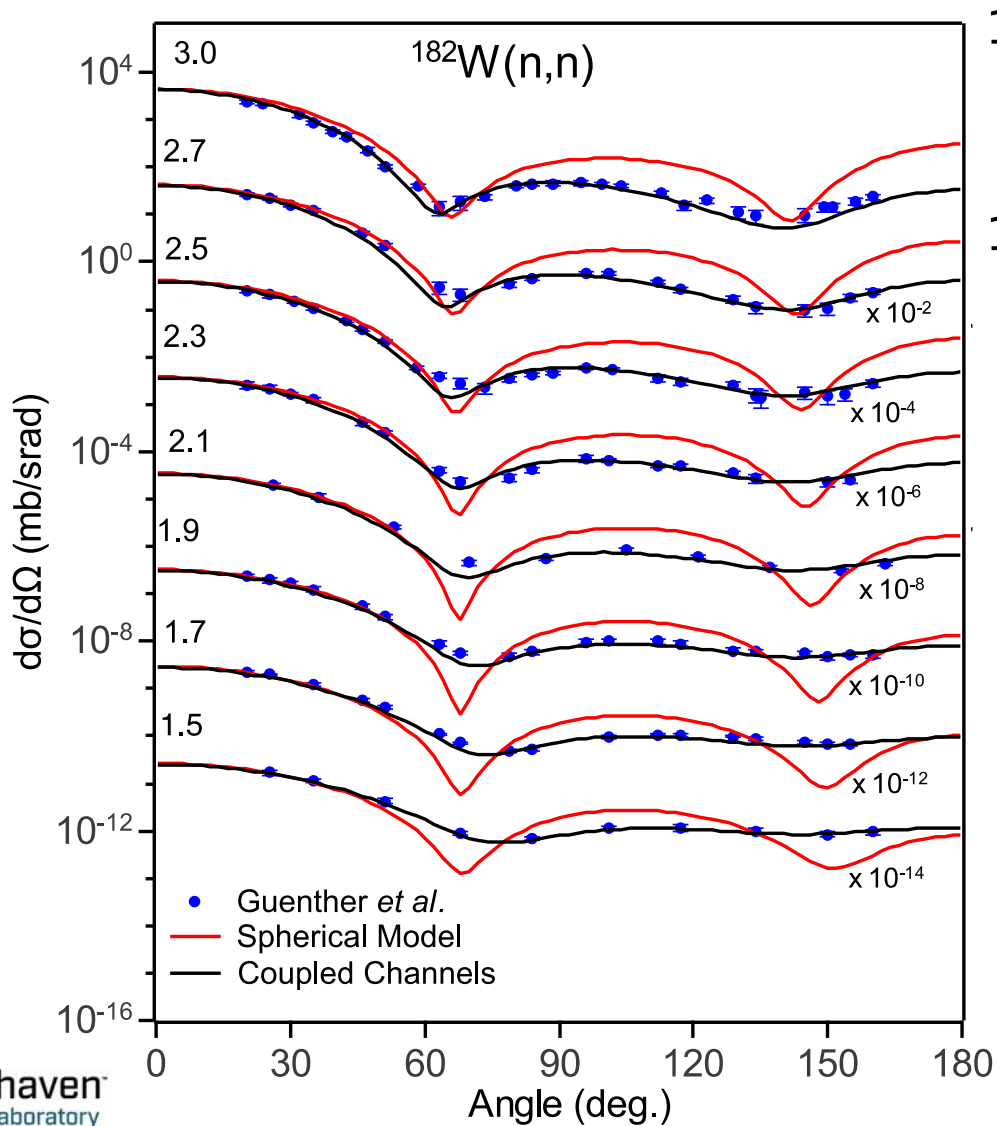
Inconsistency with other experiments

Advantage of a more fundamental (and not fitted) optical potential becomes explicit



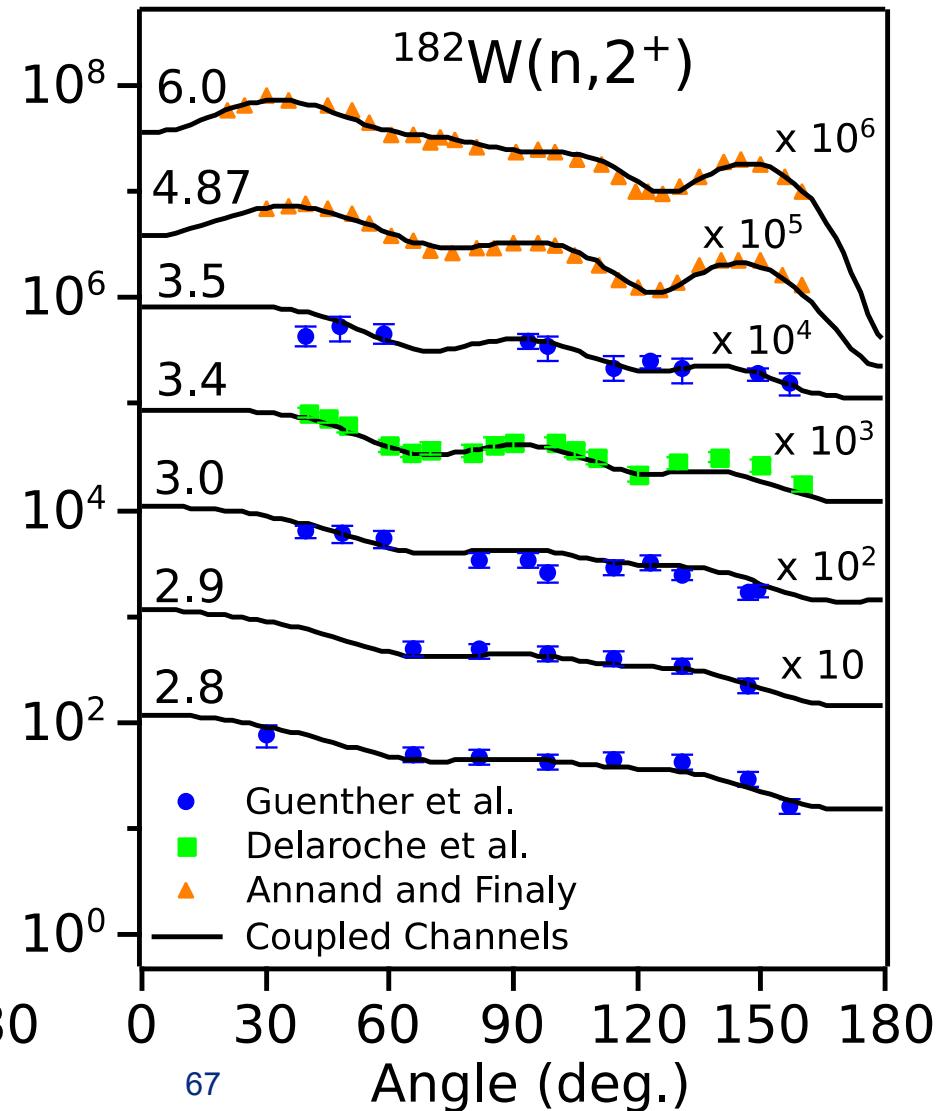
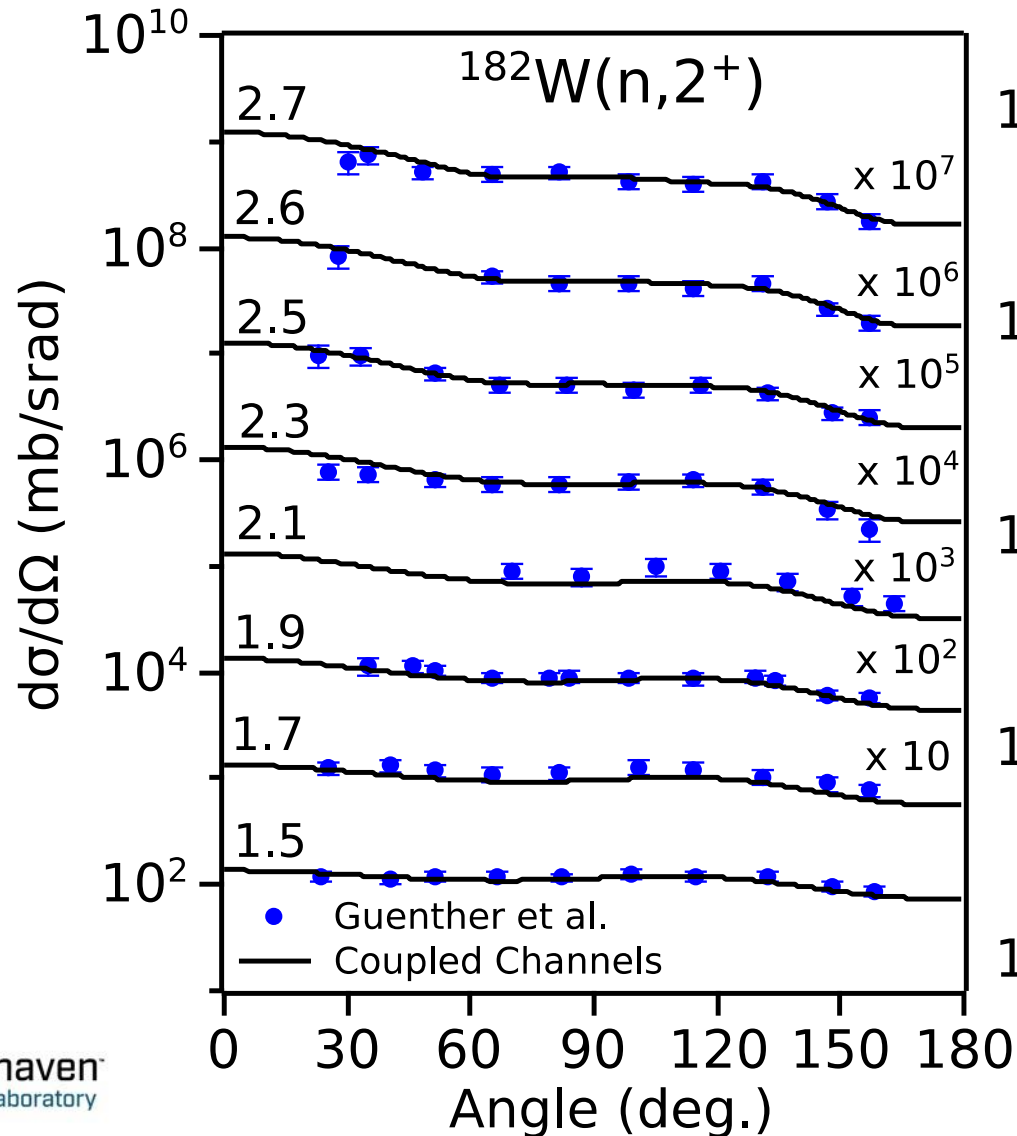
# $^{182}\text{W}$ – Elastic angular distributions

Good agreement with experimental data obtained by the model



# $^{182}\text{W} - 2^+$ Inelastic ang. dist. ( $E_2^+=0.100\text{MeV}$ )

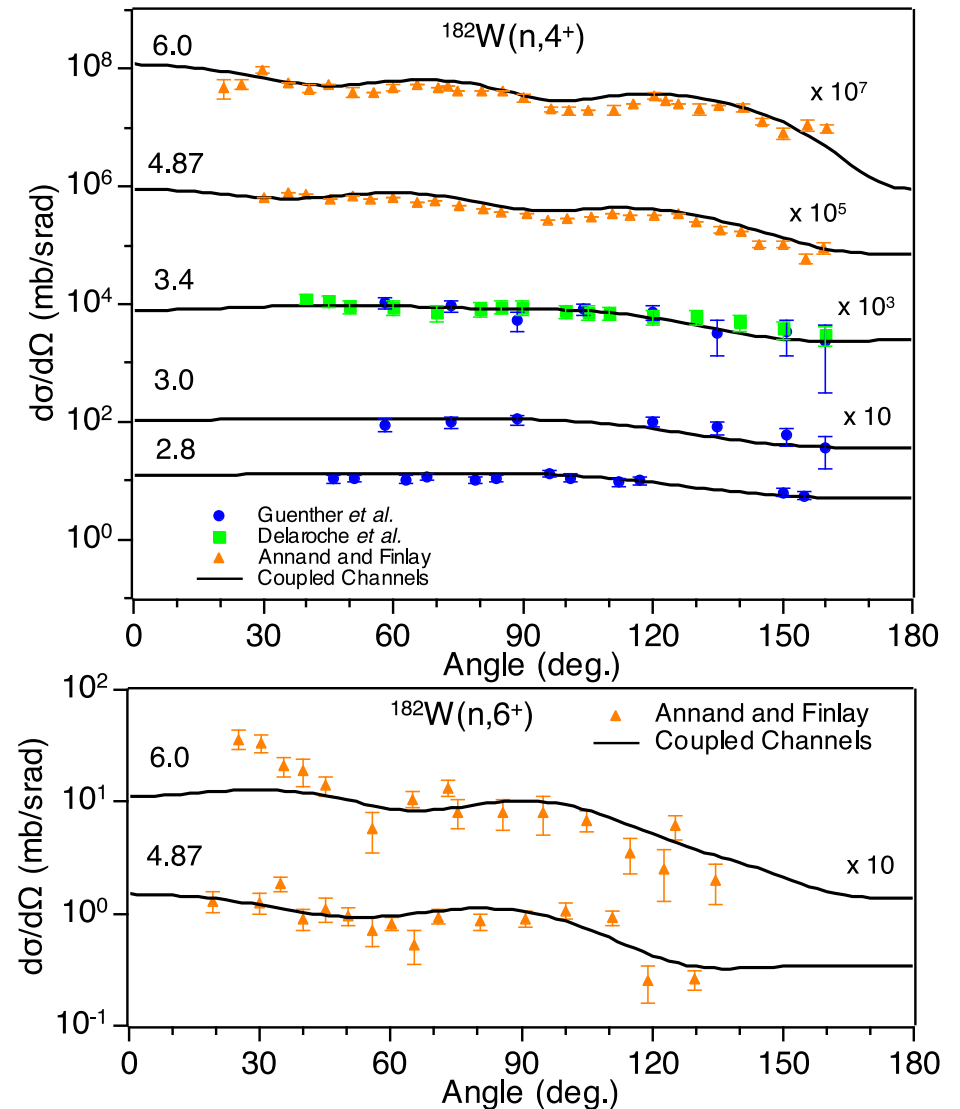
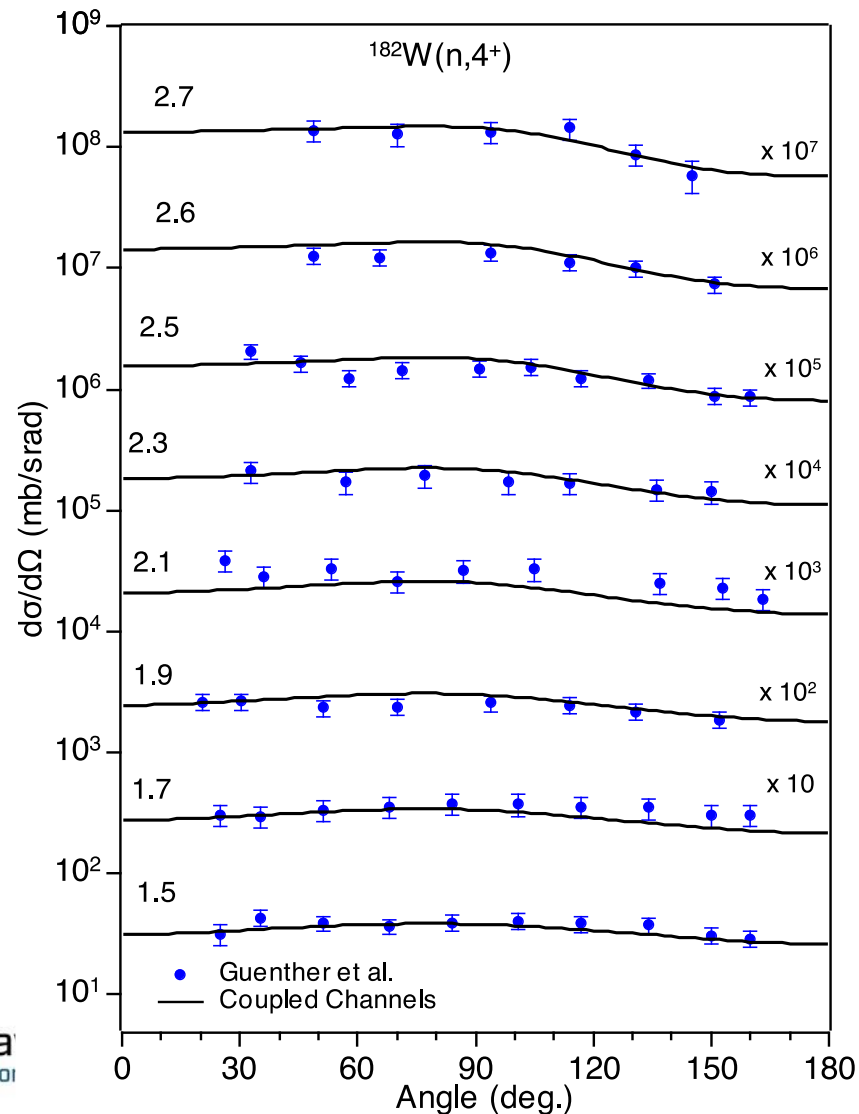
Good agreement with experimental data obtained by the model



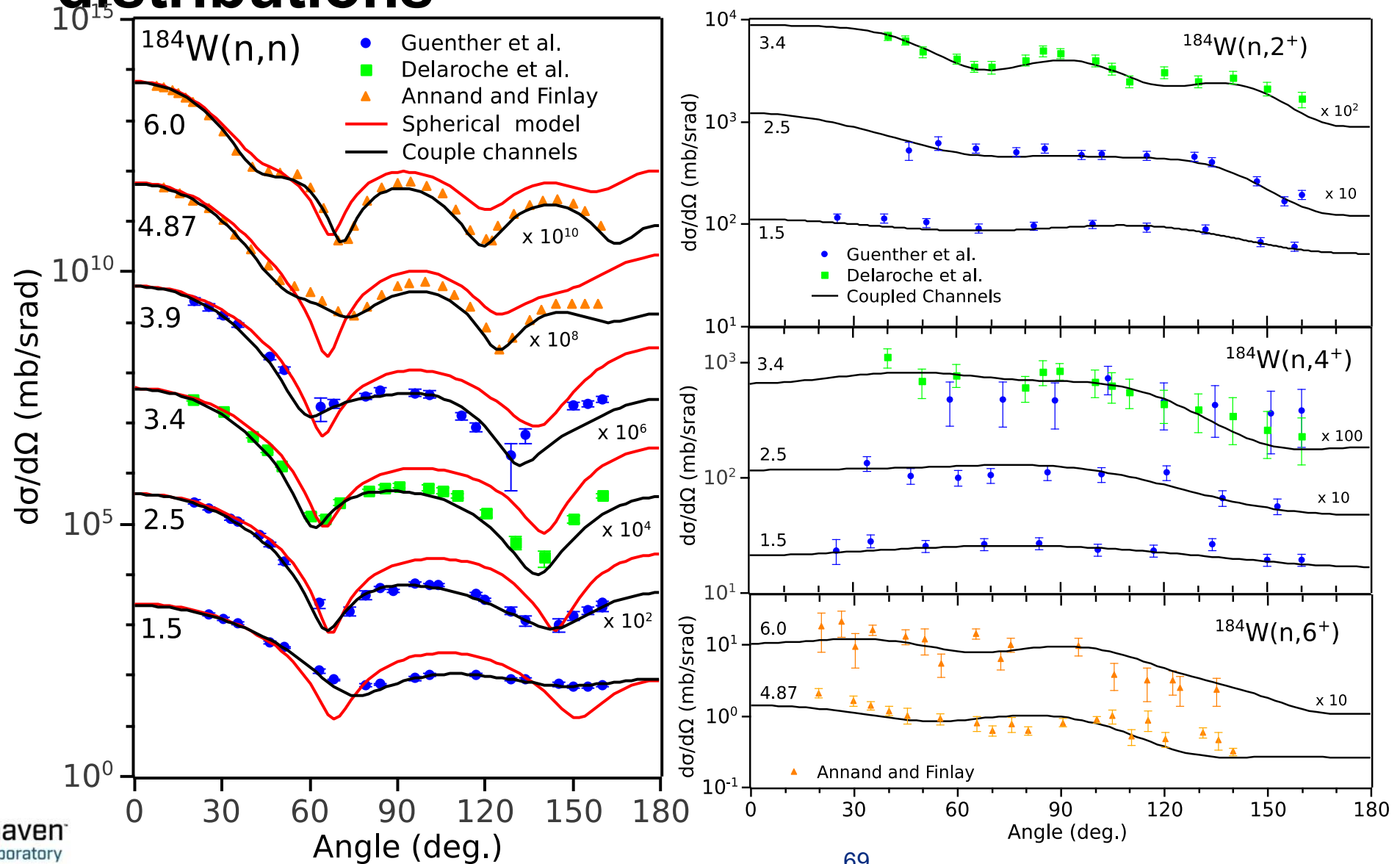


# $^{182}\text{W} - 4^+$ Inelastic ang. dist. ( $E_4^+ = 0.329\text{MeV}$ )

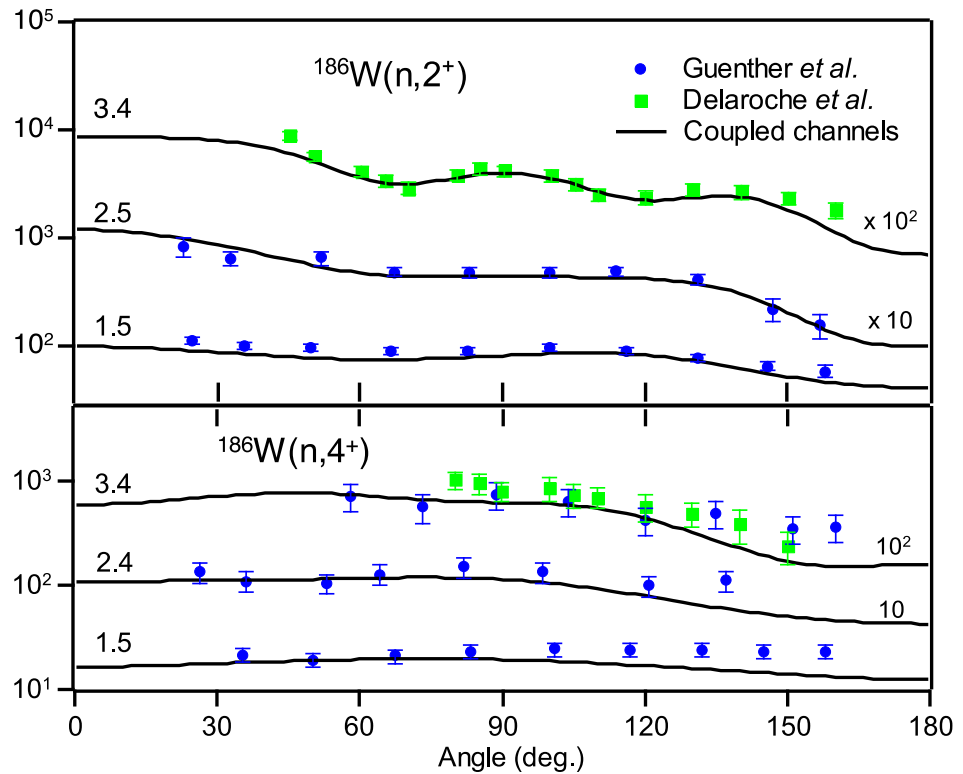
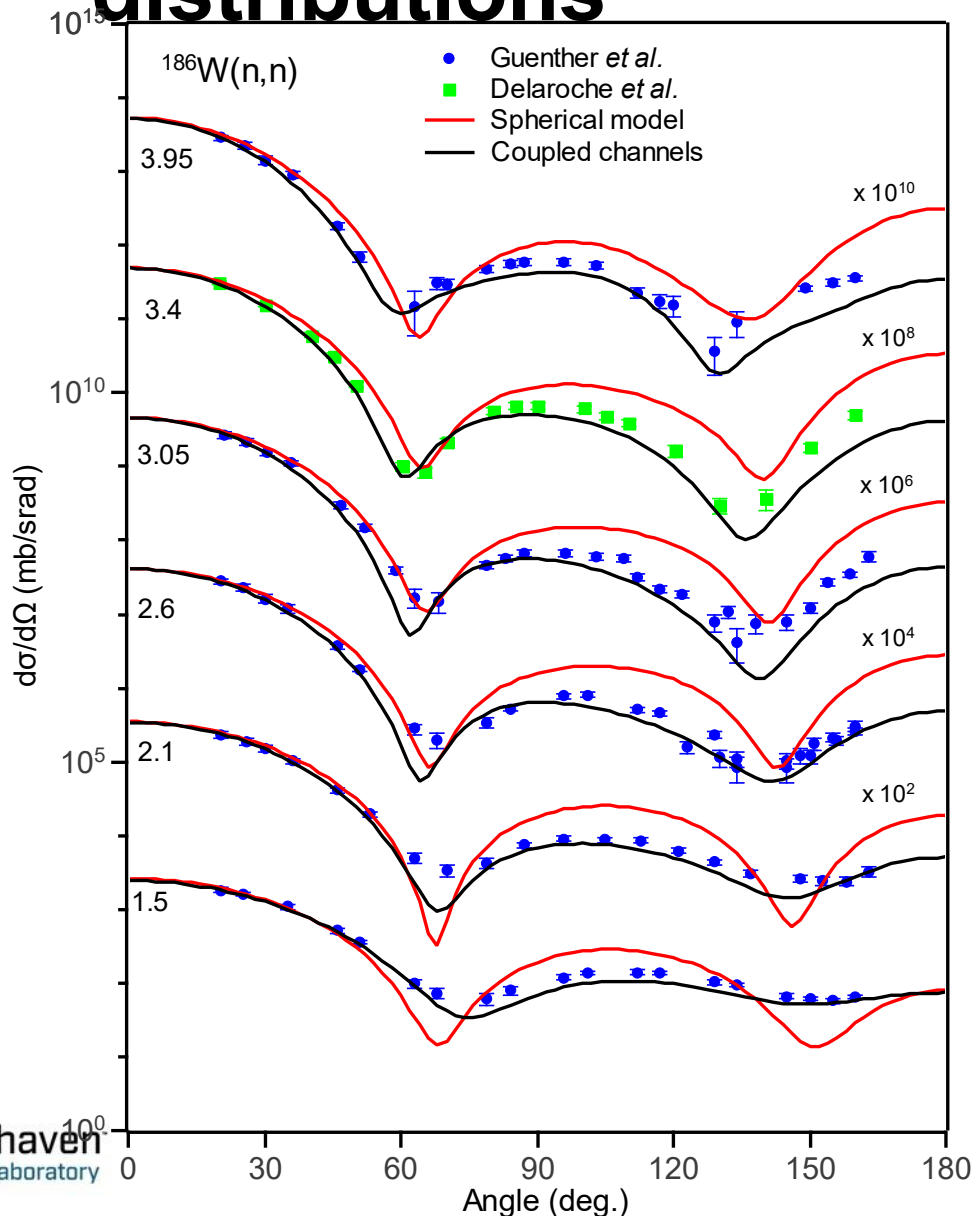
Good agreement with experimental data obtained by the model



# $^{184}\text{W}$ – Elastic and inelastic angular distributions

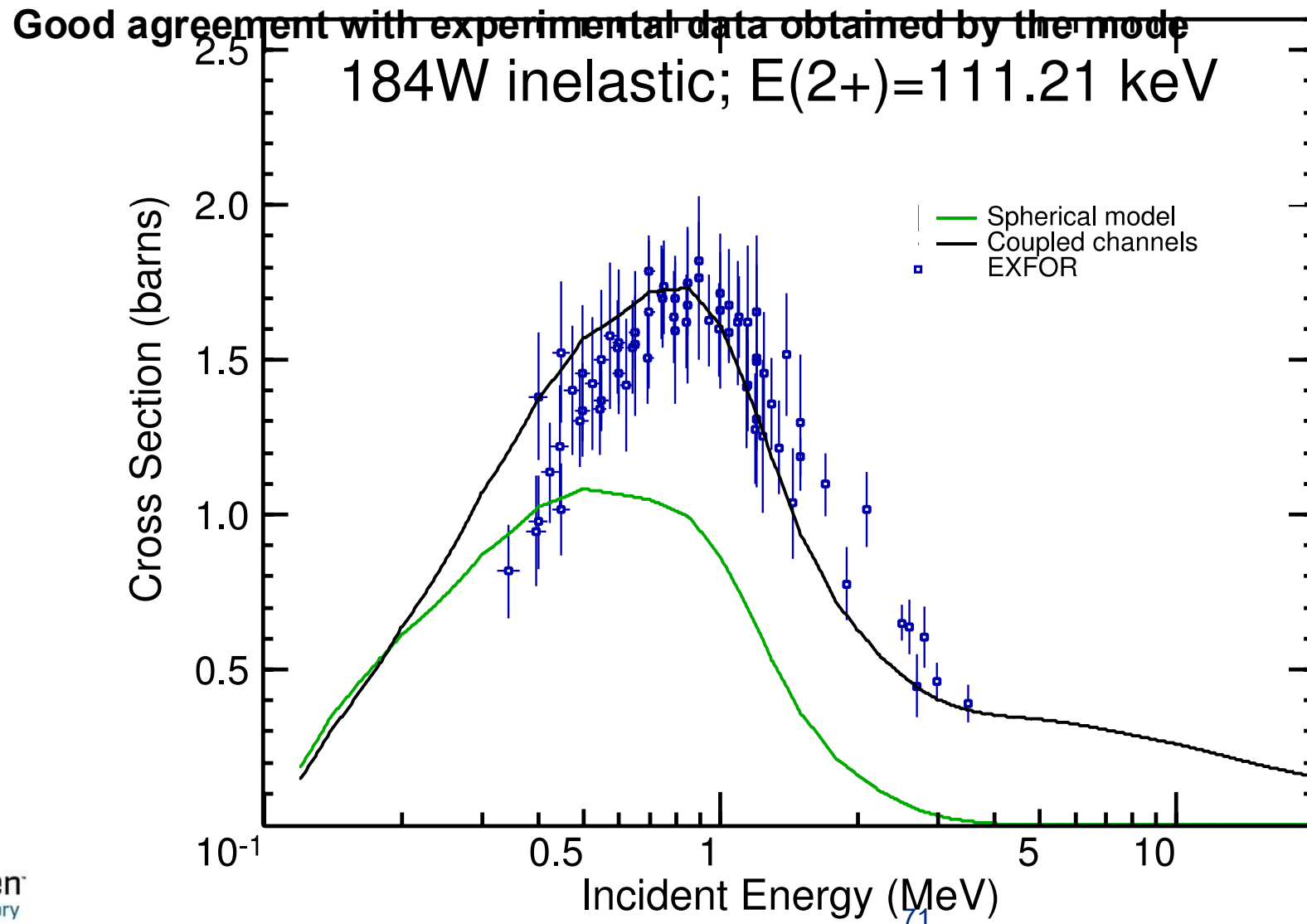


# $^{186}\text{W}$ – Elastic and inelastic angular distributions



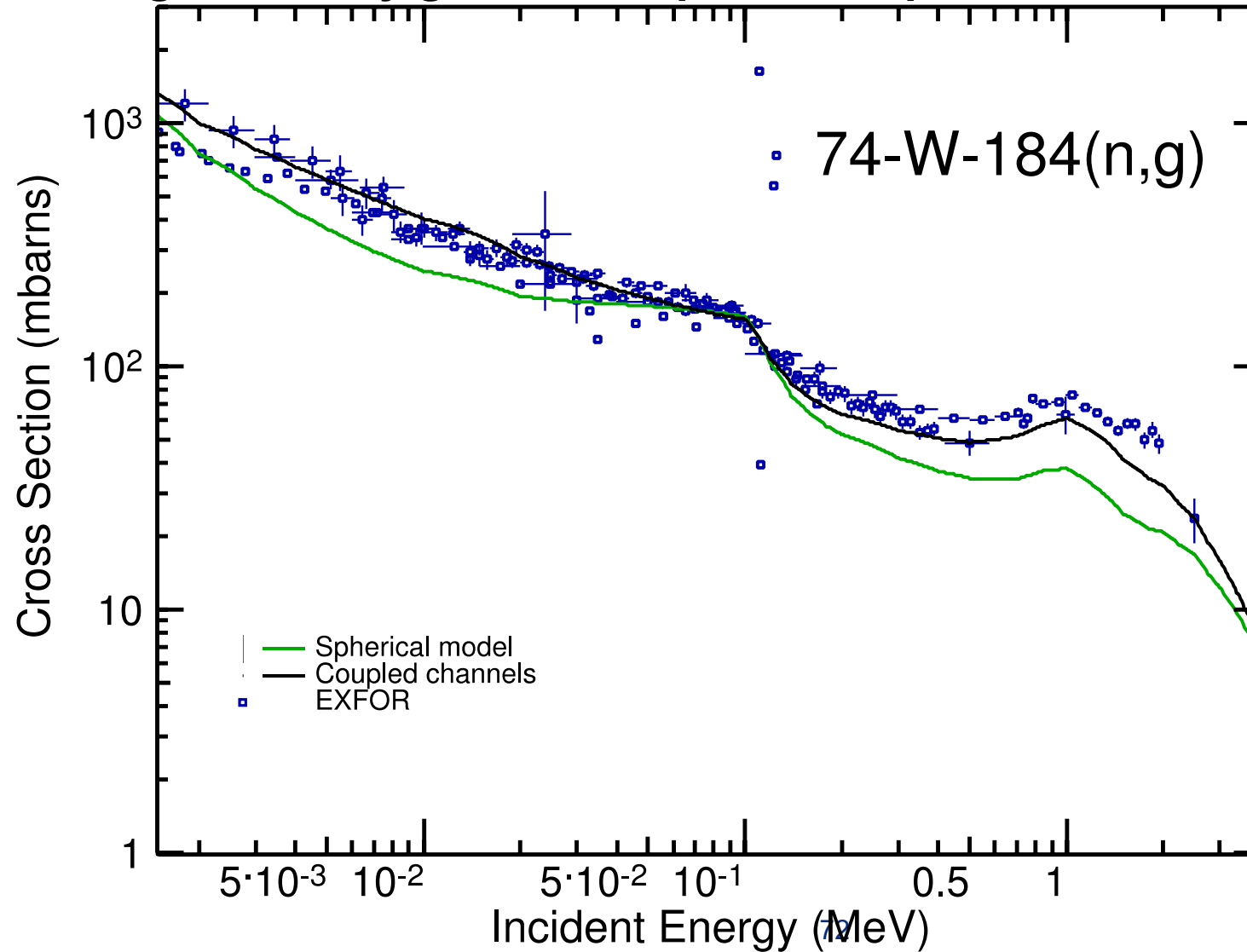
The fact that deforming KD allows to consistently describe observed elastic and inelastic angular distributions remarkably well is very supportive of the model and of the adiabatic approximation.

# Angle-integrated inelastic cross sections



# Capture cross sections

Our model gives a very good description of capture cross sections



# Conclusion

We deformed spherical KD potential in CC calculations to describe statically-deformed nuclei

- No free parameters (experimental deformations)
- Radius correction gives (small but) noticeable effect

This approach provides provides remarkable results for

- Total, elastic, inelastic cross sections
- Elastic and inelastic angular distributions

Improvement of capture cross sections, in particular their shape

This simple method is a good, consistent and general step towards an OP capable of fully describing the rare-earth region, filling the current lack in this important region.



# Experimental level density studies at Edwards lab, Ohio University

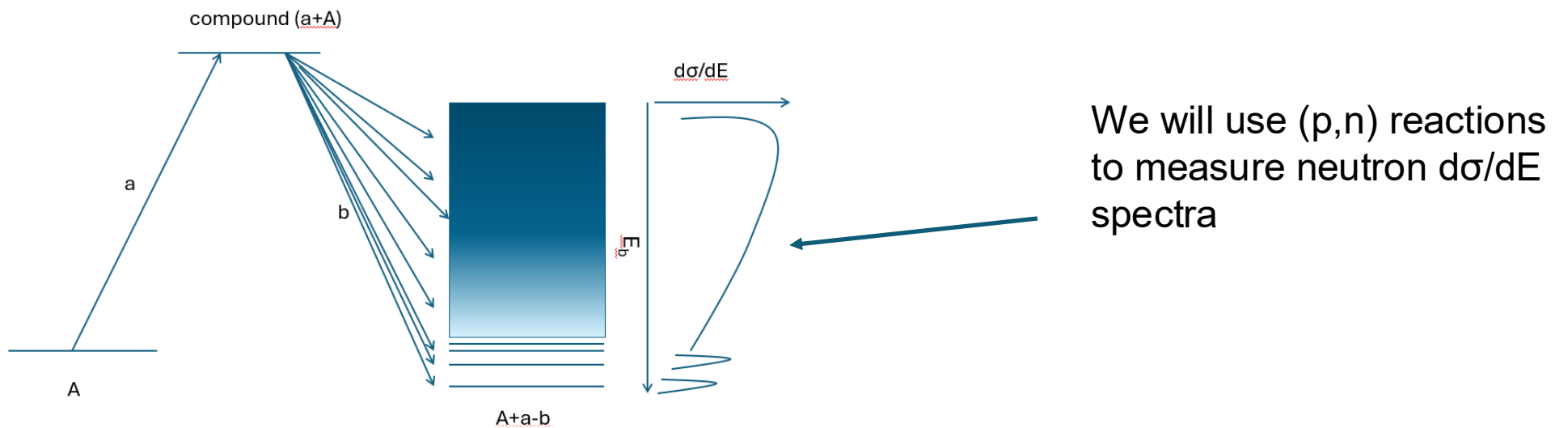
**Goal:** to improve systematics of the level density model parameters in the mass region of fission products thereby enhancing the predictive power of level density models for nuclear data evaluations.

## **Method:**

- to review and validate available literature data on level densities measured with the different techniques over the mass range of the fission products (about 20 data sets are available).
- to address gaps in level density systematics by conducting targeted experiments at the Edwards Lab and benchmark models against experimental data

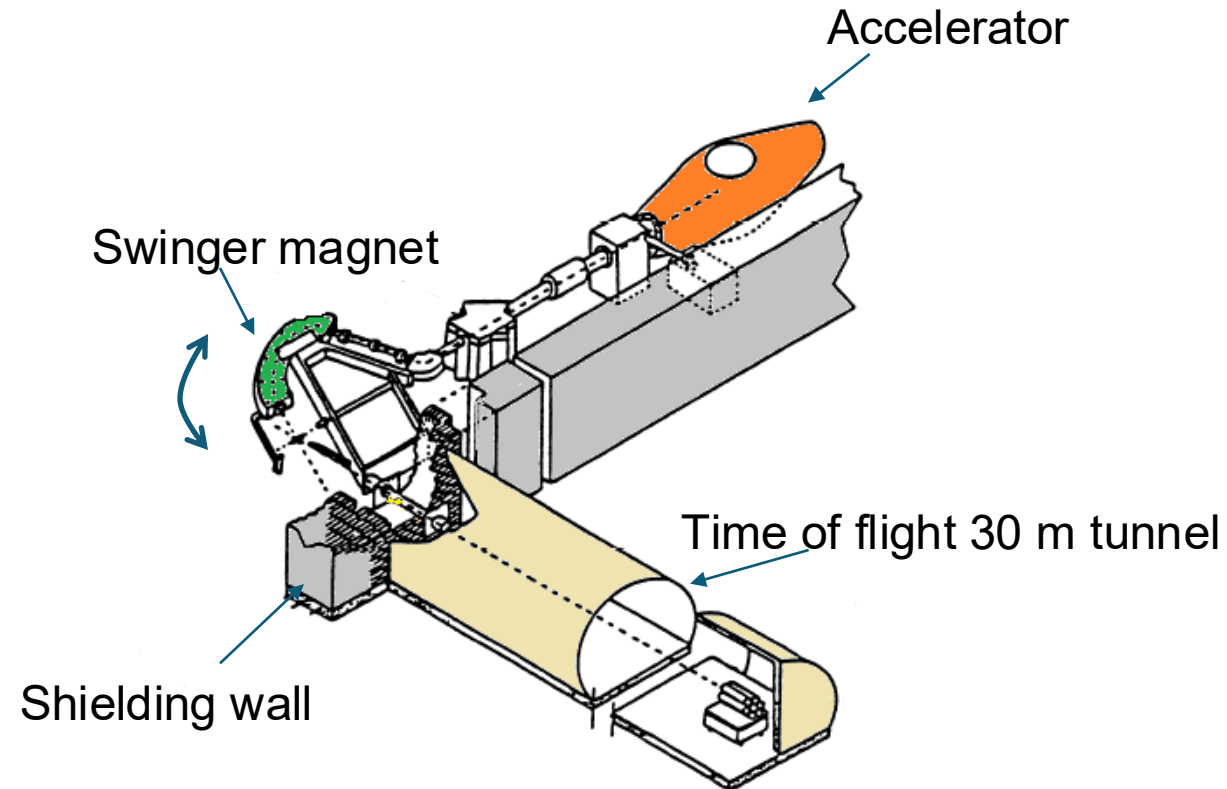
# Particle evaporation technique to study level densities at the Edwards Lab

1. Create a reaction which proceeds through the compound reaction mechanism. This implies selecting appropriate beam species and energies.
2. Differential spectra of particles emitted from compound reactions depends on level density of nuclei populated.



# Ohio University Neutron facility layout

Swinger magnet



# Proposed experimental plan

- We will study level densities for stable nuclei in the mass range of the 1-st fission yield bump. Constraining level densities for stable nuclei will make it easier to extrapolate them to neutron rich nuclei using available models
- Possible reactions (depending on target availability):

$^{74-78,80,82}\text{Se}(p,n)^{74-78,80-82}\text{Br}$ ,       $^{89}\text{Y}(p,n)^{89}\text{Zr}$ ,       $^{90-92,94,96}\text{Zr}(p,n)^{90-92,94-96}\text{Nb}$ ,

- We commit 1 experiment per year, including data analysis

# Preequilibrium: Extended microscopic QM model

- Preequilibrium emissions become dominant at high energies

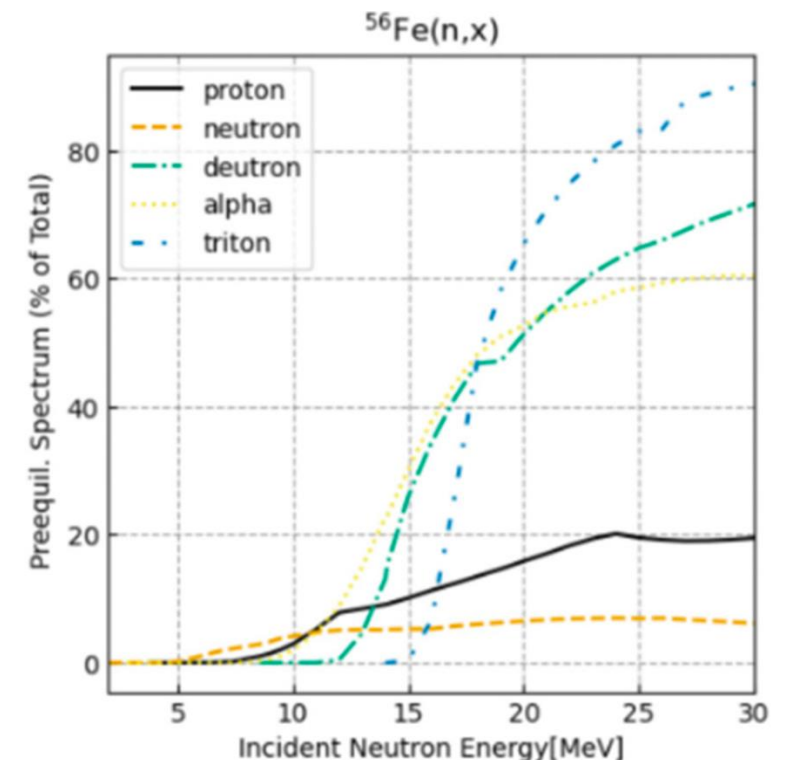
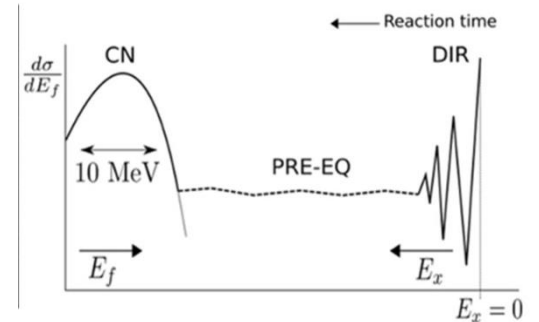
## Goal:

- Use **QM** based **ph** ( and **2p2h**) response functions  $f_{BW}$  to model these direct-like reactions

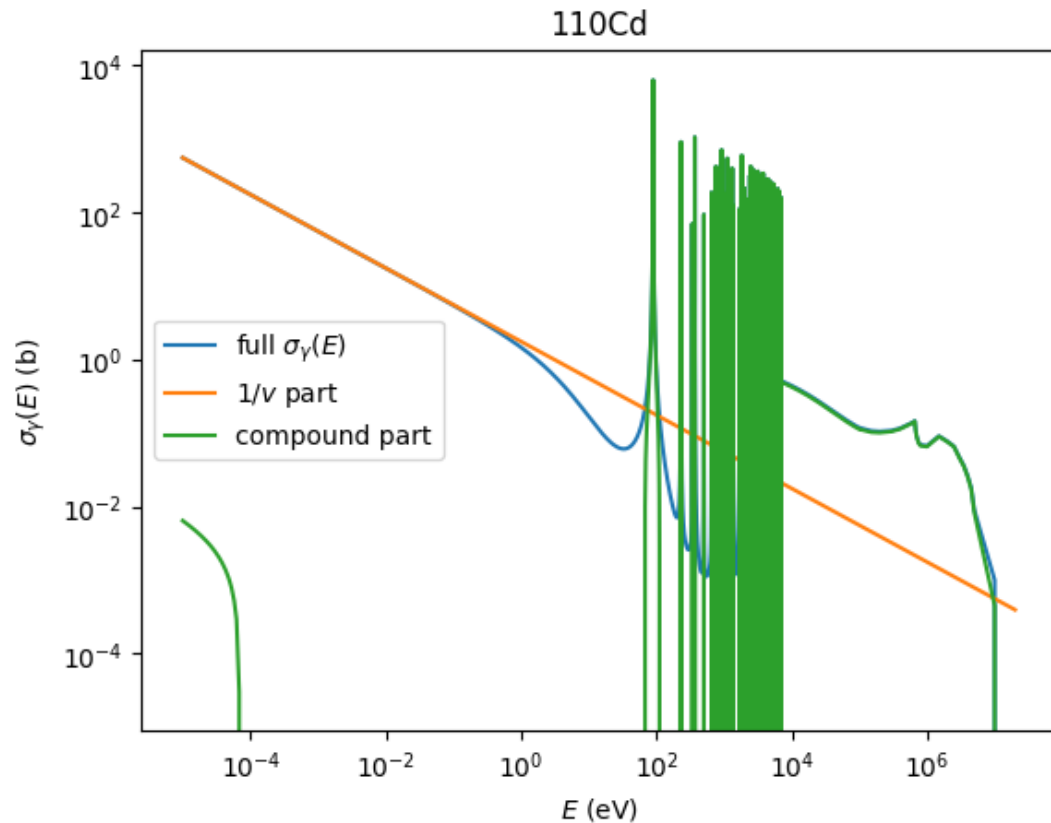
$$\sigma(E) = \sum_{ph} \int_{E-\Delta}^{E+\Delta} f_{BW}(E, E_{ph}) \sigma_{ph} dE$$

- Increase confidence in the description at stable isotopes before applying to unstable ones

✓ Extending the classical picture of exciton model



# Capture cross-sections



Capture cross-sections have

- A 1/v part – the shape is analytic, the magnitude must be measured
- A compound nuclear part consisting of many resonances
- A smooth high-energy part that peaks around 14 MeV with  $\sigma \sim 100$  mb

Practical division:

$$\sigma_\gamma(E) = \sigma_{th} \sqrt{\frac{E_{th}}{E}} + \sigma_{CN}(E)$$



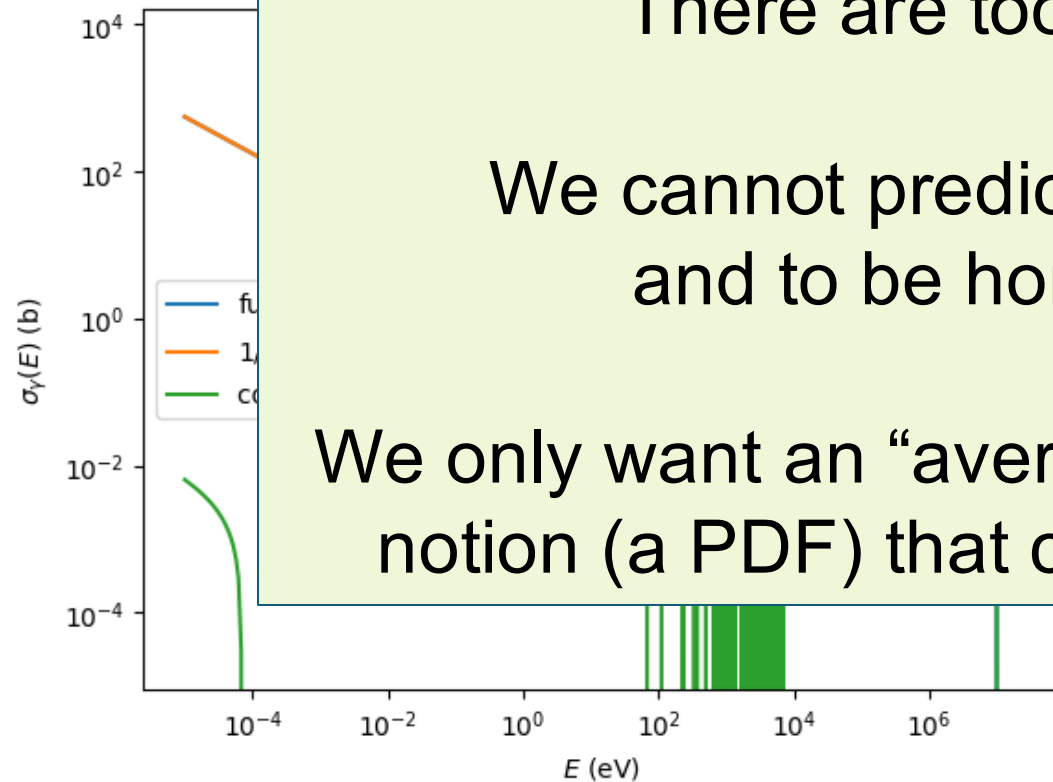
# Capture cross-sections

Capture cross-sections have

There are too many resonances.

We cannot predict their position or width,  
and to be honest, we don't care.

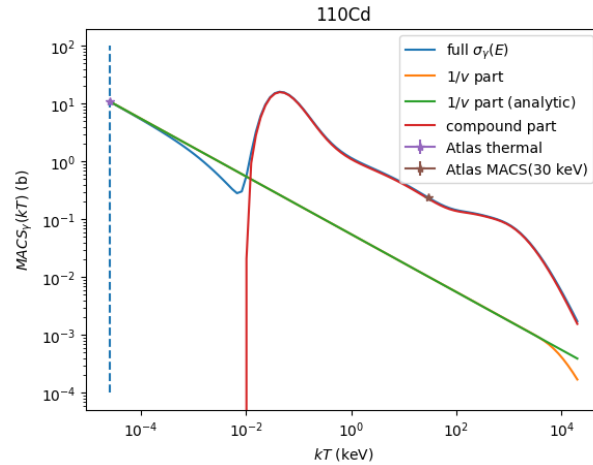
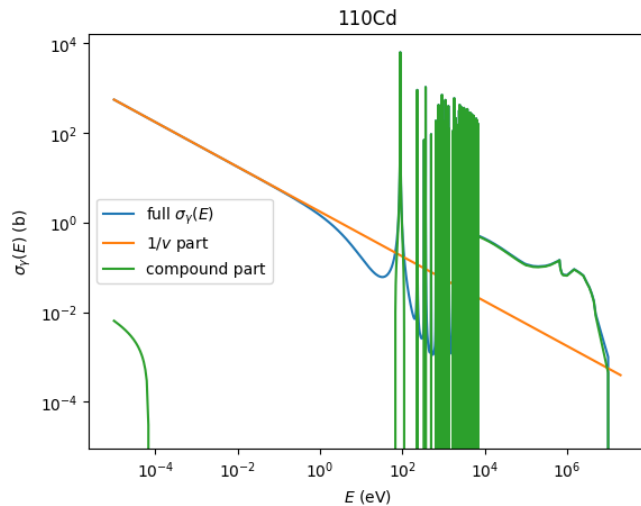
We only want an “average” cross section and some  
notion (a PDF) that captures size of fluctuations



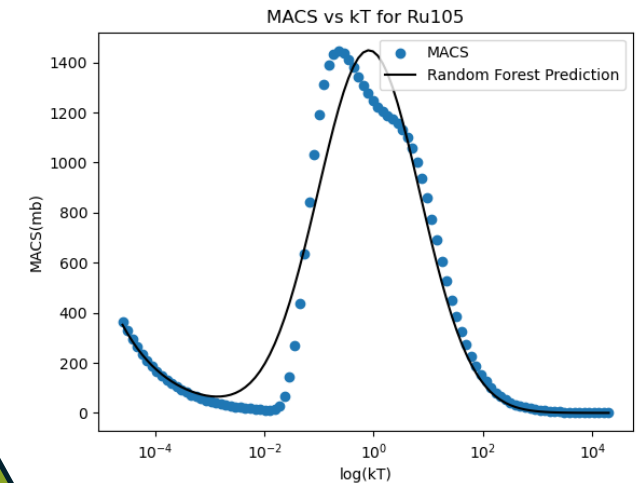
$$\sigma_{\gamma}(E) = \sigma_{th} \sqrt{\frac{v_{tr}}{E}} + \sigma_{CN}(E)$$

# Capture cross-section average values

Build reduced order model of MACS



Learn parametric (Z,A) dependence of reduced order model

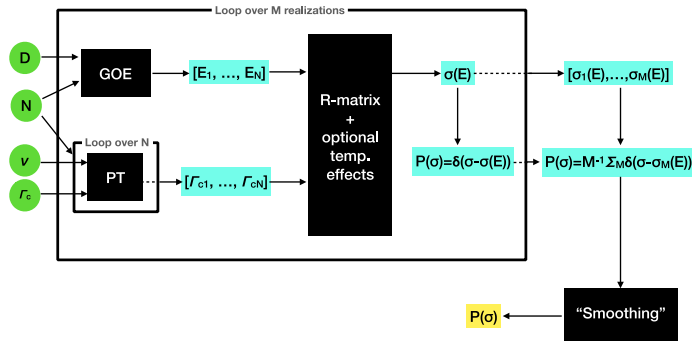


Test against original cross-sections or MACS

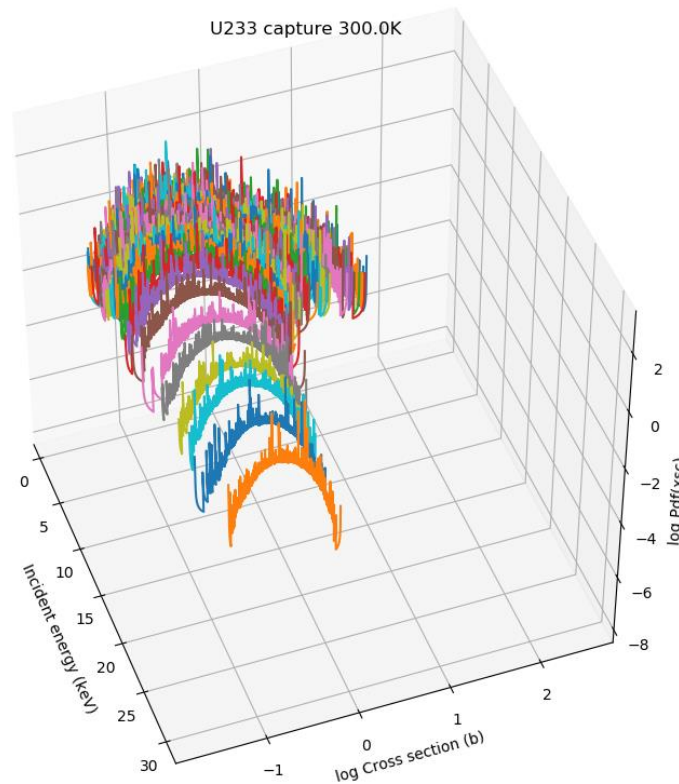
*“magic” function*  
 $\sigma_\gamma(Z,A,E)$

Transform model back to cross-section space

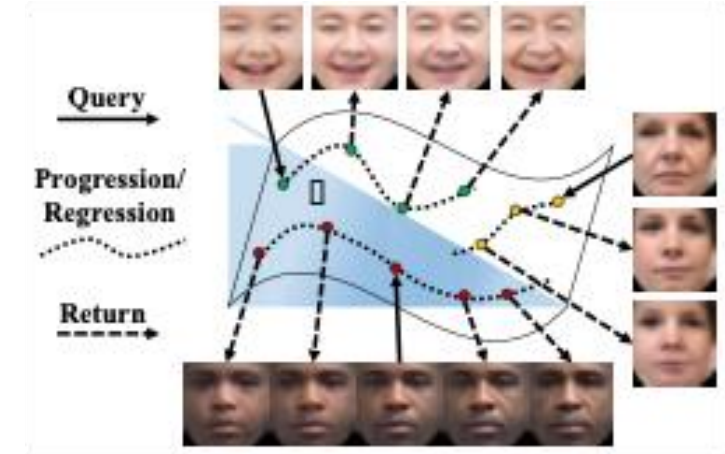
# Capture cross-section fluctuations



Use FUDGE as a generative model to simulate cross-section probability distribution function (PDF)

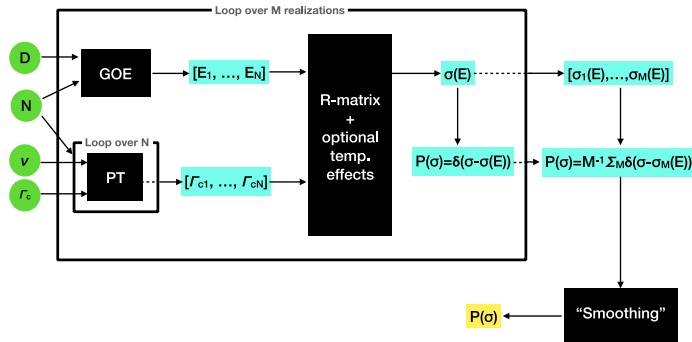


$^{238}\text{U}(n,g)$  cross-section PDF

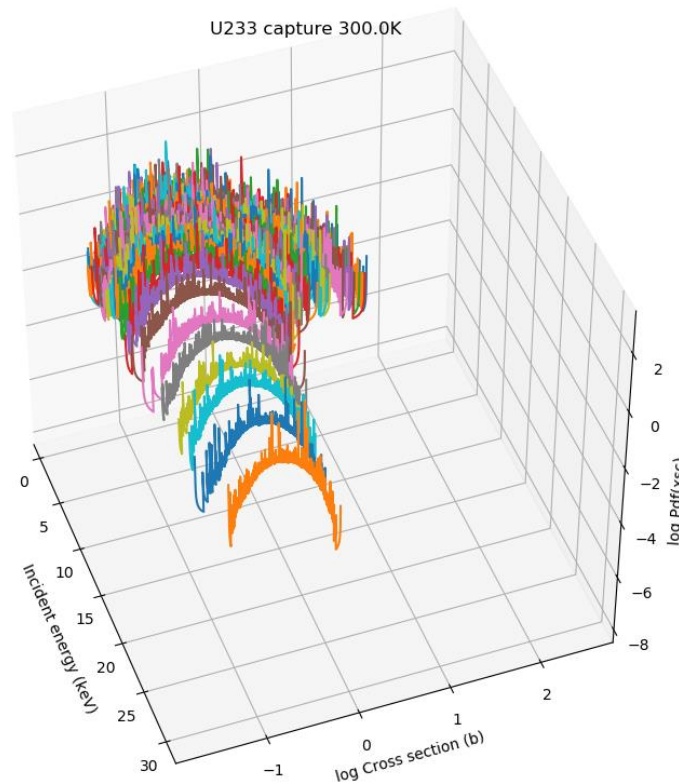


Use age-progression software to learn the temperature (and energy?) dependence of the cross-section PDF

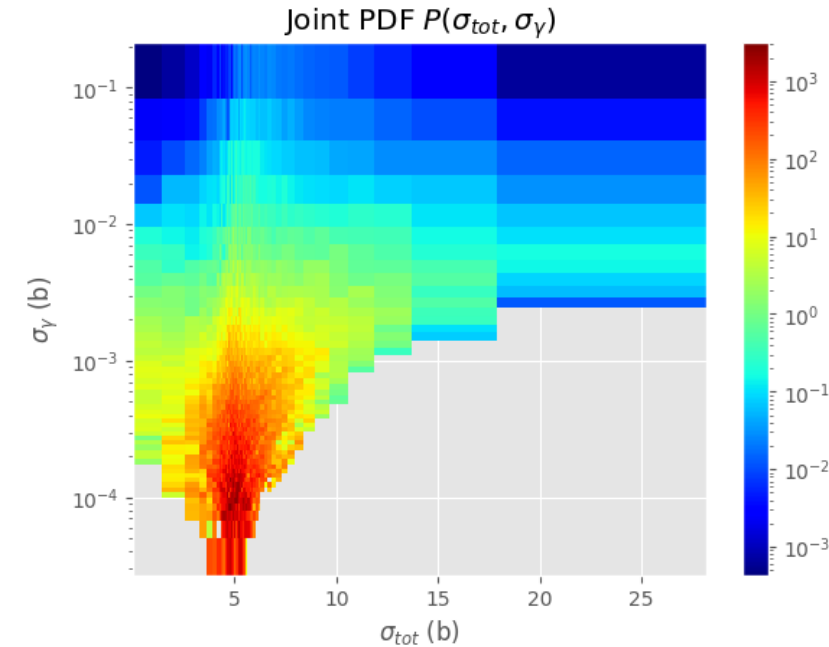
# Capture cross-section fluctuations



Use FUDGE as a generative model to simulate cross-section probability distribution function (PDF)



$^{238}\text{U}(n,g)$  cross-section PDF



As a hedge, can use the PDF's directly with estimates of RRR spacings & widths

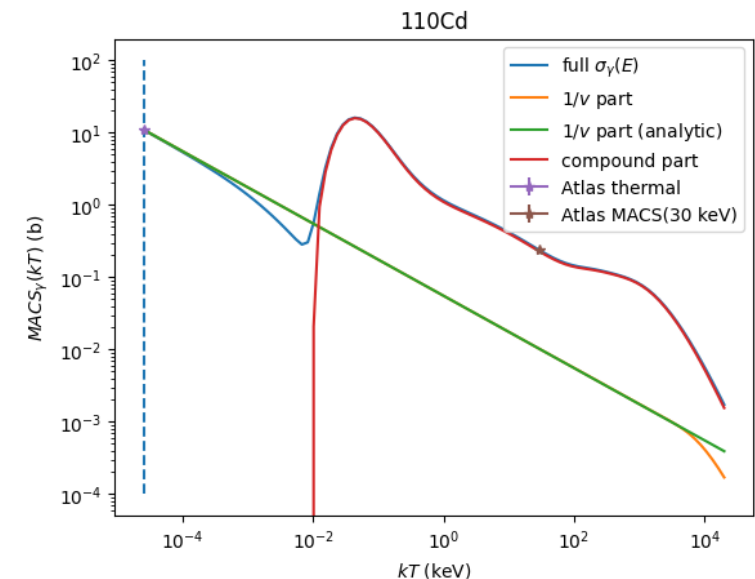
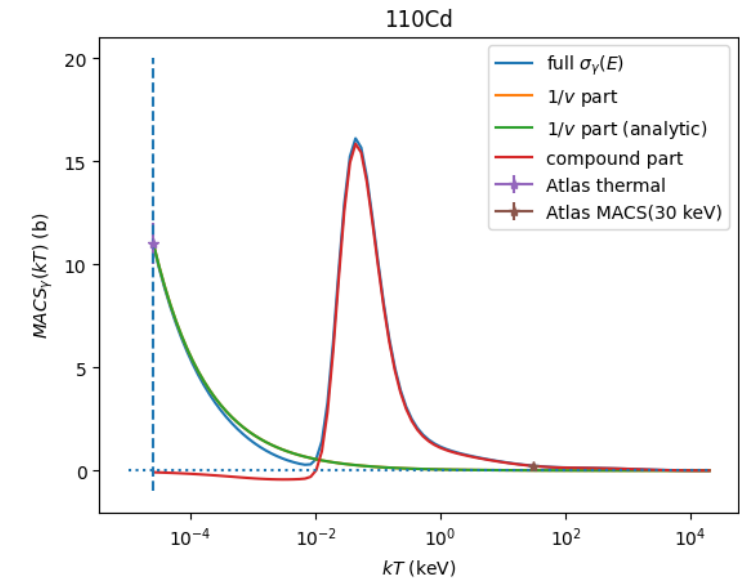
# Maxwellian Averaged Cross-Sections

The MACS is given by

$$\begin{aligned} \text{MACS}(k_B T) &= \frac{2}{\sqrt{\pi}} \frac{a^2}{(k_B T)^2} \int_0^\infty E \sigma(E) e^{-\frac{aE}{k_B T}} dE \\ &= \frac{\langle \sigma v \rangle}{v_T} \end{aligned}$$

Interestingly, the 1/v part can be done analytically, giving

$$\text{MACS}(kT) = \text{MACS}_{CN}(kT) + \sigma_{th} \sqrt{\frac{aE_{th}}{kT}}$$



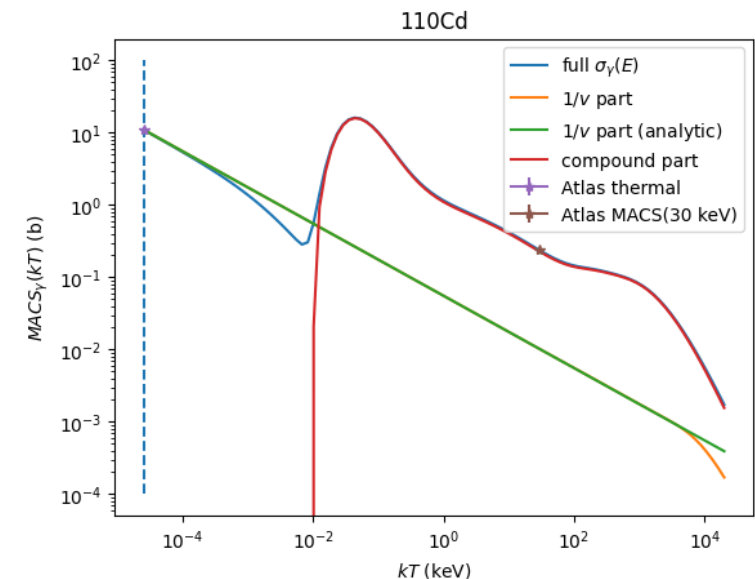
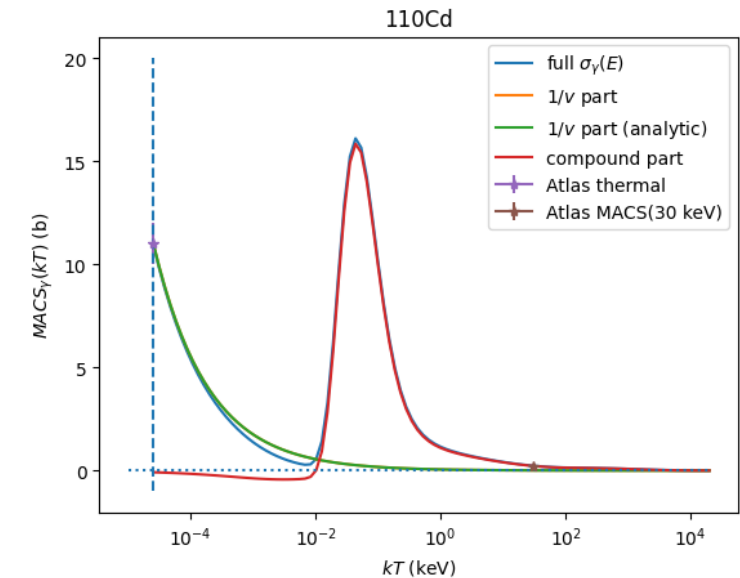
# Maxwellian Averaged Cross-Sections

The MACS is given by

$$\begin{aligned} \text{MACS}(k_B T) &= \frac{2}{\sqrt{\pi}} \frac{a^2}{(k_B T)^2} \int_0^\infty E \sigma(E) e^{-\frac{aE}{k_B T}} dE \\ &= \frac{\langle \sigma v \rangle}{v_T} \end{aligned}$$

Our reduced order model:

$$\text{MACS}(k_B T) = \frac{A_0}{\sqrt{k_B T}} + \sum_{i=1}^n A_i e^{-\left[ \frac{\log(k_B T) + B_i}{C_i} \right]^2}$$



# How to get back to “cross-section space”

Believe it or not, the MACS is actually a Laplace transform:

$$F(s) \equiv \mathcal{L}\{f\}(s) = \int_0^{\infty} f(t)e^{-st} dt$$
$$f(t) = \mathcal{L}^{-1}\{F\}(t) = \frac{1}{2\pi i} \lim_{T \rightarrow \infty} \int_{\gamma-iT}^{\gamma+iT} e^{st} F(s) ds$$

We make the following identifications:

$$f(t) \rightarrow \frac{2}{\sqrt{\pi}} \sigma_{CN}(E) E \qquad t \rightarrow E$$
$$F(s) \rightarrow \frac{(kT)^2}{a^2} MACS_{CN}(kT) \qquad s \rightarrow a/kT$$



# How to get back to “cross-section space”

Believe it or not, the MACS is actually a Laplace transform:

$$F(s) \equiv \mathcal{L}\{f\}(s) = \int_0^{\infty} f(t)e^{-st} dt$$
$$f(t) = \mathcal{L}^{-1}\{F\}(t) = \frac{1}{2\pi i} \lim_{T \rightarrow \infty} \int_{\gamma-iT}^{\gamma+iT} e^{st} F(s) ds$$

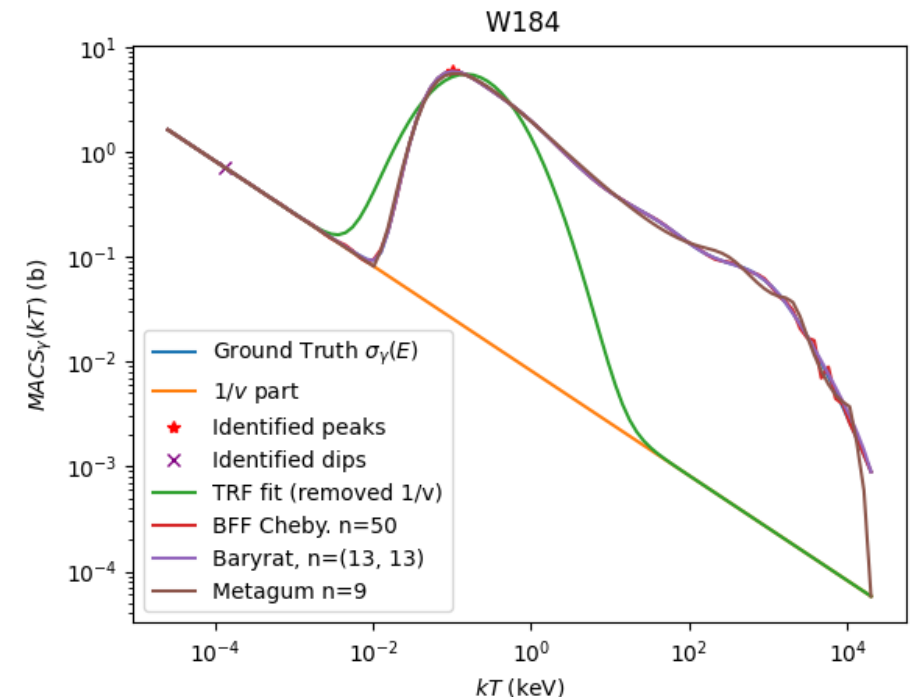
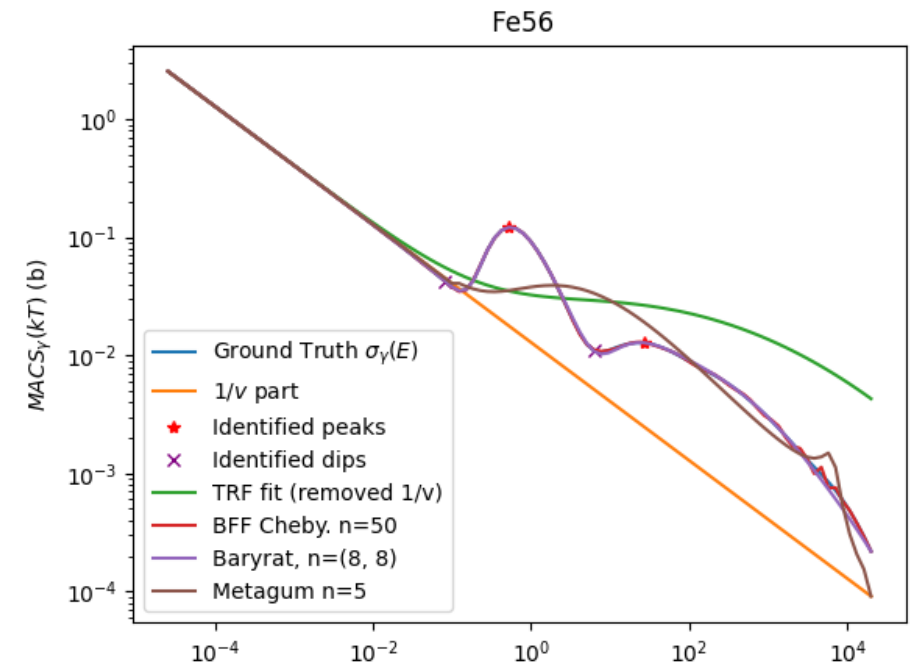
We make the following identifications:

$$f(t) \rightarrow \frac{2}{\sqrt{\pi}} \sigma_{CN}(E) E \qquad t \rightarrow E$$
$$F(s) \rightarrow \frac{(kT)^2}{a^2} MACS_{CN}(kT) \qquad s \rightarrow a/kT$$

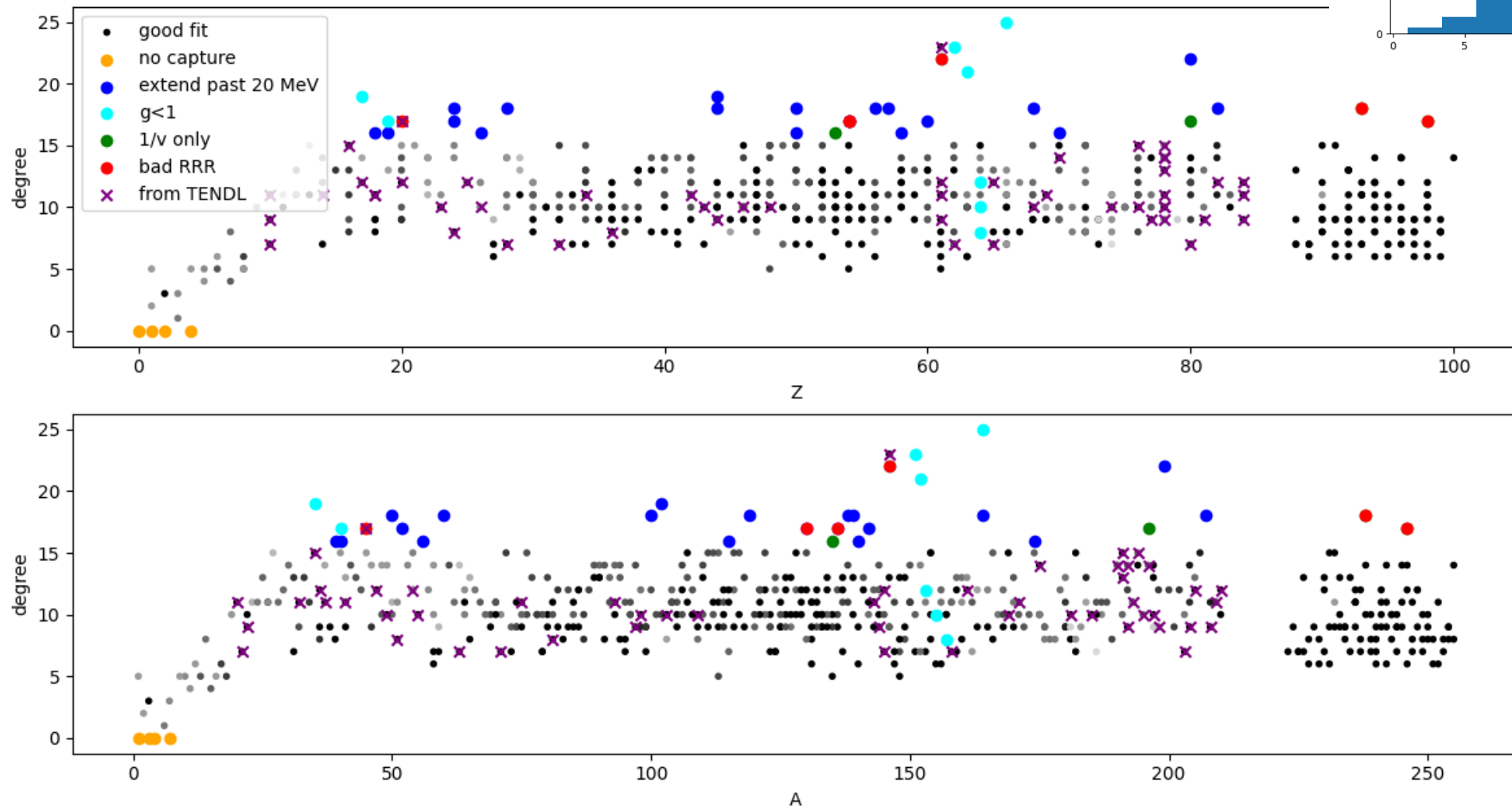
If we make a rational approximation to the MACS, the ILT is **ANALYTIC**

# 5. Rational function approximation

- Barycentric rational function approximation using adaptive Antoulas–Anderson algorithm
- Provide set of  $\{kT, \text{MACS}(kT)\}$  points, a tolerance, max order  $m$
- # parameters =  $3m$
- Robust fit
- Trade off quality of fit for dimensional reduction
- Analytic ILT
- Easily beats other schemes



# Summary of the fits, $\text{atol}=10 \mu\text{b}$ , $\text{rtol}=0.1\%$



# We have experience with that!

- Evaluated files for these nuclides are either:
  - Non-existent; or
  - Created with oversimplified modeling = poor predictability
- Technical report BNL-114256-2017-INRE (<https://doi.org/10.2172/1656598>)
- Produced evaluated files for isotopes with  $T_{1/2} \geq 1$  day and for g.s. and isomeric nuclides “bridging” them: ENDF/B-VIII.0

**Better treatment of deformed nuclei and isomeric targets**

## Comparison between EMPIRE and TENDL

G. P. A. Nobre<sup>1</sup>, D. A. Brown<sup>1</sup>, and M. W. Herman<sup>1</sup>

<sup>1</sup>*National Nuclear Data Center, Brookhaven National Laboratory, Upton, NY 11973, USA*

This report is a review of the  
also discuss additions and modifications

## 5 Differences in physics modeling

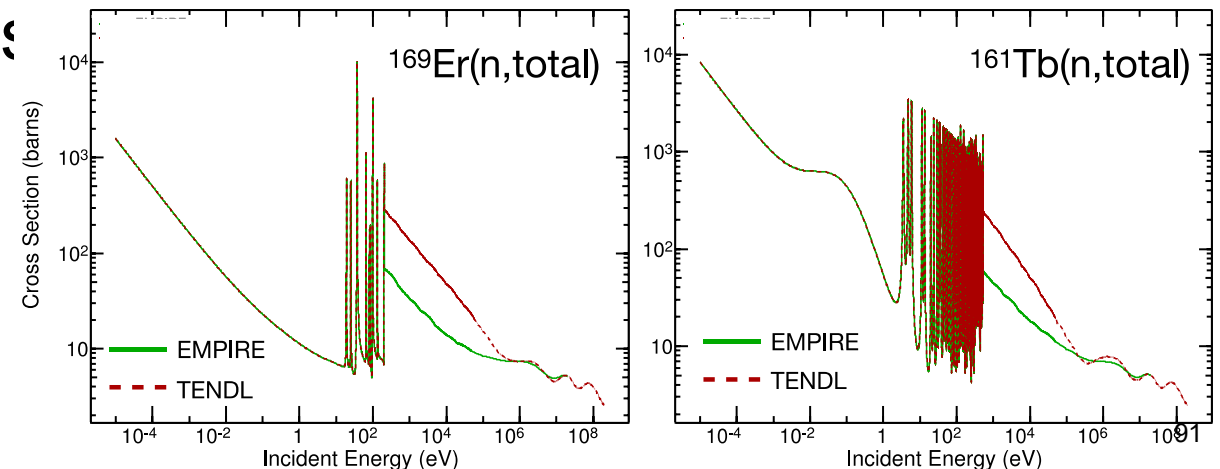
There are several physics differences between the EMPIRE based evaluations and those in TENDL-2015. We summarize them here:

- Since EMPIRE does proper deformed coupled-channel calculations, it obtains better and more reliable cross sections for the well-deformed rare-earth nuclei, as it implements the adiabatic model proposed and tested in Refs. [8, 9]
- Both codes make different choices of levels to couple in coupled-channel calculations.

- Experimental data for resonances in the cases of such unstable nuclei are inexistent, with few exceptions. However, the resonance treatment from TENDL, which artificially creates several realistic-looking resonances without any experimental grounds, may lead to misinterpretation of the evaluation considering that it is not possible within the ENDF-6 format to distinguish such resonance regions from the ones based on experimental data.
- The resonances from TENDL are extrapolated from fast region and therefore are normally 3 to 4 orders of magnitude too high.
- TENDL gets the 1 mb capture cross section at 14 MeV always right while the EMPIRE preliminary calculations have not yet been tuned to reproduce this value.

# Explain why it is challenging to produce reliable evaluations off stability

- Lack of experimental data. Perhaps show a table or plot with the number of EXFOR isotopic entries as a function of mass number for a given fission product.
- Need theory: Need to be extra careful with model choices and parametrizations
- Current solutions (TENDL, with the approach completeness before accuracy) have estimated cross as high as 50%





# We have experience with that!

- Evaluated files for these nuclides are either:
  - Non-existent; or
  - Created with oversimplified modeling = poor predictability
- Technical report BNL-114256-2017-INRE (<https://doi.org/10.2172/1656598>)
- Produced evaluated files for isotopes with  $T_{1/2} \geq 1$  day and for g.s. and isomeric nuclides “bridging” them: ENDF/B-VIII.0

**Better treatment of deformed nuclei and isomeric targets**

## Comparison between EMPIRE and TENDL

G. P. A. Nobre<sup>1</sup>, D. A. Brown<sup>1</sup>, and M. W. Herman<sup>1</sup>

<sup>1</sup>National Nuclear Data Center, Brookhaven National Laboratory, Upton, NY 11973, USA

This report is a review of the  
also discuss additions and modifications

## 5 Differences in physics modeling

There are several physics differences between the EMPIRE based evaluations and those in TENDL-2015. We summarize them here:

- Since EMPIRE does proper deformed coupled-channel calculations, it obtains better and more reliable cross sections for the well-deformed rare-earth nuclei, as it implements the adiabatic model proposed and tested in Refs. [8, 9]
- Both codes make different choices of levels to couple in coupled-channel calculations.

- Experimental data for resonances in the cases of such unstable nuclei are inexistent, with few exceptions. However, the resonance treatment from TENDL, which artificially creates several realistic-looking resonances without any experimental grounds, may lead to misinterpretation of the evaluation considering that it is not possible within the ENDF-6 format to distinguish such resonance regions from the ones based on experimental data.
- The resonances from TENDL are extrapolated from fast region and therefore are normally 3 to 4 orders of magnitude too high.
- TENDL gets the 1 mb capture cross section at 14 MeV always right while the EMPIRE preliminary calculations have not yet been tuned to reproduce this value.

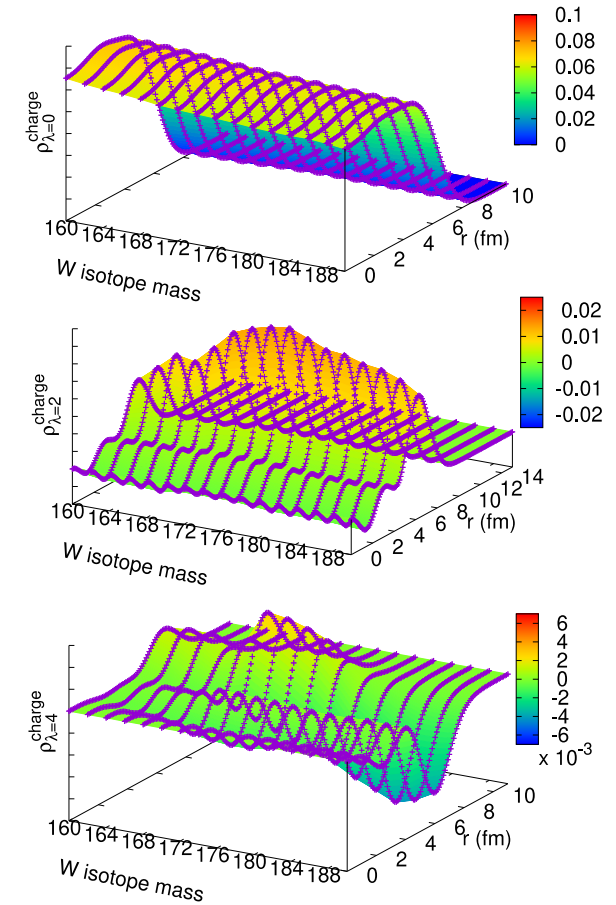
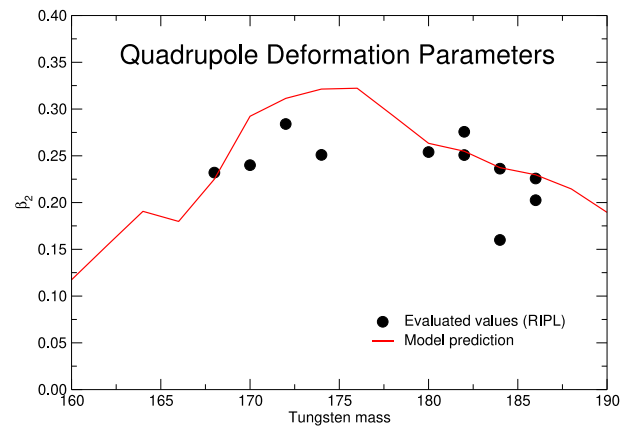
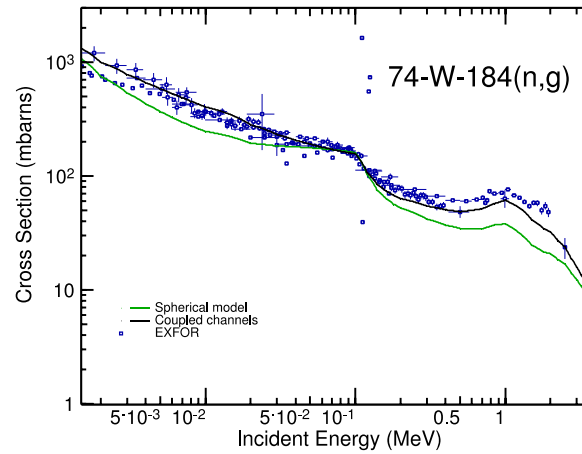


**Figure 12:** Nuclear density of charge for  $^{160-188}\text{W}$  calculated within a microscopic HFB model.



# We have experience with that!

- Predictive adiabatic model for deformed nuclei
- Proper treatment changes cross sections by orders of magnitude

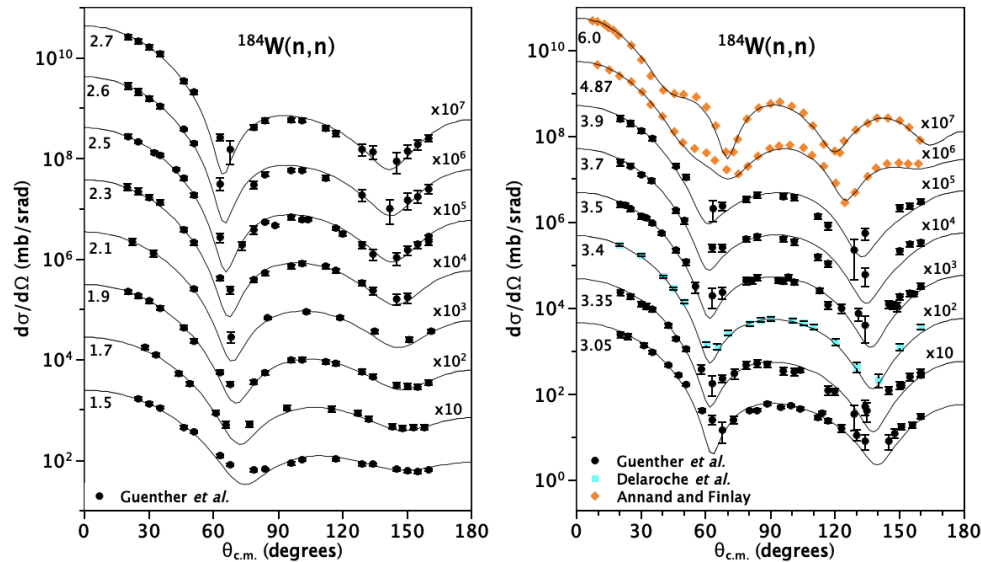
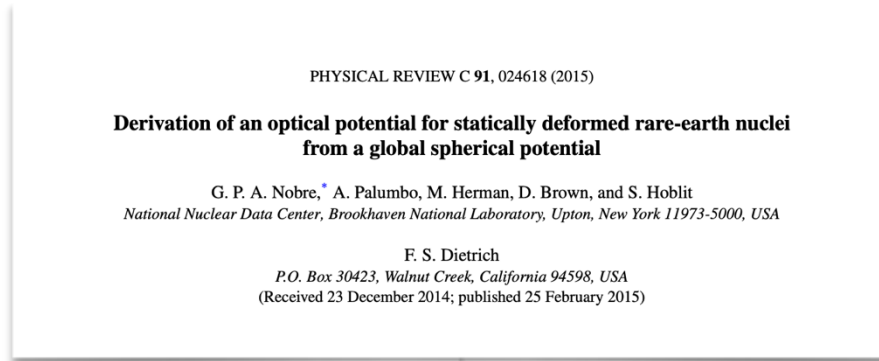


FIG. 11. (Color online) Elastic angular distributions for neutron-induced reactions on  $^{184}\text{W}$ . The curves correspond to predictions by our CC model. Numbers on the left-hand side of each plot indicate, in MeV, the values of incident energy at which the cross sections were measured, while the numbers on the right-hand side correspond to the multiplicative factor applied to be able to plot data from different incident energies in the same graph. Experimental data taken from Refs. [36–38] and their correspondence to each data set is indicated in the legends.

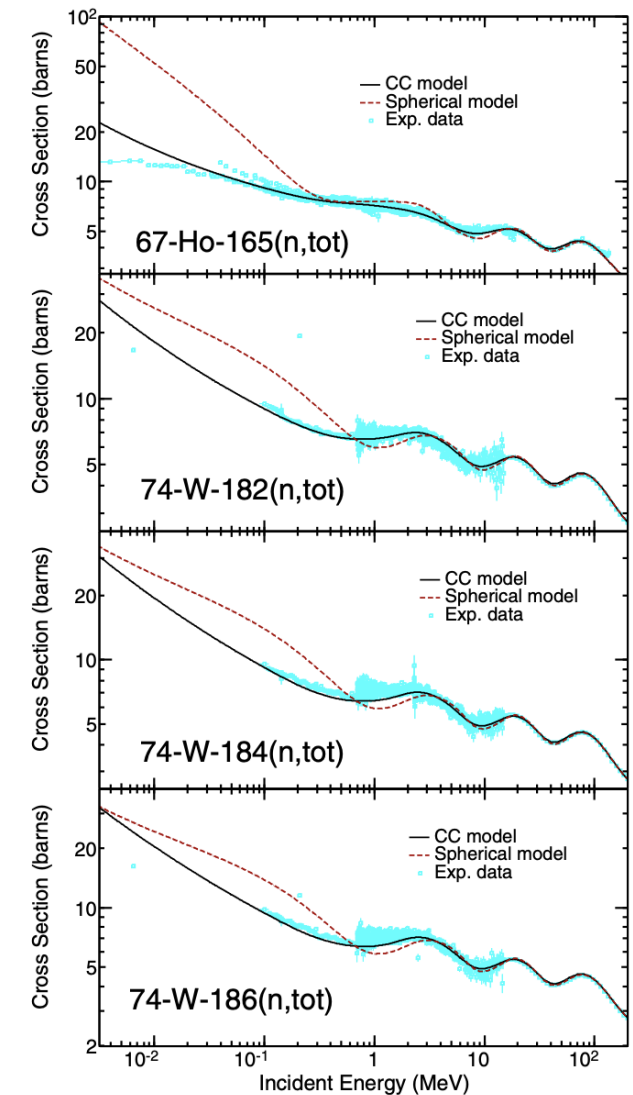
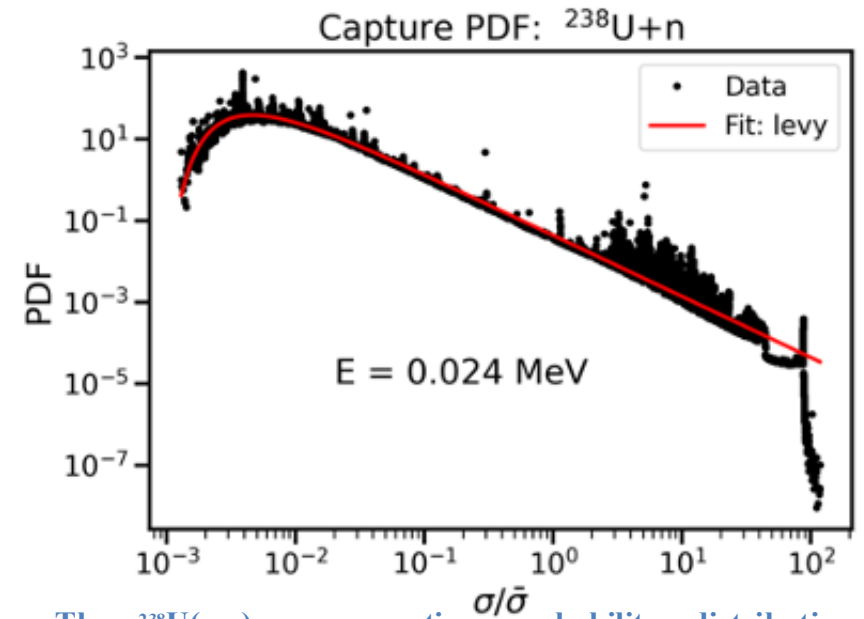


FIG. 1. (Color online) Total cross sections for neutrons scattered by a  $^{165}\text{Ho}$  and  $^{182,184,186}\text{W}$  targets for incident energies ranging from as low as  $\approx 3$  keV to as high as 200 MeV, which is the upper limit of validity for the KD optical potential [2]. The solid black curves correspond to the predictions of our CC model, while the dashed red curves are the results of calculations within the spherical model. The experimental data were taken from the EXFOR nuclear data library [39].

# We have experience with that!

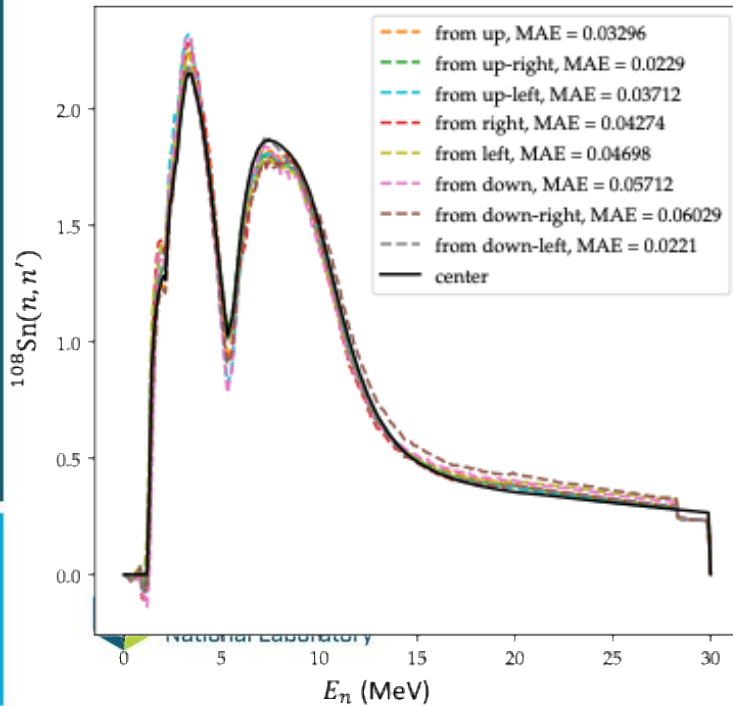
- **Neutron resonances:** On stability, we have high quality resonance data from both the ENDF/B library and from BNL's vaunted *Atlas of Neutron Resonances*. Off stability or whenever data is not available, the resolved resonance region cannot possibly be addressed reliably. Instead of generating stochastic resonances such as done for TENDL [17] with TARES [23] **we should treat the whole resonance range as unresolved.**
- **Preequilibrium:** Microscopic model from Emanuel Chimanski, constrained by on-stability data from A. Voinov



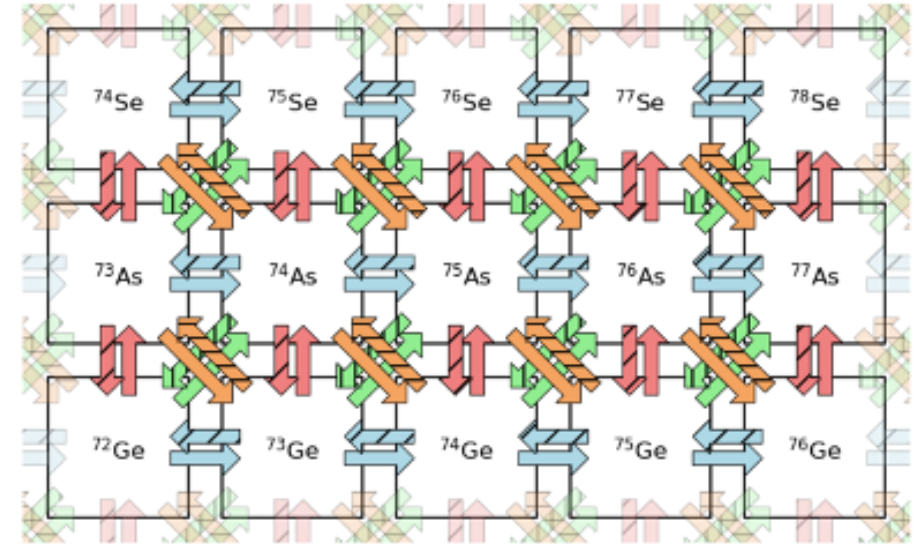
The  $^{238}\text{U}(n,g)$  cross section probability distribution at 0K stochastically generated by FUDGE and fit with a two parameter Levy Distribution. We have since found higher quality fits with a one parameter Stable Distribution.

# We have experience with that!

- Development and training of Conditional Adversarial Autoencoder (CAAE): LLNL project to use Machine Learning to train on known cross sections to make predictions for neighboring nuclei
- Will provide priors for capture and possibly inelastic cross sections
- Uncertainty quantification



Example from a preliminary trend prediction built on paired cycleGAN like architectures. The cross section is predicted using only the cross section of neighboring nuclei with high fidelity and complex feature reconstruction. This version depends on an explicit fixed energy grid whereas the transformer base networks will enable an adaptive energy grid.



Pictorial representation of the transformer's actions. The transformer is trained to directionally transform a collection of nuclear cross sections and discrete information from one nucleus to another bidirectionally (i.e., the transformer is trained as its own inverse). In this way, it learns the impact of adding or removing protons and neutrons instead of memorizing cross sections as a function of proton and neutron number. While the figure depicts only nearest neighbor connections, the networks can be tuned past nearest neighbor and with biased linkages to closed proton and neutron shells to add awareness of shell effects.

# Preequilibrium: Extended microscopic QM model

- Preequilibrium emissions become dominant at high energies

## Goal:

- Use **QM** based **ph** ( and **2p2h**) response functions  **$f_{BW}$**  to model these direct-like reactions

$$\sigma(E) = \sum_{ph} \int_{E-\Delta}^{E+\Delta} f_{BW}(E, E_{ph}) \sigma_{ph} dE$$

- Increase confidence in the description at stable isotopes before applying to unstable ones

✓ Extending the classical picture of exciton model

